STUTZMAN

NATIONAL ACADEMIES OF SCIENCE AND ENGINEERING

NATIONAL RESEARCH COUNCIL

of the

UNITED STATES OF AMERICA

UNITED STATES NATIONAL COMMITTEE

International Union of Radio Science

National Radio Science Meeting

4-6 January 1989

Sponsored by USNC/URSI
in cooperation with
Institute of Electrical and Electronics Engineers

University of Colorado
Boulder, Colorado
U.S.A.

National Radio Science Meeting
4-6 January 1989
Condensed Technical Program

Tuesday, 3 January

2000-2400
USNC-URSI Meeting — Broker Inn

Wednesday, 4 January

0835-1200
B-1 SCATTERING I — CR0-30

0855-1200
D-1 HIGH FREQUENCY DEVICES — CR0-36
F-1 EARTH AND OCEAN SENSING, AND TERRAIN EFFECTS — CR1-9
G-1 THE EARLY DAYS OF RADIOSCIENCE — CR2-28
A Commission G Memorial honoring the memory and celebrating the lives of Henry G. Booker, J.A. Ratcliffe, and Newbern Smith
J-1 VERY LONG BASELINE INTERFEROMETRY AND ASTRONOMY I — CR2-26

1335-1700
B-2 NUMERICAL METHODS — CR0-30
DB-1 MICROWAVE COMPONENTS — CR0-36
G-2 IONOSPHERIC EFFECTS ON RADAR AND SATELLITE SYSTEMS — CR2-6

1355-1535
J-2 VERY LONG BASELINE INTERFEROMETRY AND ASTROMETRY II — CR2-26

1355-1520
H-1 SPACEBORNE ELECTRODYNAMIC TETHERS AND THEIR EM EMISSIONS INTO NEAR-EARTH PLASMA — CR1-46

1355-1700
A-1 ANTENNA AND FIELD MEASUREMENTS — CR1-42
C-1 ANALYSIS OF UNEQUALLY SAMPLED EXPERIMENTAL DATA — CR1-40
F-2 RAIN, RADIOMETRY, AND RADAR MEASUREMENTS — CR1-9

1535-1700
J-3 INTERSTELLAR AND INTERPLANETARY SCATTERING — CR2-26

1555-1700
H-2 ACTIVE EXPERIMENTS WITH ELECTRON AND NEUTRAL BEAM INJECTION INTO SPACE — CR1-46

1700-1800
Commission B Business Meeting — CR0-30
Commission C Business Meeting — CR1-40
Commission G Business Meeting — CR2-6
Commission J Business Meeting — CR2-26

United States National Committee

INTERNATIONAL UNION OF RADIO SCIENCE

PROGRAM AND ABSTRACTS

National Radio Science Meeting
4-6 January 1989

Sponsored by USNC/URSI in cooperation
with IEEE groups and societies:

Antennas and Propagation
Circuits and Systems
Communications
Electromagnetic Compatibility
Geoscience Electronics
Information Theory
Instrumentation and Measurement
Microwave Theory and Techniques
Nuclear and Plasma Sciences
Quantum Electronics and Applications

Copy 8
97 + attachment
98 "
134-139
118
120 attachment
34

WAD to

NOTE:

Programs and Abstracts of the USNC/URSI Meetings are available from:

USNC/URSI
National Academy of Sciences
2101 Constitution Avenue, N.W.
Washington, DC 20418

at $2 for meetings prior to 1970, $3 for 1971-1975, and $5 for 1976-1989 meetings.

The full papers are not published in any collected format; requests for them should be addressed to the authors who may have them published on their own initiative. Please note that these meetings are national. They are not organized by the International Union, nor are the programs available from the International Secretariat.

MEMBERSHIP

United States National Committee
INTERNATIONAL UNION OF RADIO SCIENCE

Chairman:	Sidney A. Bowhill*
Vice Chairman:	Chalmers M. Butler*
Secretary:	David C. Chang*
Immediate Past Chairman:	Robert K. Crane*

Members Representing Societies, Groups, and Institutes:

American Geophysical Union	Dr. George W. Reed
American Astronomical Society	Dr. A. Richard Thompson
IEEE Antennas & Propagation Society	Dr. W. Ross Stone
IEEE Microwave Theory and Techniques Society	Dr. A. A. Oliner
IEEE Geophysics and Remote Sensing Society	Dr. Robert E. McIntosh

Members-at-Large:	Dr. Julius Goldhirsh
	Dr. James W. Mink
	Dr. Kenneth Davies
	Dr. Charles Rino
	Dr. Irene Peden
	Dr. Dave Hill

Liaison Representatives from Government Agencies:

National Telecommunications & Information Administration	Dr. Hans Liebe
National Science Foundation	Dr. Laura P. Bautz
Federal Communications Commission	Mr. William A. Daniel
Department of Defense	Mr. William J. Cook
Department of the Army	Mr. Earl J. Holliman
Department of the Air Force	Dr. Allan C. Schell

Chairmen of the USNC/URSI Commissions:	
Commission A	Dr. Edmund K. Miller
Commission B	Dr. Robert S. Elliott
Commission C	Dr. Aaron D. Wyner
Commission D	Dr. Tatsuo Itoh
Commission E	Dr. John R. Herman
Commission F	Dr. Calvin T. Swift
Commission G	Dr. Charles M. Rush
Commission H	Dr. Mario Grossi
Commission J	Dr. J. Richard Fisher

Officers of URSI resident in the United States: (including Honorary Presidents)	
Honorary President	Prof. Henry G. Booker**
Chairmen and Vice Chairmen of Commissions of URSI resident in the United States:	
Chairman of Commission B	Prof. Thomas B.A. Senior
Chairman of Commission F	Dr. Robert K. Crane
Foreign Secretary of the U.S. National Academy of Sciences	Dr. William E. Gordon
Chairman, National Research Council, Commission on Physical Sciences, Mathematics, and Resources	Dr. Norman Hackerman
Chairman, National Research Council, Board on Physics and Astronomy	Prof. Norman F. Ramsey
Honorary Members	Dr. Harold H. Beverage Dr. Ernst Weber
NRC Staff Director	Mr. Donald C. Shapero
NRC Program Officer	Dr. Robert L. Riemer
NRC Administrative Associate	Ms. Susan M. Wyatt

* Member of USNC/URSI Executive Committee
** Deceased, 1 November 1988

DESCRIPTION OF THE INTERNATIONAL UNION OF RADIO SCIENCE

The International Union of Radio Science is one of 18 world scientific unions organized under the International Council of Scientific Unions (ICSU). It is commonly designated as URSI (from its French name, Union Radio Scientifique Internationale). Its aims are (1) to promote the scientific study of radio communications, (2) to aid and organize radio research requiring cooperation on an international scale and to encourage the discussion and publication of the results, (3) to facilitate agreement upon common methods of measurement and the standardization of measuring instruments, and (4) to stimulate and to coordinate studies of the scientific aspects of telecommunications using electromagnetic waves, guided and unguided. The International Union itself is an organizational framework to aid in promoting these objectives. The actual technical work is largely done by the National Committee in the various countries.

The officers of the International Union are:

President:	Prof. A.L. Cullen (U.K.)
Past President:	Dr. A.P. Mitra (India)
Vice Presidents:	Dr. Ing. H.J. Albrecht (F.R.G.) R.L. Dowden (New Zealand) E.D. Jull (Canada) Prof. V. Zima (Czechoslovakia)
Secretary-General	J. Van Bladel (Belgium)
Honorary Presidents:	G. Beynon (U.K.) W. Dieminger (West Germany) W. Christiansen (Australia)

The Secretary-General's office and the headquarters of the organization are located at Avenue Albert Lancaster, 32, B-1180 Brussels, Belgium. The Union is supported by contributions (dues) from 38 member countries. Additional funds for symposia and other scientific activities of the Union are provided by ICSU from contributions received for this purpose from UNESCO.

The International Union, as of the XXth General Assembly held in Washington, DC in August 1981, has nine bodies called Commissions for centralizing studies in the principal technical fields.

Every three years the International Union holds a meeting called the General Assembly. The next is the XXIIIrd, to be held in 1990. The Secretariat prepares and distributes the Proceedings of the General Assemblies. The International Union arranges international symposia on specific subjects pertaining to the work of one or several Commissions and also cooperates with other Unions in international symposia on subjects of joint interest.

Radio is unique among the fields of scientific work in having a specific adaptability to large-scale international research programs, since many of the phenomena that must be studied are worldwide in extent and yet are in a measure subject to control by experimenters. Exploration of space and the extension of scientific observations to the space environment are dependent on radio for their research. One branch, radio astronomy, involves cosmic phenomena. URSI thus has a distinct field of usefulness in furnishing a meeting ground for the numerous workers in the manifold aspects of radio research; its meetings and committee activities furnish valuable means of promoting research through exchange of ideas.

Session B-1 0835-Weds. CR0-30
SCATTERING I
Chairman: Gary Brown, Virginia Polytechnic and State Univ.,
Blacksburg, VA 24061

B1-1
0840

Approximation Methods for Scattering From Rough Surfaces

John A. DeSanto
Center for Wave Phenomena
Department of Mathematics
Colorado School of Mines
Golden, Colorado 80401

Rigorous analytical methods in rough surface scattering lead to integral equations. In coordinate space these integral equations are written on the surface value of the field (Neumann, hard, TM boundary value problem), the surface value of the normal derivative of the field (Dirichlet, Soft, TE) or coupled equations on both (interface or penetrable surface or dielectric problem). An additional integration is necessary to find the scattered or transmitted field. In Fourier transform space the corresponding equations are on the scattering and/or transmission amplitudes with a direct interpretation as scattered or transmitted fields as a function of angle.

The integral equations express the full multiple scattering solution and this must be treated numerically. Truncation of the equtions can lead to analytical results for single scattering (which is well known) and for double scattering. We describe here the approximations necessary to analytically evaluate to closed form the double scattering term. Specifically for plane wave incidence on a Gaussian distributed rough surface with a Gaussian correlation function we analytically evaluate the mean incoherent intensity representing double scattering.

B1-2
0900

BACKSCATTERING ENHANCEMENT BY RANDOMLY DISTRIBUTED VERY LARGE PARTICLES

Yasuo Kuga
Department of Electrical Engineering and Computer Science
The University of Michigan
Ann Arbor, Michigan 48109

Akira Ishimaru
Department of Electrical Engineering
University of Washington
Seattle, Washington 98195

Recently, the backscattering enhancement by densely distributed particles of a size comparable to the wavelength was reported. It has been explained as the constructive interference of the two waves traveling in opposite directions. This enhancement was observed only in densely distributed particles, and its existence in sparsely distributed media has not been verified yet. In this paper we present the experimental evidence of the backscattering enhancement by sparsely distributed very large particles. Experiments are conducted using 45-mm latex particles which are approximately 100 times the wavelength. Both co- and cross-polarized components are measured for different particle concentrations. Unlike for small particles, the backscattering enhancement is most noticeable when the particle concentration is low. The angular width of the peak is comparable to the ratio (wavelength)/(particle size) and is independent of the optical distance.

B1-3
0920

TWO-DIMENSIONAL ELECTROMAGNETIC SCATTERING BY A COMPOSITE ANISOTROPIC STRUCTURE

H. Massoudi, N.J. Damaskos
Damaskos, Inc., P. O. Box 469,
Concordville, PA 19331

The two-dimensional (2D) problem of electromagnetic (EM) scattering by a composite anisotropic cylindrical structure, with arbitrary cross section, is treated in this paper. The scatterer consist of a collection of infinitely long cylinders which are made of perfectly electric conductors, of anisotropic lossy and inhomogeneous media, and of anisotropic impedance sheets. The impressed fields are either the EM fields of a normally incident plane wave or those of an electric or a magnetic line source located parallel to the axis of the cylinder.

The problem is formulated as a set of coupled integral equations with induced electric and magnetic currents as unknowns. Method of moments, Galerkin's method with pulse basis functions, and extended operators, are utilized to transfer the coupled integral equations into a set of linear equations for the unknown secondary sources. The secondary sources are solved for via matrix inversion and then the far-field data are calculated for the 2D problem.

Curves showing the bistatic and monostatic scattering cross-sections, for a variety of composite anisotropic geometries, are presented. For the case of plane wave irradiation two different polarizations are considered: E- and H-polarization. For some composite anisotropic structures with circular cross sections, the results obtained from our numerical code are compared with those of the exact series solutions (H. Massoudi, N.J. Damaskos, and P.L.E. Uslenghi, Electromagnetics, 8:71-83, 1988). Our numerical results are found to be quite accurate and convergent. Some numerical aspects of the scattering problem such as the optimum mathematical cell size and shape, matrix size, and criteria for converged solutions will also be discussed.

B1-4
0940

Numerical Simulation of Radar Doppler Spectra From Ocean Surfaces

Charles L. Rino, Thomas L. Crystal, and Alan K. Koide
Vista Research Inc.
100 View St. P.O. Box 998
Mountain View, Ca. 94042

Numerical simulations of backscatter from rough surfaces have been used to test the range of validity of theoretical results obtained by using perturbation theory, the Kirchoff approximation, full-wave methods, and composite theories. Essentially exact calculations from simulated random one-dimensional surfaces have been demonstrated by Fung and Cheng [JOSA-A, Vol. 2, No. 12, 1985] and by Thorsos [J. Acoust. Soc. Am, Vol. 83, No. 1, 1988] for EM scatter from perfectly conducting boundaries and acoustic scatter from pressure-release boundaries. These results, however, only consider the backscatter cross-section and its angular distribution for static surfaces. In this paper we report numerical simulations of Doppler spectra from simulated ocean surfaces.

The ocean surface is simulated by using the modified Peirson-Stacy model proposed by Donelan and Pierson [JGR, Vol 92, No. C5, 1987] with a time evolution imposed by the *linear-wave* dispersion relation. Simulations using meter wavelengths show the rapid evolution from simple Bragg scatter to highly nonlinear spectra with increasing wind speed. Because the Doppler simulations use phase as well as amplitude, they provide a more complete picture of the scatter characteristics –polarization sensitivity, grazing-angle dependence, etc.–and the sensitivity of the numerical methods used.

The results presented to date have used spatial-domain implementations of integrals containing the one-dimensional Green's function. Our method uses a direct implementation of DeSanto's [JOSA-A, Vol. 2, No. 12, 1985] spectral-domain formulation of the problem. The relative advantages and disadvantages of the different approaches will be discussed.

B1-5
1020

HYBRID RAY-MODE-(BOUNDARY ELEMENTS) METHOD FOR WAVE SCATTERING BY OBSTACLES IN LAYERED MEDIA

I-Tai Lu
Department of Electrical Engineering/Computer Science
Weber Research Institute
Polytechnic University, Farmingdale, NY 11735

Wave scattering by obstacles in layered media is studied by a new method which combines the hybrid ray-mode method and the boundary elements methods. The latter is used to formulate the scattering process and the former to provide the Green's function of the layered environment. Following standard procedures of the boundary elements method, we first formulate integral equations for field distributions along the boundaries of the obstacles. By expressing these unknown distributions in terms of appropriate basis functions, the integral equations are then reduced to algebraic equations which are solved numerically. In the integral equations, one needs to compute the Green's function of the layered environment for various arrangements of locations of source and receiver. None of these conventional approaches (rays, modes and spectral integration) to evaluate the Green's function is satisfactory for all possible arrangements. Only the newly developed hybrid ray-mode method is best suited for this purpose because it combines rays and modes self-consistently within a single framework and optimizes the advantage of each. Numerical implementation illustrates these aspects.

B1-6
1040

WAVE SCATTERING FROM ROUGH SURFACES USING THE "SHOOTING AND BOUNCING RAYS" (SBR) TECHNIQUE

Adel M. Marzougui and Steven J. Franke
Department of Electrical and Computer Engineering
University of Illinois
Urbana, IL 61801

The problem of wave scattering by rough surfaces has been studied extensively by scientists and engineers because of its wide applications in science and technology. In this talk a new approach to the rough surface scattering problem, namely, the "shooting and bouncing rays" (SBR) technique is presented. This method is based on geometric optics (GO) where a dense grid of geometric optics rays representing an incident plane wave is "shot" onto the surface through a flat aperture located directly above the surface and followed as the rays bounce between the irregularities of the surface and eventually return to the aperture. Then, in order to obtain the scattered field, the physical optics theory is used to integrate the aperture field. This approach requires the radius of curvature of the surface to be much greater than the wavelength (gently undulating surfaces), yet the effects of multiple scattering and shadowing are automatically included. Another advantage of this numerical technique is its straightforward implementation on the computer because of the fact that the incident wave is represented by a sum of rays that can be easily vectorized. Furthermore, this method can be extended to solving the problem of scattering by rough interfaces between two media, backscattering by curved surfaces and scattering of spherical and beam waves.

Some preliminary results are provided where the testing of the SBR technique is restricted to scattering of horizontally polarized electromagnetic plane waves from a perfectly conducting rough surfaces with sinusoidal profiles in one direction only (i.e. a scattering problem in two space dimension). The results are compared to those obtained using the Kirchhoff approximation method. The agreement of these results has proven the feasibility and the accuracy of this new technique.

B1-7
1100

THE SECOND-ORDER MULTIPLE SCATTERING THEORY FOR THE VECTOR RADIATIVE TRANSFER EQUATION

Yasuo Kuga
Department of Electrical Engineering and Computer Science
The University of Michigan
Ann Arbor, Michigan 48109

Akira Ishimaru and Qinglin Ma
Department of Electrical Engineering
University of Washington
Seattle, Washington 98195

Vector radiative transfer (RT) and first-order multiple scattering (FOMS) theories are often used for analyzing the depolarization effect by the random medium. However, the numerical solution for the RT theory is limited to moderate sized particles because of the numerical stability. In order to analyze the depolarization effect by large particles near the backscattering direction, we obtained the second-order multiple scattering (SOMS) theory for the vector radiative transfer theory. The derivation was based on the second-order solution of each Fourier component of the Stokes vector. The numerical results were compared with FOMS and RT theories. It was shown that the SOMS theory was most useful for large particles and near the backscattering direction. Experimental results for large spherical particles were compared with the SOMS theory. The second-order ladder term which was included in the SOMS theory was not sufficient to explain the sharp peak observed in the backscattering direction in the depolarized intensity. The peak appears to be caused by the backscattering enhancement effect.

B1-8
1120

BACKSCATTERING OF LIGHT FROM A RANDOMLY ROUGH GRATING

A. A. Maradudin and T. Michel
Department of Physics and
Institute for Surface and Interface Science
University of California
Irvine, CA 92717

With the use of Green's second integral theorem we obtain exact expressions for the scattered electromagnetic fields produced by p-polarized and s-polarized beams of finite width incident from the vacuum side onto a random grating whose grooves are perpendicular to the plane of incidence. The scattered field is expressed in terms of the values of the magnetic (electric) field and its normal derivative on the surface of the grating in the case of p- (s-) polarization. These two source functions satisfy a pair of coupled, inhomogeneous, integral equations, which are solved numerically by the method of moments for ~ 1000 realizations of the surface profile, each of which is generated numerically and is a stationary, Gaussian stochastic process. Strongly corrugated as well as weakly rough surfaces are studied. The differential reflection coefficients are averaged over these realizations of the surface profile, and the specular component is subtracted off. The resulting angular dependence of the diffuse component of the differential reflection coefficient in p-polarization displays a well-defined peak in the retroreflection direction in the case that the random grating is ruled on the planar surface of a lossy metal and of a perfect conductor, but not when it is ruled on the surface of a nearly transparent dielectric. Similar results are obtained in s-polarization for strongly corrugated surfaces. We have also calculated the diffuse component of the differential reflection coefficient in approximations that correspond to single-scattering and double-scattering of light from the surface of a perfect conductor in order to ascertain whether the peak in the backscattering direction is due to multiple scattering or can be reproduced by a single scattering theory, and whether the subsidiary maxima observed in scattering from a metal or perfect conductor at normal incidence can be obtained from a double-scattering approximation. Our results indicate that a single-scattering calculation does not produce a peak in the backscattering direction, while a double-scattering calculation yields both the backscattering enhancement and the subsidiary maxima.

B1-9
1140

UNIFORM HIGH-FREQUENCY SOLUTION TO SCATTERING FROM THE STRIP

Robert A. Shore and Arthur D. Yaghjian
Electromagnetics Directorate
Rome Air Development Center
Hanscom AFB, MA 01731

Integration of incremental diffraction coefficients (multiplied by the incident field) along the edges or boundaries of 3-D scatterers provides a convenient, efficient way to obtain the high-frequency diffracted fields for arbitrary angles of incidence and scattering. Recently, it has been shown that 3-D incremental diffraction coefficients can be found by direct substitution of the far fields of corresponding planar 2-D canonical scatterers (Shore and Yaghjian, IEEE AP-S Trans., 55-70, Jan. 1988). For example, one could obtain from a simple line integration the high-frequency scattered fields of an arbitrarily shaped flat plate for all angles of incidence and scattering, provided one could obtain a high-frequency solution to the 2-D canonical problem of scattering from the infinite strip that is valid for all angles of incidence and scattering. Although the infinite strip has an exact scattering solution in terms of an infinite summation of Mathieu functions or alternatively a double integral (Bowman, Senior, and Uslenghi, Electromagnetic and Acoustic Scattering by Simple Shapes, North-Holland 1969, Ch. 4), we have been unable to find in the literature a computationally efficient asymptotic high-frequency solution valid for all angles of incidence and scattering.

Therefore, the purpose of this paper is to present a uniformly valid high-frequency solution for 2-D scattering from the infinite strip. A uniform asymptotic solution for both normal and oblique incidence is derived by first integrating the exact non-uniform currents of the leading-edge half-plane over the strip, and then repeating this procedure for the trailing edge. The final expressions for the scattered fields involve Fresnel functions, but not integrals of Fresnel functions, and thus can be computed extremely fast. Numerical evaluation of this high-frequency solution to the strip shows excellent agreement with the exact solution over the entire range of incident and scattering angles. In particular, for grazing H-wave incidence the non-uniform scattered field reduces to the negative of the physical optic's scattered field, and thus the total scattered field vanishes, as it should, at grazing incidence.

Session D-1 0855-Weds. CR0-36
HIGH FREQUENCY DEVICES
Chairman: T. Itoh, Dept. of Electrical and Computer Engineering,
Univ. of Texas, Austin, TX 78912

D1-1
0900

VERTICAL AND LATERAL BALLISTIC DEVICES

Michael Shur
Department of Electrical Engineering
University of Minnesota,Minneapolis, MN 55455

In short semiconductor devices the velocity of charge carriers is enhanced because of ballistic (collisionless) transport. The electron velocity enhancement has been observed in conventional short-channel Field Effect Transistors, and the effective electron velocities well above peak velocities in bulk material have been reported for short-channel FETs. However, the direct observations of the ballistic transport have only been achieved in vertical devices (Hot Electron Transistors). In these devices, electrons are injected into the active region with large velocities, in contrast to conventional field-effect transistors where electron acceleration in the channel is gradual.

In this talk we discuss various approaches to the design of vertical and lateral ballistic devices. As an example of new vertical ballistic devices, we discuss a Double Base Hot Electron Transistor (DBHET) and Tunneling Emitter Bipolar Transistor (TEBT). In the DBHET, the first (doped and/or graded) base region acts as an "electron gun" accelerating electrons and as a "lens" providing a better focused ballistic electron beam that is injected into the second base where an input signal is applied. In the TEBT, the emitter and base region are separated by a thin barrier. A much smaller tunneling probability for holes then for electrons greatly improves the emitter injection efficiency. Another advantage is the focusing effect caused by the electron tunneling, similar to that previously reported for the Hot Electron Transistors.

As an example of a lateral ballistic device, we consider a field-effect transistor with a variable gate-voltage swing along the channel. This may be achieved either by varying the device threshold voltage in the lateral direction (from the source to the drain) or by using two or more "split" gates (a Split-gate FET), with adjacent gates separated by a very small distance. By choosing a larger gate-voltage swing near the gate, an electric field distribution along the channel is made more uniform. Even in conventional (collision-dominated) devices, a more uniform field distribution leads to a shorter transit time and to a larger device transconductance. The advantages should be especially pronounced in low-mobility high-velocity materials, such as diamond or silicon carbide. In the ballistic regime of operation, the velocity enhancement is even larger. This concept is illustrated by the results of the calculations based on a new charge-control model.

We conclude that the new device designs for vertical and lateral devices will allow us to realize the benefits of ballistic transport.

D1-2
0940

MILLIMETER/SUBMILLIMETER WAVE RECEIVER ELEMENTS

Robert J. Mattauch and Thomas W. Crowe
Semiconductor Device Laboratory
Department of Electrical Engineering
University of Virginia
Charlottesville, VA 22901

The nonlinear element of choice for millimeter and submillimeter wave heterodyne receivers has been the Schottky barrier diode. Recently the SIS element has exhibited near quantum limited noise and conversion gain in the 100 GHz range. While this device offers great promise for application at frequencies as high as twice the gap frequency, the Schottky barrier device remains the principal heterodyne receiver element of the submillimeter wavelength region. Current research at the University of Virginia Semiconductor Device Laboratory on both Schottky barrier diodes and SIS elements will be reviewed.

Parameters of critical importance to the operation of heterodyne receiver elements are (a) maximum frequency of device operation, (b) conversion loss, and (c) noise temperature. The Schottky barrier diode has been shown to operate as a heterodyne element at frequencies in excess of 4 THz and is known to suffer no degradation of conversion loss upon cooling. A study of the dependence of mixer noise temperature on device parameters will be reviewed. Device design based upon conclusions of this study will be presented along with experiment results. Also presented will be recent experimental and theoretical results on a non-whisker contacted, mechanically robust Schottky barrier mixer diode having minimized parasitic element values.

Recent SIS element research on both Nb and Nb-PbBi structures will be reported upon for trilayer and edge junction configurations, respectively. Projected RF performance will also be discussed.

D1-3
1040

INTERVALLEY SCATTERING EFFECTS IN PHOTOCONDUCTIVE SWITCHES

S. Chamoun, R. Joshi and R.O. Grondin, Center for Solid State Electronics Research, Arizona State University, Tempe, AZ 85827

By using laser pulses whose duration is less than 0.1 ps. extremely fast photoconductive transients can be excited in gaps in microstrip-lines (D.H. Auston, *IEEE J. Quantum Electronics, QE-19,* 639, 1983;J.A. Valdmanis et al., *IEEE J. Quantum Electronics, QE-19,* 664, 1983; Meyer et al., *Appl. Phys. Lett.*, accepted for publication). Risetimes of significantly less than a picosecond can be obtained. These risetimes are the shortest obtainable by any switching technique and they are presently being employed in a variety of experimental settings. This risetime is not limited by the optical pulse length and in fact is several times longer than the pulse. The limiting factor is the transformation of the photogenerated carrier cloud from a state with zero average momentum to one which provides conduction current flow.

We have investigated this rise using Monte Carlo techniques. We find that there is an important qualitative difference between long and short excitation wavelengths (R.O. Grondin and M.-J. Kann, *Solid State Electronics, 31,* 567-570, 1988) which arises when electrons are photogenerated near the energy threshold for intervalley scattering. The initial 0.3 ps of the response then is dominated by negative velocity electrons produced a mechanism similar to the one noted in certain Gunn diode transients (D. Jones and H.D. Rees, *J. Phys. C., C6,* 1781, 1973). Here we will explain this affect and show how it produces a deay of 0.1 to 0.2 ps. in the onset of the rise of the photocurrent. The roles of bias, energy band structure and optical excitation level and wavelength in establishing limits to ultrafast photoconductive switching will be discussed.

D1-4
1100

MONTE CARLO STUDIES OF ELECTRONIC TRANSPORT IN COMPENSATED InP

Julio Costa and Michael Shur
Department of Electrical Engineering
University of Minnesota
Minneapolis, Minnesota 55455

Andrzej Peczalski
Systems & Research Center
Honeywell
Minneapolis, Minnesota 55418

Recently, there has been a strong interest in electronic devices which utilize InP as the bulk semiconductor. InP Gunn diodes capable of delivering 34 mW at 94 GHz, with a potential 3dB cuttoff of 200 GHz have been available commercially. Many of the devices currently built with GaAs such as MESFETs, MISFETs and HWMTs, as well as heterojunction bipolar structures have been successfully implemented in InP. With a direct energy gap of 1.42 eV, it also has been used successfully in opto-electronic devices, such as in a wide-bandwidth LED, laser diodes, and solar cells. Although many fabrication difficulties such as mechanical fragility, low chemical reactivity, and unreasonable wafer yields have yet to be tackled, indium phosphide is establishing itself as the material of choice for high-millimeter-wave frequency operation.

The Monte Carlo program used in this work is similar to the one used previously for GaAs by Xu and Shur (J. Xu, B. Bernhardt, and M. Shur, C.H. Chen, A. Peczalski, "Electron mobility and velocity in compensated GaAs," Appl. Phys. Lett., 49 (6), pp 342-3, 11 August 1986). It utilizes a standard Monte Carlo approach in the sense that it tracks the motion of one electron inside of an infinitely long semiconductor body, where it is subject to the accelerating force of the applied electrical field and many scattering mechanisms. The following scattering mechanisms are included in this calculation: a) impurity scattering; b) polar optical phonon scattering; c) acoustic phonon scattering; d) intervalley scattering between nonequivalent valleys; and e) intervalley scattering between equivalent valleys. For these calculations we simulated three electrons per value of the applied electric field, with each electron trajectory being followed for 500,000 scattering events. The drift velocity was then obtained by averaging the electron velocities throughout its trajectory. The simulations were performed using a Honeywell/NEC SX-2 Supercomputer and approximately 65 hours of CPU time were used. The SX-2 vectorization compiler capabilities and higher data throughput improved the code runtime by a factor of four over the Cray-2 supercomputer.

We present the results for the Monte Carlo calculations for the electron drift velocity versus applied electric electric field for the temperature range from 77°K to 400°K and degree of compensation from 0 to 0.9. We assumed an InP sample doped with $N_d=10^{16}cm^{-3}$ impurities. The InP curve presents a higher peak drift velocity and higher peak electric field than in GaAs. This implies that the low-field mobility regime persists for a much wider range of the applied electric field. Velocity saturation values and negative differential mobilities are comparable for both InP and GaAs. The electron drift mobility in InP is, as expected, affected similarly to GaAs with respect to temperature and compensation dependencies. We observed that the drift mobility in highly compensated InP was only weakly dependent on temperature, this value being somewhere between 2100 and 2250 cm^2/Vs. The mobility values obtained for InP in this simulation are smaller than those reported for GaAs. The negative differential mobility was defined as the largest negative derivative of the v(F) curve and the saturation velocity, was the minimum value of the drift velocity after the peak was reached. These parameters were found to be just weakly dependent on the degree of compensation Na/Nd; however, in a highly compensated material, the negative differential mobility regime is narrowed significantly, and the Gunn effect may not be easily observed. Simulation results reveal that the low-field mobility regime is expected to persist for higher values of electric field in InP than in GaAs due to a higher Γ-L energy valley separation. As a result, higher peak velocities and peak electric fields occur in InP. We investigate the dependency of the low-field electron drift mobility, peak drift velocity, threshold electrical field, saturation velocity and negative differential mobility on temperature and compensation ratio. We show that compensation in InP significantly reduces the electron peak velocity and low-field drift mobility. Empirical relationships will be presented which describe these quantities within reasonable accuracy.

D1-5
1120

ON THE POTENTIAL OF THE TRAVELING-WAVE INVERTED-GATE FIELD-EFFECT TRANSISTORS

T. Itoh* and S. El-Ghazaly**
* Dept. of Electrical and Computer Engineering
The University of Texas at Austin
Austin, Texas 78712
** Dept. of Electrical and Computer Engineering
Arizona State University
Tempe, Arizona 85287

Traveling-wave transistors are believed to provide a high power over a very wide frequency band. Moreover, in the mm-wave range, the electrodes of the conventional MESFET structure act as transmission lines, with different phase velocities. This phase velocity mismatch limits the device width to 0.1 wavelength. To remove this limitation, the Inverted-Gate FET, INGFET, which has a symmetrical electrode structure may be used in the traveling wave mode (S. El-Ghazaly *et al., IEEE Trans. Electron Devices, ED-35, no 7, 810-817, 1988).* We will present a complete analysis of the traveling-wave INGFET. Its potential to provide a high gain over a very wide bandwidth will be presented as well.

The D.C. characteristics of the INGFET is obtained using a two-dimensional computer simulation with energy dependent parameters. The passive transmission-line parameters are are obtained using a quasi-TEM wave mode. The conductor loss and the channel loss are taken into consideration as resistive elements in the transmission-line model. To obtain the characteristic equation, the passive and active aspects of the device are linked together using the coupled mode formulation. The resulting equations are solved for the possible modes and their propagation constants of this active transmission-line.

The results show that two modes can exist on this device. One mode is lossy and the other mode is gainful (i.e. its amplitude is increasing along the device width). The excitation of these modes depends on the device terminations as well as the feed arrangements. High gain was observed over a very wide bandwidth (about 30 GHz).

D1-6
1140

DISTRIBUTED MODEL FOR HIGH FREQUENCY ANALYSIS OF HIGH ELECTRON MOBILITY TRANSISTOR

D.H. Huang and H.C. Lin, Electrical Engineering Dept., Univ. of Maryland, College Park, MD 20742

This paper describes a lossy transmission line model for high frequency analysis of HEMT. The a.c. analysis is preceded with d.c. analysis to determine the resistance and transconductance of the incremental transistors. The d.c. analysis is conducted by using a more accurate empircal formula for velocity vs. electric field. The transmission line model for high frequency a.c. analysis is then introduced. Both d.c. and a.c. models agree with experimental data well.

F1-1
0900

AN INVESTIGATION OF WAVENUMBER FILTERING TO ENHANCE THE INTERPRETATION OF THREE-DIMENSIONAL MAGNETOTELLURIC DATA

R. Clark Robertson
The Bradley Department of Electrical Engineering
Virginia Polytechnic Institute and State University
Blacksburg, VA 24061

The magnetotelluric (MT) method is an electromagnetic sounding technique used in geophysical exploration that is based on the measurement of surface electric and magnetic fields. The presence of three-dimensional (3-D) conducting heterogeneities near the surface of the Earth obscures conducting regions buried deeper in the Earth and leads to interpretational errors. A procedure referred to as "wavenumber filtering" has the potential to dramatically reduce the undesirable effects of 3-D heterogeneities on the Z_{xy} and Z_{xx} components of the MT impedance tensor, where the x-axis is arbitrarily determined by the line of the MT survey. The Z_{yx} and Z_{yy} components of the MT impedance tensor are also improved to some extent by wavenumber filtering, but the amount of improvement depends on the location with respect to the anomalous region and does not, in general, result in a correct interpretation.

The wavenumber filtered elements of the MT impedance tensor are computed as

$$Z_{ij}^{f}(\omega,x) = \int_{-\infty}^{\infty} Z_{ij}(\omega, x')K(x - x')dx'$$

where K(x) is some low pass filter function in plane wave space. Hence, the wavenumber filtering process implies that the MT impedance at a given test site will be computed as a weighted average of the measured MT impedance at all test sites in the survey. In this paper, the effects of the shape of the filter function and the filter cutoff wavenumber on the wavenumber filtering process are examined in order to optimize the procedure. In addition, the manner in which the finite length of an actual MT survey affects the wavenumber filtering process is investigated so that the procedure can be more easily applied to actual MT data. The wavenumber filtering process is evaluated by comparing the filtered and the unfiltered apparent resistivities and the corresponding MT impedance phases derived from the MT impedance tensor for a particular 3-D model consisting of a heterogeneous region on the surface of an otherwise homogeneous earth.

F1-2
0920

Borehole Radar Clutter

R. Greenfield
Geosciences Department
The Pennsylvania State University
University Park, PA 16802

Borehole pulse radar operating around 30 M Hz is used to look for voids and tunnels in the earth, and can also be used to determine rock properties. Propagation paths are on the order of 25 m. The signal waveform and propagation characteristics in homogeneous material are fairly well understood. However in many places earth material is not homogeneous. Thus records contain clutter due to spatial variations of conductivity and dielectric constant in the subsurface. To look at these effects I model the earth as a complex series of layers. Planewaves with realistic waveforms are propagated through the layers to look at the level of scattered power levels with time, signal attenuation, and signal distortion. The propagation is done using layer transmission matrix methods in the frequency domain, then inverse transforming to give time domain records. This gives exact solutions. Layered models with a modest number of discrete layers, and models with random variation are examined. Random models are used which have a variety of different spatial wavenumber spectra.

F1-3
0940

GRAZING INCIDENCE MEASUREMENTS OF OCEAN WAVE SPECTRA USING THREE-FREQUENCY K_U- AND L-BAND RADARS

Dale L. Schuler
William J. Plant
William C. Keller
Wah P. Eng
Naval Research Laboratory
Washington, DC 20375-5000

Extensive experimental measurements using both L- and K_u-Band radars have been made from a pier-site located on the coast of the Atlantic Ocean at Duck, NC. These measurements provided a test for a new microwave technique designed to make directional measurements of ocean wave spectra. The theory for this new three-frequency scatterometer products a significant improvement in output signal quality and, ultimately, in the accuracy of directional measurements of ocean wave spectra. Measurements of wave height spectra for waves of wavelength λ in the range $7m \leq \lambda \leq 100m$ will be reported on. Measurements on shorter waves in the 1-10 meter regime are, however, feasible using this microwave technique. Such short wave measurements are hard to make with microwave systems and are important in (a) wave growth studies, (b) two-scale surface wave modulations, and (3) interactions of internal waves with the surface wave field.

Three separate measurement campaigns conducted during 1983, 1984, and 1988 will be reported. Ocean wave spectra compare favorably with non-directional in-situ Baylor gauge data obtained during all periods.

The theory that has been developed for this technique appears to be will founded and indicates that the measurement signal quality should equal, or exceed, that available from the short pulse measurement technique.

A multiplexed version of the basic three-frequency scatterometer has been shown to be a practical means of collecting data during acquisition times that are short enough so that naturally occurring dynamic, geophysical changes in the wave field may be studied.

F1-4
1000

SEA SURFACE SLOPES INFERRED FROM QUASI-SPECULAR SEA SCATTER DATA

Frederick C. Jackson
NASA Goddard Space Flight Center
Laboratory for Oceans/Code 671
Greenbelt, Maryland 20771

It is well known that geometrical optics (GO) provides a good approximate description of near-nadir microwave backscatter from the sea surface. However, on account of diffraction, care must be taken in the use of GO in the analysis and interpretation of actual scattering data. In particular, a distinction must be made between the slope pdf and mean square slope (mss) parameter that might be used, for example, to best fit experimental data and the slope pdf and mss that enter into a two-scale (2-S) composite surface scattering model. Further, it is important to know quantitatively the relationship between the two above interpretations of the pdf and mss, which we shall refer to as the 'gross fit GO' and '2-S' interpretations.

For near-vertical incidence, physical optics (PO) provides a paradigm of scattering from the sea surface, inasmuch as it can be shown in this case to subsume 2-S scattering theory as well as GO. Hence it may be used to address the above problem. To begin with, we assume a Gaussian, isotropic k^{-4} spectral-law sea surface and calculate the exact PO scattering integral for this case. The 'exact' result is then used (e.g., as 'data') to least squares fit (over an angular range $< 1.7 \times$ mss) both the GO and the 2-S model forms. The residuals are found to be $< 7\%$ for the gross fit GO case and $< 4\%$ for the 2-S model case, and the scale separation wavelength for the 2-S model fit is found to be approximately three electromagnetic wavelengths. Next, assuming the scale separation wavelength to be fixed, we calculate the 2-S model cross section for a wind-speed dependent model spectrum in order to determine the relationship between the gross fit GO and 2-S model mss parameters as a function of wind speed. The model calculations are found to agree well a consensus of Ku-band frequency sea-scatter data (these include some new observations reported here) as well as optically-inferred mss data. The agreement lends credibility to the model sea spectrum adopted for the present analysis and recommends its usefulness for large-angle sea scatter studies among other applications.

F1-5
1020

FULL-WAVE COPOLARIZED NONSPECULAR TRANSMISSION AND REFLECTION SCATTERING MATRIX ELEMENTS FOR ROUGH SURFACES

Ezekiel Bahar and M. A. Fitzwater
Department of Electrical Engineering
University of Nebraska-Lincoln
Lincoln, Nebraska 68588-0511

A 2 x 2 scattering matrix for rough surfaces that separate two different media is derived. To this end, explicit closed-form expressions for the nonspecular transmission scattering coefficients are derived for the rough-surface elements to complement previous derivations of the nonspecular reflection scattering coefficients. Both vertically and horizontally polarized electromagnetic excitations are considered here. Thus the elements of scattering matrices represent the polarization-dependent nonspecular transmission and reflection properties of each arbitrarily oriented and elevated element of the rough surface. The total nonspecularly transmitted and reflected fields are expressed as integrals (not integral equations). The full-wave solutions derived here are compared with the corresponding high-frequency physical-optics results, and the low-frequency perturbation results are also derived. They are shown to satisfy the reciprocity and duality relationships in electromagnetic theory, and they are invariant to coordinate transformations. These results may be applied to both deterministic and random rough surfaces.

F1-6
1040

AN EXAMINATION OF THE "FULL-WAVE" METHOD FOR ROUGH SURFACE SCATTERING: PART II

Eric I. Thorsos
Applied Physics Laboratory
University of Washington
1013 N.E. 40th Street
Seattle, WA 98105

Results were presented previously (National Radio Science Meeting, Boulder, Jan 5-8, 1988: Paper B/F1-1) for Bahar's full-wave approach to rough surface scattering. It was shown using Monte Carlo methods that when the surface heights and slopes become small, the full-wave prediction does not reduce to first-order perturbation theory results. Instead, the full-wave prediction agrees closely with the Kirchhoff solution. The case examined assumed the Dirichlet (zero field) boundary condition using one-dimensional surfaces with a Gaussian roughness spectrum. In this paper the full-wave method has been applied to the same case, but the average scattered intensity is found using a "formal average" rather than a Monte Carlo average. To obtain the formal average, the four-dimensional normal probability density is used to account fully for correlations between heights and slopes. It is found that the formally averaged full-wave predictions are completely consistent with the original Monte Carlo results. This work shows even more convincingly that the full-wave solution does not reduce to the first-order perturbation solution when the heights and slopes become small. [Work supported by ARO.]

F1-7
1100

AN EMPIRICAL MODEL FOR MILLIMETER-WAVE BACKSCATTER FROM SNOW-COVERED GROUND

Ram M. Narayanan
Department of Electrical Engineering
University of Nebraska-Lincoln
209N Walter Scott Engineering Center
Lincoln, NE 68588-0511

An empirical model is presented to predict the millimeter-wave co- and cross-polarized backscatter from multi-layered snow surfaces above bare ground. The backscatter coefficient, σ°, is assumed to be of the form:

$$\sigma^\circ = \frac{A \cos^B\theta \; 10^{-Cm_v}}{\sigma_s^D}$$

where θ is the angle of incidence, m_v is the "effective" volumetric moisture content in %, σ_s is the RMS surface roughness in mm, and A, B, C and D are empirically fitted parameters for each frequency and polarization combination. The "effective" volumetric moisture content is computed from the measured values in each individual layer weighted by a linear weighting function.

This model was applied to data gathered from a comprehensive set of snow backscatter measurements at 215 GHz (R. M. Narayanan, et al., Proc. IGARSS'88, paper WEA-7-11, Edinburgh, 1988) to obtain the following values for the A, B, C and D parameters in the above equation using least-squares fitting:

(a) Co-polarized (VV/HH) : A = 4.68, B = 3.22, C = 0.23, D = 1.50

(b) Cross-polarized (VH/HV) : A = 2.00, B = 3.45, C = 0.46, D = 2.00

The RMS error between the data and model-derived values was 3.0 dB for the co-polarized and 3.3 dB for the cross-polarized cases. The model is valid in the range $25^\circ \leq \theta \leq 85^\circ$, $0 \leq m_v \leq 1.5\%$ and 0.8 mm $\leq \sigma_s \leq$ 1.6 mm.

F1-8
1120

PROPAGATION OF CERTAIN DIGITAL MODULATIONS AT MICROWAVE FREQUENCIES IN THE PRESENCE OF TERRAIN MULTIPATH

E. J. Dutton
National Telecommunications and Information Administration
Institute for Telecommunication Sciences
325 Broadway
Boulder, CO 80303-3328

Three of the most commonly used digital modulation techniques with point-to-point terrestrial applications at microwave/millimeter wave frequencies are

1) 8-PSK
2) 16-QAM
and 3) 64-QAM.

These modulation types are increasingly sensitive to terrain multipath as the signal space becomes more dense.

Terrain multipath is modeled as two-ray multipath and treated as a form of interference in order to investigate the consequences on the bit-error-rate under such propagation conditions. There are various applications (e.g., mobile communications and military battlefield environments) where LOS propagation over terrain that causes terrain multipath is a distinct possibility. The effects of terrain multipath on digitally-modulated systems can be severe, because of the large spectral requirements of these high-data-rate systems.

F1-9
1140

SHORT RANGE PROPAGATION ABOVE L BAND – A QUASI CYLINDRICAL APPROXIMATION

Hung-Mou Lee (Code 62Lh)
Department of Electrical and Computer Engineering
Naval Postgraduate School, Monterey, California 93943-5100

The propagation of radio waves above 1 GHz in a spherically stratified atmosphere is considered. The receiving antenna height is assumed to be short compared to the radius of earth but may be large compared to the wavelength. The transmitting antenna is placed along the polar axis centered at the earth. If, in evaluating the fields at the receiving antenna, the contribution from outside the conical region $\theta = \theta_0$ can be neglected, and if the receiving antenna is located at a range such that $\theta_0 \ll 1$, then the expressions for the fields are greatly simplified. For frequencies above 1 GHz, it is reasonable to assume that θ_0 should lie beyond the optical horizon of the receiving antenna. With an earth radius a of 6368 km, a receiving antenna at a height of 40 m subtends a 0.2° angle to its horizon. If $\theta_0 = 0.01$ radian, the receiving antenna can be 40 km away. If θ_0 is relaxed to 0.05 radian, a range of a little over 295 km is allowed.

Observe that the distance between two points $\vec{r}$ and $\vec{r}'$ in the spherical coordinate can be written as:

$$|\vec{r} - \vec{r}'|^2 = (r - r')^2 + \frac{rr'}{a^2}[4a^2\sin^2(\frac{\theta - \theta'}{2}) + 4a^2\sin\theta\sin\theta'\sin^2(\frac{\phi - \phi'}{2})]$$

It is recognized that, on the right hand side of the equation, the expression in the bracket is the square of the projected distance between $\vec{r}$ and $\vec{r}'$ on earth. The metric on a cylindrical coordinate system can thus be adapted for this distance if $\theta, \theta' < \theta_0 \ll 1$. Specifically, $2a\sin|\frac{\theta - \theta'}{2}|$ is replaced with $|l - l'|$ and $a^2\sin\theta\sin\theta'$ is replaced with ll' where $l = 2a\sin\frac{\theta}{2}$ and $l' = 2a\sin\frac{\theta'}{2}$.

For a homogeneous atmosphere, by matching the EM boundary conditions exactly, contour integral representations for the field components can be derived without ever encountering the residue series (H. Bremmer, *Handbuch der Physik*, 16, 423-639, 1958). The singularities of the integrands are only branch cuts. There is no pole present. In the flat earth limit, these integrands reduce exactly to those of the Sommerfeld integrals. Note that the exact integrands could never have been recovered if the impedance boundary (Leontovich) conditions were applied in the derivation (H. Bremmer, *IRE Trans. AP*-6, 267-272, 1958; J. R. Wait, *J. Res. Nat. Bur. Stand.* 56, 237-244, 1956). Since this theory is formulated entirely in the spherical coordinate system, there is no need to 'flatten' out the propagation path of the ray through the use of the modified refractivity. The modified refractivity appears naturally as the branch points in the integrand of the field representations.

For a layered atmosphere, the poles of the integrands are determined by a combination of algebraic and exponential functions. They are much simpler than the Hankel or the Airy functions which appear in a more traditional approach that does not employ this short range approximation (G. B. Baumgartner Jr. et. al. *IEE Procedings, Pt. F*, 630-642 1983).

Session G-1 0855-Weds. CR2-28

THE EARLY DAYS OF RADIOSCIENCE

A Commission G Memorial Session honoring the memory and celebrating the lives of Henry G. Booker, J.A. Ratcliffe, and Newbern Smith

Chairman: E.K. Smith, Department of Electrical and Computer Engineering, University of Colorado, Boulder, CO 80309-0425

G1-1 0900 IONOSPHERIC RADIO BEFORE WW II: S. Gillmore

G1-2 0940 THE RADIO GROUP AT THE CAVENDISH LABORATORY: S.A. Bowhill

G1-3 1000 REFLECTIONS OF HENRY BOOKER: W.E. Gordon

G1-4 1040 THE RADIO SECTION AT NBS, IRPL, AND CRPL: W.F. Snyder

G1-5 1100 SHORTENING THE TIME BETWEEN INSPIRATION AND APPLICATION: ONE ENGINEERING SCHOOL'S EXPERIENCE WITH RADIOSCIENCE: O.G. Villard and R.A. Helliwell

G1-6 1120 RADIO PROPAGATION STUDIES AT CORNELL IN THE FORTIES AND FIFTIES: B. Nichols

G1-7 1140 SOME MEMORIES OF NEWBERN SMITH: R. Silberstein and J.V. Lincoln

Session J-1 0855-Weds. CR2-26
VERY LONG BASELINE INTERFEROMETRY AND ASTRONOMY I
Chairman: James M. Moran, Harvard-Smithsonian Center for Astrophysics,
60 Garden St., Cambridge, MA 02138

J1-1 0900 **OVERVIEW OF THE VLBA PROJECT**

P. J. Napier
National Radio Astronomy Observatory
Socorro, New Mexico, USA.

The Very Long Baseline Array (VLBA) radiotelescope, currently under construction and scheduled for completion in 1992, is a dedicated VLBI array to be used for very high resolution imaging of bright, compact sources. The principal classes of observations to be made with the VLBA include quasars and active galactic nuclei, maser sources, pulsars, active stellar objects, and astrometric and geodetic measurements. The ten 25m diameter antennas comprising the array are located from the Virgin Islands in the east to Hawaii in the west, providing baselines up to 8000 km. The antennas are equipped with receivers for nine bands over the frequency range 330 MHz to 43 GHz, with the antenna being designed for useful operation up to 86 GHz in the future. Data will be recorded on tape recorders having a maximum record rate of 256 Mbit/sec. Tapes will be processed on a twenty station correlator located in the Array Operations Center in Socorro.

The first of the ten sites, located at Pie Town, New Mexico, has been participating in VLBI observing sessions since early 1988. The current status of the project construction and testing will be reviewed.

J1-2
0920

THE VERY LONG BASELINE ARRAY CORRELATOR

Jonathan D. Romney
National Radio Astronomy Observatory
Edgemont Road
Charlottesville, Virginia 22903-2475

The Very Long Baseline Array (VLBA), currently under construction by the NRAO, will consist of ten new, dedicated VLBI antennas. It is designed as a multi-purpose instrument, supporting continuum, spectroscopic, astrometric/geodetic, multi-frequency, bandwidth synthesis, polarization, and pulsar measurements — with a variety of bandwidths, sampling rates, quantization schemes, and multi-band modes. Frequent joint observations will combine the Array with existing telescopes to produce global and/or extremely sensitive arrays. The VLBA correlator forms spatial coherence functions for all baseline pairs between these interferometer elements, and is intended to support routine processing of all observations involving the Array, in all operating modes. It will be by far the largest such system ever built for VLBI.

These requirements impose severe cost/performance constraints on design of the correlator. This challenge has been met by adopting an 'FX' or spectral-domain correlator architecture which achieves significant cost efficiencies and introduces a number of important technical advantages as well. This scheme differs from conventional lag correlation essentially in the sequence of operations performed to calculate baseline cross-power spectra from the input station samples. It exploits the efficient FFT algorithm, and organizes as much processing as possible on a station basis, to minimize the number of operations required. Despite the increased precision required for these operations a significant net economy is realized, for any large and/or high-resolution system. Accompanying advantages include superior performance for spectroscopic and pulsar observations, enhanced sensitivity, minimization of closure errors, and straightforward adaptability to unusual "stations" such as orbiting antennas.

The VLBA correlator will be a 20-station system, to accommodate extended-array observations, extreme wideband measurements using two recorders at each of 10 stations, or simultaneous correlation of two normal 10-station programs. Multiple baseband channels can be traded off in binary steps against spectral resolution, or other features such as interleaved or overlapped correlation and spectral interpolation; extremes range from 8 channels of continuum (low resolution) data, to a single channel resolved into 1024 spectral points.

A 7-station, 2-channel subset of the full correlator is planned to become operational by mid-1990, which will allow extensive testing of both the correlator and VLBA station equipment. This subsystem will then be moved to the new Array Operations Center in Socorro, NM, where it will be available for correlation (initially at twice real time or faster) of data from all VLBA stations then in operation, while being expanded to its final configuration.

J1-3
0940

THE VERY LONG BASELINE ARRAY (VLBA) TAPE RECORDER

H.F.Hinteregger
Haystack Observatory
Westford, MA 01886

The VLBA consists of 10 new 25-meter antennas with 8 in the continental U.S. plus one in Hawaii and one in St.Croix, Virgin Islands. The array forms a single aperture synthesis instrument by recording signals from radio stars on magnetic tape and subsequently processing them at a correlator in New Mexico. The new high performance recording system required by VLBA must be able to sustain an average data rate of 100 Mb/s continuously at each site with tape changes only once per day. The recording technology chosen for the VLBA is an upgraded version of the "narrow track" Mark IIIA recorder developed for the NASA Crustal Dynamics Project. The longitudinal Honeywell 96 drive is outfitted with a headstack consisting of 36 (32 user +4 system) heads which are 38 microns wide. The headstack is moved between successive tape passes to record a total of 512 user tracks in 16 passes. The VLBA spec (128 Mb/s at 78% duty) is just met at a longitudinal density of 39 Kfci with 13-micron (thin) tape on 14-inch reels and two recorders at each site.

The rapid evolution of digital tape recording technology applied to Very Long Baseline Interferometry (VLBI) is discussed: Volume density has increased 6400-fold since the days of 800 bpi computer tape; the capacity of a single 14(16) inch diameter reel of inch-wide 13-micron D1-equivalent tape has reached .69(.92) terabytes. The standard 14-inch reel now sustains a data transfer rate of 128 Mb/s for 12 hours at 50 Kfci (with 12.5% format overhead). Bit height (tape thickness) has gone from 40 to 13, width (trackwidth plus guardband) from 1400 to 43, length from 31 to 0.5 microns.

A further 64-fold increase in volume density is projected when ultrathin evaporated metal coated tape becomes commercially available; bit height should go to 2.2, width to 8, and length to 0.25 microns. A new base film with 3 times the tensile strength of polyester makes ultrathin tape practical. Reputedly fully engineered as an alternative for the 8mm camcorder application, the evaporated metal (EM) coating process yields the highest output and resolution of any tape yet developed and should make a 7.3 micron trackwidth and 100 Kfci (4 transitions/micron) safe. Sustained gigabyte/sec operation could be made practical and promises an 8-fold increase in VLBI sensitivity.

J1-4
1000

VLBI DATA PROCESSING IN AIPS

W. D. Cotton
NRAO
Edgemont Road
Charlottesville, VA 22901

There is now a nearly complete set of programs in the NRAO AIPS package for processing astronomical VLBI data from both Mk II and Mk III correlators. The data are kept in multisource files with calibration and editing information kept in auxillary tables. The software attempts to maintain the total geometric model applied to the data. The use of calibrator sources to determine amplitude, delay, rate, and bandpass calibration values is supported.

The general calibration functions available include: global fringe fitting, amplitude calibration, instrumental polarization calibration, correlator offset calibration, interactive and traditional editing, and self-calibration. Additional calibrations for spectroscopic observations include bandpass calibration from cross- or autocorrelations, phase referencing to a set of spectral channels, and diurnal Doppler corrections.

J1-5
1020

PHASE REFERENCED VLBI AND APPLICATION TO ALGOL

A.E. Niell
Haystack Observatory, MIT, Westford, MA 01451

Differences in the frequency systems, electronics, atmospheres, and ionospheres at the various elements of a VLBI network make it difficult to maintain phase coherence. Observations of one source can provide a reference phase for other (signal) sources if they are close enough on the sky that the spatially and temporally varying atmosphere and ionosphere, and the differentially changing frequency systems, do not introduce ambiguities in phase in the time between observations of the reference and signal sources. These requirements place limits on the angular separation between the reference and signal sources and on the duration of the scans of each. In addition the reference source must itself introduce no unpredictable phase variations as a function of time and/or baseline due to its structure; it must be unresolved or its structure must be known.

This technique has been applied to strong extragalactic sources by Bartel et al. (Nature 319, 733-738, 1986) to set limits on motion of the core of 3C345 relative to NRAO512. The sources were observed alternately, and detection of the source was required in every scan that was to be usable in order to make a map of each prior to phase-referencing (although NRAO512 was in fact unresolved).

A similar technique can be applied to objects which are too weak to be detected in the time allowed by the phase coherence requirements, provided the reference source is detectable. The (very) noisy amplitude and phase for each observation of the object are evaluated at the delay and rate extrapolated (or interpolated) from adjacent observations of the reference source. At a grid of "sky" points centered on the expected position of the object these complex visibilities of the weak source are coherently added over the duration of the experiment, producing a "dirty map".

We will illustrate the use of phase referencing for structure and astrometry as applied to the ternary stellar system Algol, observed at a flux density as low as 4 milli-Jansky, when the SNR for each scan was approximately 1. From these observations we are able to conclude that the radio emission is from the close binary component, and we resolve the ambiguity in the line of nodes of the ternary system.

J1-6
1040

WATER VAPOR RADIOMETRY: APPLICATIONS TO GEODETIC VERY LONG BASELINE INTERFEROMETRY

T.A.Herring
Harvard–Smithsonian Center for Astrophysics
60 Garden Street,
Cambridge, MA 02138.

The current limiting error source in geodetic applications of very–long–baseline interferometry (VLBI) is modeling the delays due the propagation of the radio signals through the Earth's atmosphere. For over a decade, water vapor radiometry (WVR) has been studied as a means for calibrating the propagation delays due to atmospheric water vapor which is thought to be the most difficult part of the propagation delay to calibrate. However, even now it is not clear that these instruments are able perform this calibration with sufficient accuracy to be useful in improving the precision of most geodetic VLBI experiments. When the elevation angle dependence of the water–vapor delays is known, these delays can be estimated from the VLBI data themselves. The use of stochastic estimation techniques in the analysis of VLBI data allows changes in the water–vapor delay during a (typically 24 hour) experiment to be estimated. Comparisons of these estimated delays with those obtained from simultaneously operating WVR's have yielded root–mean–square (RMS) differences as small as 3 mm in the zenith direction. These comparisons also show biases of typically 10 to 30 mm between the estimated and WVR–calibrated delays. Some part of these biases are thought to arise from errors in converting sky brightness temperatures to water–vapor delays, and the remainder from errors in modeling the delay due to the dry constituents in atmosphere. We will examine the data base of VLBI experiments for which WVR data is available, the likely origins of the biases discussed above, and we will assess the usefulness of WVR's for improving the precision of geodetic VLBI experiments. Currently, it appears that the most accurate radiometers available measure sky brightness temperatures with sufficient accuracy to be useful and that progress must now be made in the algorithms used to convert these temperatures to propagation delays, and in modeling the delays due to the dry constituents in the atmosphere.

J1-7
1100

ASTROMETRIC VLBI AT THE NAVAL OBSERVATORY

Kerry A. Kingham
U. S. Naval Observatory
Washington, D.C. 20392

In order to meet increasing demands by the Department of Defense for more accurate ties between celestial and terrestrial reference frames, the Naval Observatory has been developing an astrometric VLBI program. This began with participation in building and operating the Washington Mark IIIA VLBI Correlator Facility in cooperation with NGS, NASA, and NRL. The Naval Observatory is expanding its VLBI activities by conducting its own VLBI Earth Orientation observations and planning its own VLBI network for reference frame determination.

Since DoD requires a reliable, secure system with minimum delay between observation and results, this puts severe restrictions on possible network geometries. In order to gain experience with the limitations of these restrictions, the Naval Observatory has been conducting its own series of weekly Earth Orientation observations. These observations, using existing Mark III VLBI stations in networks which approximate possible geometries within mission restrictions, have been giving accuracies in the 1 to 2 milliarcsecond range.

As a result of this experience, plans are proceeding for the establishment of a Navy VLBI Network. Radio telescopes in West Virginia, Alaska, Florida, and Hawaii will form this network. Work on refurbishing two telescopes in West Virginia, one for the Green Bank site, the other to be moved to Florida is proceeding. Site selection for the telescope in Hawaii should be completed by September, 1989. An existing telescope in Alaska will be used. A new Navy Correlator which will be located alongside the existing Washington Correlator will be available for processing the observations of the new network. The planned network and logistical support system should allow routine daily UT1, weekly Earth Orientation, and monthly reference frame observations from this All-U.S. network with accuracies at the 0.5 milliarcsecond level, thus meeting Naval Observatory mission requirements.

J1-8
1120

VLBI IN THE NASA CRUSTAL DYNAMICS PROJECT: AN OVERVIEW

Tom Clark someone else and paper

Jim Ryan
NASA/Goddard Space Flight Center
Greenbelt, MD 20771

The NASA Crustal Dynamics Project (CDP) was established in 1979 to pursue the application of space techniques to the study of geophysics, principally plate tectonics. The techniques of very-long-baseline interferometry (VLBI) and satellite laser ranging were developed with equal vigor so that they could complement each other and by comparing results establish the validity of both. This paper will discuss the VLBI aspects of the CDP.

The Mark-III VLBI system was developed as a part of the CDP. Since 1979 the CDP and the National Geodetic Survey's IRIS program, which uses CDP-developed technology, have used the Mark-III system to carry out more than 700 observing sessions. More than 330,000 observations have been acquired with stations spanning the globe. Important results from CDP VLBI include confirmation of the opening of the Atlantic, and accurate measurement of the large scale motions along the San Andreas Fault, the motions of islands in the central Pacific, spreading of the Basin and Range, and the motions of sites in Alaska. The CDP has also developed an accurate catalog of 182 radio source positions.

17 mm/yr is movement level at OSO - this is a real movement in Atlantic plate region
46 mm/yr in pacific region
In CA motions are parallel to San Andreas fault
An area in Japan this summer started moving at 80 cm/yr. a big earthquake will happen.

J1-9
1140

VLBI OBSERVATIONS USING AN ANTENNA ON A TDRSS SATELLITE

R. P. Linfield
Jet Propulsion Laboratory
Mail Code 238-700
Pasadena, CA 91109

Very Long Baseline Interferometry (VLBI) observations have been successfully conducted using the combination of one antenna in earth orbit and antennas on the surface of the earth, in Japan (Usuda, Nobeyama, and Kashima) and Australia (Tidbinbilla). The antenna in earth orbit was of 4.9 m diameter, part of the Tracking and Data Relay Satellite System (TDRSS), in geosynchronous orbit over the east coast of Brazil. Observations were conducted in three sessions: July-Aug. 1986, Jan. 1987, and Feb.-Mar. 1988. Data were taken at 2.3 GHz during all three sessions, and at 15 GHz during the third session. The 4.9 m TDRSS antenna has receivers at only 2.3 and 15 GHz.

During the observations, local oscillator phase was transmitted from a frequency standard at White Sands, NM to the satellite. Intermediate frequency (IF) data were transmitted from the satellite to White Sands, where they were digitized and time tagged. Doppler and range measurements between the satellite and two widely separated ground transponders were processed into an accurate orbit ephemeris. This ephemeris was used to generate delay and phase models on the space-ground baselines, for use during data correlation on the Haystack Mk IIIA correlator.

Extragalactic radio sources were successfully detected on space-ground baselines at 2.3 GHz from all three sessions, and at 15 GHz from the third session. Brightness temperatures greater than 10^{12} K were measured for ten sources. This result, which could not be obtained with ground-based arrays, suggests that bulk relativistic motion occurs in these objects. The mean coherence at 2.3 GHz on space-ground baselines during the second session was 87% at 180 seconds and 78% at 360 seconds. Data reduction for the third session is in progress. Our results demonstrate the technical feasibility of space VLBI observations. Furthermore, it is clear that the resolution of space VLBI is necessary to measure the structure of many extragalactic radio sources.

14 MHz BW at 2.3 GHz, 88 MHz at 15 GHz

Session A-1 1355-Weds. CR1-42
ANTENNA AND FIELD MEASUREMENTS
Chairman: E.K. Miller, General Research Corp., Santa Barbara, CA

A1-1
1400

Theoretical and Experimental Data Comparison of the Radiating Near-Field of an Open-Ended Rectangular Waveguide

by

Doris I. Wu
Dept. of Electrical and Computer Engineering
University of Colorado
Boulder, CO 80309

Motohisa Kanda
Electromagnetic Fields Division
National Institute of Standards and Technology
Boulder, CO 80303

Abstract

A comparison between theoretical and experimental data on the radiating near-field of an open-ended waveguide (OEG) is presented. Two theoretical methods are examined. The first one is an approximation based on simple plane wave equations with the electric field expressed in terms of the gain of the OEG. The gain equation is an empirical equation obtained from scaled measured data. The second approach is based on far-field to near-field transformations. Its purpose is to provide an alternate method for computing the fields as well as to provide a means of assessing the accuracy of the first approach. Theoretical data computed using both methods are presented along with measured data obtained in the anechoic chamber. The discrepancy between the two theoretical approaches is typically less than 0.5 dB, while the discrepancy between the theoretical and experimental results varies slightly depending on the distance between the OEG and the field point.

A1-2
1420

NUMERICAL EM MODELING DATA REQUIREMENTS FOR INTERIOR EM COUPLING

K. S. Kunz and D. Steich
The Pennsylvania State University
Electrical Engineering Department
129 Electrical Engineering East Bldg.
University Park, PA 16802

A current, but little appreciated problem in numerical electromagnetic modeling of interior coupling is the very demanding data requirements associated with an accurate characterization of the coupling responses. The seemingly simple problem of a rectangular box (2.4 x 0.8 x 0.8 m) over a ground plane with a varying size aperture (0.8 x 0.4, 0.6 x 0.4 or 0.4 x 0.2 m) at the ground plane with a central wire running up from the ground plane to near the top of the enclosure clearly illustrates this. A physically important response characterization is the current flow at the base of the wire. This current response can be readily found at the wire base using the time domain finite difference technique (K. S. Kunz, et al., IEEE Trans. EMC 20, Parts I&II, 1978). Complete characterization of the response requires the resonance frequency, amplitude and width. Of special interest is the response at the lowest lying resonances where the energy flow across the aperture is most restrictive, leading to high Q resonances.

We have discovered that we must stay with a modest problem space size (32 x 16 x 16 cells) to encompass our object (28 x 16 x 16 cells) and still have the computer resources to go the one million time steps needed to accurately characterize the lowest lying resonance when a perfectly conducting enclosure is modeled. Truncation errors are extreme, unless such long run times are used, leading to severe errors in the amplitude and resonance width characterization and to the energy content of each resonance. The truncated time domain data can be used after filtering to select a single resonance to obtain time domain parameters, namely peak amplitude and decay rate, from which the frequency domain parameters can be inferred approximately. In this case somewhat less of a run length is required, on the order to 128k time steps.

Comparison of different run lengths shows the wide variations in the response parameters. Large amounts of computer time (100's of hours per VAX 8550 run) are required for the accurate characterization of the response. Great care must therefore be taken to insure that any numerical or experimental technique has accurately characterized such highly resonant responses with Q's in the thousands. If past experience is any indication, we have all greatly underestimated the difficulties with this seemingly simple problem.

A1-3
1440

An Iterative Technique to Correct Probe Position Errors in Planar Near-Field to Far-Field Transformations

by

Lorant A. Muth and Richard L. Lewis
Electromagnetic Fields Division
National Institute of Standards and Technology
Boulder, Colorado 80303

Abstract

We have developed a general theoretical procedure to take into account probe position errors when planar near-field data are transformed to the far field. If the probe position errors are known, we can represent the measured data as a Taylor series, whose terms contain the error function and the ideal spectrum of the antenna. Then we can solve for the ideal spectrum in terms of the measured data and the measured position errors by inverting the Taylor series. This is complicated by the fact that the derivatives of the ideal data are unknown; that is, they can only be approximated by the derivatives of the measured data. This introduces additional computational errors, which must be properly taken into account. We have shown, that the first few terms of the inversion can be easily obtained by simple approximation techniques, where the order of the approximation is easily specified. A more general solution can also be written by formulating the problem as an integral equation and using the method of successive approximations to obtain a general solution. An important criterion that emerges from the condition of convergence of the solution to the integral equation is that the total averaged position error must be less than some fraction of the sampling criterion for the antenna under test.

A1-4
1500

COUPLED ELECTRIC FIELD DISTRIBUTION OF LONG AXIALLY SLIT CYLINDERS WITH CONCENTRIC LOADING

D.C. Fromme, R.M. Sega, J.D. Norgard
Department of Electrical Engineering
University of Colorado
Colorado Springs, CO 80933-7150

The electromagnetic field structure within cylinders with axial slits can be accomplished with various theoretical methods. This paper extends previous work in experimental determination of these fields for various angles of incidence and slit widths, and includes concentric cylinders.

Recent developments in both theoretical and experimental methods for viewing cross-sectional electric fields in slit cylinders lend themselves to examination and subsequent comparison. Experimental techniques developed at the University of Colorado are based on infrared (IR) measurements of Joule heating induced when electromagnetic energy is absorbed by lossy dielectric materials. The surface temperature patterns correspond to the field intensities in the surface. An infrared scanning system detects the thermal radiation and the actual field strengths are empirically related to the surface temperature variations on a pixel by pixel basis. The detection screen material is of planar construction and thus provides a two-dimensional field mapping. By moving the screen along the axis of the cylinder the three dimensional field is obtained.

Comparisons are made between the theoretical and experimental approaches for various slit cylinder configurations for frequencies from 1 to 8 GHz. Internal measurements are presented for various aperture sizes, TE illumination angles, and the inclusion of concentric cylinders. The field intensity distributions, determined experimentally, are compared with contour maps of the electric field generated by a theoretical technique based on the generalized dual series solution.

A1-5
1540

USING A NETWORK ANALYZER TO MEASURE ANTENNA FACTOR AT A GROUND SCREEN FIELD SITE

R. L. Ehret, E. B. Larsen and D. G. Camell
National Institute of Standards and Technology
Electromagnetic Fields Division
Boulder, CO 80303

The present NIST technique of using a standard (calculable) dipole for calibrating antenna factor at frequencies from 25 to 1000 MHz is compared with a 3-antenna method using an automatic network analyzer. The proposed technique involves the measurement of insertion loss between transmitting and receiving antennas at a field site having a good 30 x 60 meter ground screen reflector. Antenna factor calibrations using an "open circuit" $\lambda/2$ dipole as a standard receiving antenna are compared with the 3-antenna insertion loss method. The latter approach would lead to faster measurements with greater repeatability and reduced uncertainty, especially at frequencies above 80 MHz.

A1-6
1600

ON THE USE OF PROBE ARRAYS FOR RAPID NEAR-FIELD MEASUREMENTS

by
B.J. Cown, C.E. Ryan, Jr. and J.P. Estrada
EMED/ECSL/GTRI
Georgia Institute of Technology
Atlanta, Georgia 30332 USA

J. Ch. Bolomey
Groupe D' Electromagnetisme
LSS-SUPELEC
Gif-Sur-Yvette, FRANCE

Measurement times associated with the conventional near-field techniques employing mechanical positioning of a single probe and/or the test antenna can become excessively long for electrically large targets or for sophisticated antennas-- telecommunication antennas, phased arrays, multi-beam antennas, reconfigurable antennas, -- especially those which have to be tested for several possible excitations or configurations. The long measurement times and cumbersome and expensive mechanical positioning assemblies associated with conventional near-field scanning are a serious impediment to the on-site testing of antennas installed on vehicles, aircraft, ships, or located at field sites.

This paper summarizes results of research and development efforts to significantly reduce near-field measurement time by utilizing arrays of electrically small probes in lieu of the single probe ordinarily used in conventional near-field measurements techniques. Results of numerical and experimental investigations show that the Modulated Scattering Technique (MST) employing arrays of hundreds of modulated scattering probes can be used to rapidly map the complex near-field of antennas or scatterers in a few seconds or minutes. The results also strongly indicate that classical receiving/transmitting arrays can be adapted for rapid near-field data collection and that MST or classical probe arrays can be used for rapid near-zone RCS data acquisition. Basic factors influencing the accuracy, speed, and cost of probe array measurement systems--element sensitivity and NF sample denisity, multiple interactions between the probe array and test antenna, interelement mutual coupling and probe correction, element dispersions, parasitic scattered signals--will be discussed in the light of available analytical, numerical and/or experimental results obtained at GTRI and SUPELEC.

GTRI tests

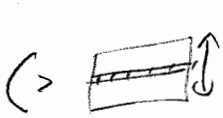

SUPELEC

Session B-2 1335-Weds. CR0-30
NUMERICAL METHODS
Chairman: Don Dudley, Electrical Engineering Dept., Univ. of Arizona, Tucson, AZ 85721

B2-1
1340

MULTIGRID METHODS FOR SOLVING THE HELMHOLTZ EQUATION

Bjorn Engquist*, Anne Greenbaum**, and William D. Murphy***

*Department of Mathematics
University of California
Los Angeles, CA 90024
(213) 825-4340

**Department of Computer Science
New York University
New York, NY 10012
(212) 998-3145

***Rockwell International Science Center
P.O. Box 1085
Thousand Oaks, CA 91360
(805) 373-4130

ABSTRACT

TM-wave scattering from a conducting two dimensional object is modeled by solving Helmholtz's equation with the standard far field radiation boundary condition replaced by a global far field boundary condition allowing it to be applied very near the scatterer surface. The discrete problem is solved by a multigrid procedure. That is, the equation is differenced on grids of several sizes, say, h, 2h, 4h,..., giving rise to a sequence of matrices $A \equiv A_0$ from the finest grid, A_1 from the next coarser grid, A_2 from a still coarser grid, and so on, down to A_C from the coarsest level grid. Each cycle of the multigrid algorithm loops over the different grid levels, performing relaxation steps on the finer grids and solving the linear system directly on the coarsest grid. Residuals are projected from fine to coarse grids, and solution vectors are interpolated from coarse to fine grids. This technique is compared with known solutions and more conventional approaches in regard to computational efficiency and accuracy.

B2-2
1400

FAST INTEGRAL EQUATION SOLVERS USING GENERALIZED CONJUGATE RESIDUAL TECHNIQUES

W. D. Murphy*, V. Rokhlin**, and M. S. Vassiliou*
(alphabetical)

* Rockwell International Science Center
P. O. Box 1085
Thousand Oaks, CA 91360

** Department of Computer Science
Yale University
New Haven CT 06520

ABSTRACT

While much progress has been made recently in the numerical solution of integral equations in electromagnetics, conventional integral equation solvers are often plagued with two problems: (1) The accuracy of the solution does not always increase as the number of points per wavelength is increased, and (2) Condition numbers in the matrices to be inverted can be large, leading among other things to slow convergence in iterative inversion methods.

We present a second-kind integral equation solver which addresses these problems. The method has been used to compute electromagnetic scattering from perfect electrical conductors of arbitrary closed geometry in two dimensions. It employs accurate, fourth-order-convergent quadrature formulas using endpoint corrections. The resulting discrete matrix has a condition number bounded by a constant as the sampling is refined. We use generalized conjugate residual techniques to solve the linear system of equations. Because of the low condition numbers, these methods converge extremely fast, and because of the accurate quadrature formulas the solution is of very high quality.

B2-3
1420

A NEW "EXACT" INVERSE SCATTERING/INVERSE SOURCE THEORY FOR THE DISCRETE CASE

W. Ross Stone
Stoneware Ltd.
1446 Vista Claridad
La Jolla, CA 92037

This paper presents a method for solving inverse scattering and inverse source problems. The method is "exact", in that no approximations regarding the characteristics of the source, scatterer, or scattering process are made, save possibly for a very weak restriction on the source frequency or time dependence. However, it is derived from the start, and inherently applies to, the discrete case: problems in which the scattering data is known only at discrete positions in space, in which the solution is sought only for discrete positions in space, and in which the data and solutions are discrete functions of frequency or time. The solution is derived by starting with an explicit, discrete representation of the source term in the wave equation in terms of a set of unknown complex coefficients. This source term and these coefficients may represent actual sources, equivalent sources containing the information about the scatterer and scattering process, or both. This discrete representation is substituted into the expression for the total fields (sum of scattered and incident fields, if any). A matrix equation relating the fields measured at discrete points in space (the scattering data) to the unknowns representing the source term is obtained. This explicit dependence on the data is significant, because it avoids calculating auxiliary functions used in other formulations which can cause problems.

This matrix equation (or series of three matrix equations in the vector case) has several very significant properties: (1) The knowns consist of the scattering data and a discrete representation of the *free space* Green's function; (2) solution of the matrix equation involves inverting a Toeplitz or block Toeplitz matrix; (3) the matrix equation to be solved is demonstrably nonsingular; (4) the solution is in terms of functions for which the numerical behavior is well understood, and for which the ill-conditioned behavior inherent in such inverse problems can be controlled; and (5) the formulation is such that the matrix to be inverted can be expressed so that it depends only on the geometry of the problem (and/or solution) space, and can therefore be inverted once and then used to solve all problems associated with the same geometry. Here, the "geometry" depends only on the points at which the data are recorded and the points at which the solution is sought. The use and implications of the approach are demonstrated and discussed.

B2-4
1440

APPLICATION OF THE FIELD-NETWORK ANALOGUE TECHNIQUE TO INTERIOR EM BOUNDARY VALUE PROBLEMS

Christof Pfeifer and Jovan Lebaric
Rose-Hulman Institute of Technology
5500 Wabash Av., Terre Haute, IN 47803

Numerical solutions of time and frequency responses for lossy, inhomogeneous, rotationally symmetric cavities have been obtained using field-network analogues first proposed by Kron (G. Kron, Proceedings I.R.E., 289-299, 1944). The cavities are represented, for TE and TM modes, by an equivalent planar network of lumped RLC elements whose voltages and currents correspond to cavity electric and magnetic fields.

The media properties (permittivity, permeability and losses) are accounted for by the choice of network elements and their values. The boundary conditions on the cavity surface and along the axis of symmetry are satisfied by appropriate network terminations.

Transient and frequency responses of the network are calculated using a standard circuit analysis program SPICE. Comparisons of numerical results and analytic solutions for cylindrical, homogeneous cavities show good agreement even for a moderate number of network elements.

B2-5 1500 ACCIDENTAL BUT EFFECTIVE CORRECTIONS DUE TO PREMATURE TRUNCATION OF CONJUGATE GRADIENT ITERATION

Francis X. Canning
Rockwell International Science Center
1049 Camino Dos Rios
Thousand Oaks, CA 91360

Recent work has clarified the connection between the conjugate gradient algorithm as used for electromagnetic scattering computations and the standard method of moments (meaning direct solution of the matrix equation). In particular, that work (S.L. Ray and A.F. Peterson, "Error and convergence in numerical implementations of the conjugate gradient method, I.E.E.E. Trans. AP," to have appeared) established that both techniques are based on the same matrix equation, so the only basic difference is in how that equation is solved. However, it would be erroneous to conclude that solutions using the conjugate gradient method cannot be more accurate than solutions using matrix inversion. To illustrate this, we consider a matrix equation containing an ill-conditioned but non-singular matrix. By augmenting that equation with a statement of its accuracy, we obtain a more physically correct solution than the exact mathematical solution.

The mathematical procedure mentioned above is compared to the conjugate gradient method. It is found that under general conditions, stopping the conjugate gradient iteration at a certain point (before convergence) has approximately the same effect as the "augmentation" mentioned above. This is different than the minimum norm property of the conjugate gradient method, which says that for a singular matrix if one starts the iteration from an appropriate trial solution, the fully converged result will be the minimum norm solution.

A conclusion of particular computational significance arises from considering the ill-conditioned problem that arises near resonant frequencies. We find that by halting the iteration before mathematical convergence is reached, one obtains a current that is approximately orthogonal to the nearly resonant mode. This will be true even though, due to approximations made in deriving the matrix equation, the mathematical solution to the matrix equation contains a large component of this nearly resonant mode. Finally, we show that one is likely to halt the iteration at the appropriate point, simply by accident. To summarize, near a resonance one is likely to find the physically correct answer from an inaccurate equation by accidentally terminating the conjugate gradient iteration before convergence. A similar correction is possible using direct methods, but does not occur by accident.

B2-6
1520

TRANSITION REGION CAUSTIC PROBLEMS AND SOLUTIONS FOR DUAL-SHAPED REFLECTOR ANTENNAS

Victor Galindo-Israel, Thavath Veruttipong,
Sembiam Rengarajan*, and William Imbriale

JPL, California Institute of Technology
Pasadena, CA 91109

*Cal State University, Northridge, CA 91330

The GTD diffraction analysis of dual-shaped reflectors that are synthesized for high gain and low spillover past the subreflector can lead to erroneous results. The errors are particularly significant for the fields computed in the vicinity of the edge of the main reflector. Thus the computation of spillover energy past the main reflector and the noise figure of the high-gain system can be very much in error.

The cause of the problem is a ring or ribbon caustic of the subreflector scattered field behind the edge of the main reflector. For subreflector edge illuminations of the order of -20 dB and high-gain main reflector aperture distributions, the geometrical optics (GO) rays scattered from the subreflector converge, rather than diverge, toward the main reflector edge. This problem was first studied for its effect upon far-field computations of subreflector scattering by Kildal, and then it was studied by Kildal to determine its effect upon errors in efficiency prediction. Finally, a study was made by Cwik to illustrate the difference between physical optics (PO) and GTD computations in the vicinity of the caustic in cylindrical geometries.

Not only does the GO field have a ring caustic near the main reflector edge, but so also does the Keller edge diffracted field and also the edge slope diffracted field have the same ring caustic. An analytic study of the ring caustic illustrates that the slope diffracted field has the strongest caustic singularity, while the Keller field and the GO field have weaker singularities at the caustic. Computational results from GTD and PO analysis of a 34-meter ground station dual-shaped reflector confirm the analytical formulations.

The principal utility of GTD in the analysis of large shaped subreflectors lies not in its accuracy but rather in its speed. Since the caustic is ring shaped, the stationary phase region on the subreflector is found to be elongated -- narrow in the ϕ-direction of subreflector integration and long in the θ-direction (r, θ, ϕ spherical coordinates). We thus find that a solution to the problem of obtaining both accurate and fast computations in the vicinity of the main reflector edge is to perform the subreflector scattering integral as a stationary phase evaluation in ϕ and as a PO integral in θ. The two-dimensional PO integral is thus reduced to a one-dimensional PO integral that is readily computed for even very large subreflectors.

This method of evaluation is found to be valid, accurate, and fast for near field computations as well as offset geometries. Note that no end point or edge diffraction computations are required for the θ-integral or for the ϕ-integral. A full GTD computation can and should be used for observation points far from the ring caustic. In the vicinity of the caustic, the PO or θ-integration can be made more rapid if appropriate use is made of the phase function behavior near the surface inflection region of the subreflector. For example, an asymptotic PO evaluation of the θ integral can be made away from the stationary phase region. GTD, PO, and $PO_\theta GO_\phi$ results have been obtained for both symmetric and offset geometries to illustrate the principles.

B2-7
1540

AN EFFICIENT NUMERICAL METHOD FOR THE MULTI-REGION VERTICALLY STRATIFIED MEDIA

Q. H. Liu and W. C. Chew
Electromagnetics Laboratory
Department of Electrical and Computer Engineering
University of Illinois
Urbana, IL 61801

The response of a source in the presence of a N-region, vertically stratified medium shown in the figure is an unsolved problem. The two-dimensional finite element method is not appropriate for this problem because of the infinite size of the scatterer. In this paper, the numerical mode matching method is used to solve this problem. By treating the fields propagating in the direction parallel to the subboundaries of the stratified media in terms of the propagators, and by introducing the concept of reflection operators, transmission operators, and generalized reflection operators, we reduce this two-dimensional problem into many one-dimensional problems which are solved by the one-dimensional finite element method. A formulation valid for a general N-region vertically stratified medium is derived, where the generalized reflection operators and the field amplitudes are found recursively. Because of the small sizes of the matrices involved, this formulation is very efficient for the numerical implementation compared to the two-dimensional finite element method. When there are only three regions, the comparison of the results with those in the literature (W. C. Chew, *IEEE Trans. Geosci. Remote Sensing*, vol. 26, 382–387, 1988) is very good. Some typical numerical results for $N > 3$ are also shown. This solution can be applied to many areas including geophysical prospecting, integrated optics, nondestructive testing, and biological sensing.

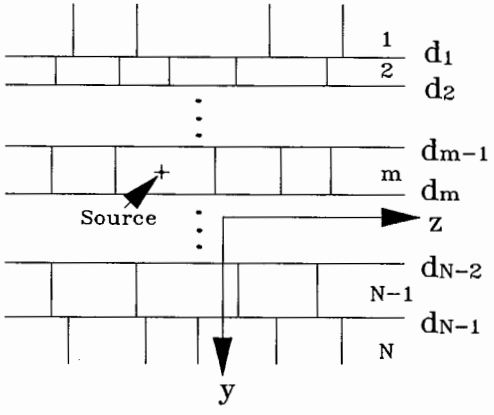

B2-8
1600

RESONANCES OF A CURVED STRIP

J. D. Kotulski
Sandia National Laboratories
Div 2322
Albuquerque, NM 87185–5800

The natural frequencies of a curved strip are obtained by using the relationship between the high–frequency expansions and the resonance condition on the object. The high–frequency expansions are associated with the GTD(Geometric Theory of Diffraction) as it is applied to the curved strip. The curved strip has contributions due to creeping waves and whispering gallery modes and by using a wavefront–resonance condition the natural frequencies can be determined. These are compared to the resonances obtained numerically from a moment–method formulation of the problem.

B2-9
1620

MATRIX SOLUTIONS TO RADIATION AND SCATTERING PROBLEMS USING THE HYPERCUBE PARALLEL PROCESSOR

Tom Cwik and Jean Patterson
Jet Propulsion Laboratory
California Institute of Technology
Pasadena, CA 91109

With the advent of concurrent processors, limits on the size of problems which may be efficiently solved numerically have increased. A program running concurrently can execute faster and have access to more memory than the same program running sequentially. The concurrent processor can allow aggregate execution times and total memory equaling the largest sequential supercomputer at a cost which is cheaper by an order of magnitude. Concurrent processing though will not achieve this performance for the general problem, but rather for those problems which can be adapted to the parallel nature of the computations. To explore the use of concurrent processing in electromagnetic applications, the JPL/Caltech Mark III Hypercube is used to solve method of moment (MoM) formulations of radiation and scattering problems. The processor consists of upwards of 128 nodes connected in a hypercube architecture. Each node contains a microprocessor and associated memory and is capable of communicating with all other nodes and a sequential host machine.

In this talk we will describe the parallel implementation of a MoM solution to scattering and radiation problems. Matrix elements are computed and distributed equally over the nodes to create uniform load balance. The matrix solution is also realized in parallel leading to high speedup and efficiency in the numerical solution. Furthermore, a stepwise solution to partitioned matrix problems (matrix Green's function solution) is developed--a method which can be a powerful tool in the design of complex structures. Capabilities on the order of 10,000 unknowns are being explored.

B2-10
1640

A NUMERICAL METHOD FOR THE SLANTINGLY STRATIFIED HALF-SPACE

Q. H. Liu and W. C. Chew
Electromagnetics Laboratory
Department of Electrical and Computer Engineering
University of Illinois
Urbana, IL 61801

The response of a source in the presence of a slantingly stratified half-space as shown in the figure is an unsolved problem. The two-dimensional finite element method is not appropriate for this problem. The numerical mode matching method cannot be applied to this problem because of the inherent hypothesis that the reflected waves propagate only in one direction. In this paper, we develop a surface integral equation method to solve the radiation problem of a line source in the presence of the slantingly stratified half-space shown in the figure. We first derive an extinction theorem for the stratified media, and then convert this theorem into surface integral equatons. In order to solve the surface integral equations to find the fields in the space, we find the approximate Green's functions for the stratified media by the eigenfunction expansion method instead of the conventional Fourier integral technique. The integral equations are then solved to find the surface unknown fields by a one-dimensional finite element method, which will economize on computer memory. After the unknown surface fields are found, we can find all the fields everywhere. This method is general for any slantingly stratified half-space with arbitrarily many layers in each region. For some special cases where the tilt angles are zero, the results obtained by this method agree very well with those obtained by the numerical mode matching method. When the two regions are homogeneous, the results can be compared with those for the Fourier integral technique. Excellent agreement has been observed between them. Numerical results for nonzero tilt angles, inhomogeneous media in both regions will be presented to demonstrate the use of this method.

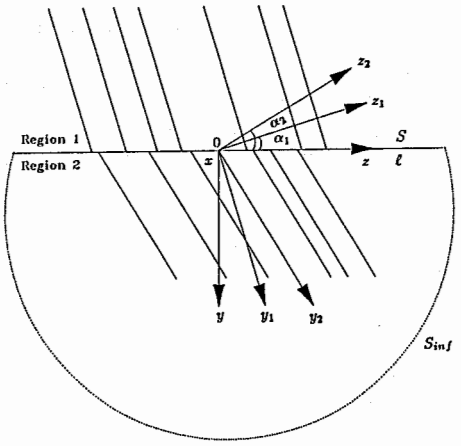

Session C-1 1355-Weds. CR1-40
ANALYSIS OF UNEQUALLY SAMPLED EXPERIMENTAL DATA
Chairman: Aaron D. Wyner, AT&T Bell Laboratories, Murray Hill, NJ 07974

C1-1 1400

Maximum Likelihood Estimation of Power Spectra from Unequally Sampled Data

Louis Scharf
Li Du

Electrical and Computer Engineering
University of Colorado
Boulder, CO 80309

Abstract. We develop a theory for computing maximum likelihood estimates of narrowband power spectra from unequally sampled data. The estimates are obtained by projecting the sample data onto a low rank subspace that describes the part of the unequally sampled data that lies in the narrow spectral band of interest, and then computing the power of that part. We present numerical results and discuss the delicate problem of selecting an appropriate order for the projection operator.

C1-2
1420

KERNEL SMOOTHING OF IRREGULARLY SPACED DATA AND ADDITIVE MODEL DECOMPOSITIONS

Trevor Hastie

AT&T Bell Laboratories, Murray Hill, N.J. 07974

The FFT provides an efficient method for computing a kernel smooth of regularly spaced time series data. I will describe an FFT based algorithm for irregularly spaced data, which also deals naturally with repeated observations.

I will also describe an additive model procedure for decomposing a series into a sum of components:

$$Y = f_1(X_1) + f_2(X_2) + \cdots + f_p(X_p) + error$$

Two scenarios come to mind:

1) Each of the X_i is *time* and the functions represent *trend* and different *seasonal components* (e.g., see Cleveland et al, 1988).

2) The variables X_i are explanatory variables measured jointly with Y.

The kernel smoother is used repeatedly to estimate all the functions in an iterative fashion.

C1-3
1520

INTERPOLATING TIME-SERIES FOR ESTIMATING SPECTRA

David J. Thomson
AT&T Bell Laboratories, Murray Hill, N.J. 07974

We study the interpolation of irregularly sampled time-series with the goal of estimating the spectrum and related functions from the equally-spaced interpolates. This approach is necessary because available non-parametric spectrum estimation procedures designed for irregular sampling become numerically unstable at moderate sample sizes. Thus, in contradistinction to standard smoothers in the literature which use a smoothness constraint, performance is measured by closeness of the Fourier transforms within the resulting Nyquist bandwidth.

Based on a band-limited L_2 norm our smoother uses the following steps: 1) We assume that the actual time samples are integer multiples of some basic epoch which we standardize to be 1 second. Choose a bandwidth $B < \frac{1}{2}$ and an equivalent integer resampling step $\Delta t = \lfloor 1/2B \rfloor$; 2) Choose a time interval T long enough so that all segments of the data contain at least $2BT$ distinct time points; 3) Compute a set of $K = 2BT$ discrete prolate spheroidal sequences $v_i^{(k)}(T, B)$; 4) Using a sequence of overlapped block positions, fit the data falling within the block to the prolate basis using a minimum-norm singular value decomposition; 5) Using the coefficients found in step 4, compute the interpolates at the output mesh points and average over block positions.
This framework easily incorporates handling of replicated observations, outlier rejection, optimum weighting of the expansion coefficients, as well as providing a variety of diagnostics.

We conclude with comparisons between this and conventional smoothers and interpolators using variations in ^{14}C abundance determined by differences from dendochronology as an example.

C1-4
1540

ANALYSIS OF UNEQUALLY SPACED EXTINCTION RATE DATA

Craig Lindberg,[1] Institute of Geophysics and Planetary Physics, Scripps Institution of Oceanography, University of California, San Diego, La Jolla, CA 92093; and David J. Thomson, AT&T Bell Labs, Murray Hill, NJ 07974
[1]Now at Mathematical Sciences Research Center, AT&T Bell Labs, Murray Hill, NJ 07974

A time series consisting of the number of species extinctions per unit time as a function of time has been compiled by David Raup and J. John Sepkoski, Jr. of the University of Chicago. This time series spans the last 277 million years of earth history and incorporates the extinction records of more than 22,000 separate species.

The time series is produced by examining samples of ocean bottom mud for the skeletons of tiny sea creatures. The sedimentation rate in the oceans has not been uniform with time, however, so it is not easy to produce equally spaced data. The time series consists of 51 unequally spaced data points.

Analysis of the extinction rate time series by various methods has led to controversy about the existence of periodic components in the data. We present the result of a multiple taper harmonic analysis to this very short, unequally-spaced noisy time series.

C1-5
1620

SPARSITY CONSTRAINED SIGNAL RECOVERY

Philip B. Stark, Dept. of Statistics, University of California, Berkeley, CA 94720

(Joint work with David L. Donoho.) Recovery of missing low frequency information is a problem in seismic petroleum prospecting. In some cases geological information indicates that the signal to be recovered is *sparse*: zero except on a set of small density. This may occur when drill cores or road cuts show the region to consist of sedimentary strata—the reflectivity sequence is then mostly zero, nonzero only at layer boundaries. We develop inequalities which imply that sparsity of the unknown signal allows stable reconstruction of the original wide band signal from low-cut filtered data containing noise.

Session DB-1 1335-Weds. CR0-36
MICROWAVE COMPONENTS
Chairman: K.C. Gupta, Dept. of Electrical and Computer Engineering,
Univ. of Colorado, Boulder, CO 80309-0425

DB1-1
1340

Progress in Microstrip-based Quasi-optical Circuits

Joel Birkeland and Tatsuo Itoh

Department of Electrical and Computer Engineering
The University of Texas at Austin
Austin, Texas 78712

Two major forces currently influencing the design of microwave systems are the push towards higher frequencies and the desire to incorporate low-cost planar components such as mixers, amplifiers, and oscillators instead of their waveguide counterparts. However, at high frequencies, componment interconnections which are compatible with planar structures, such as microstrip and coplanar waveguide, tend to exhibit high loss. An alternative to connecting circuits with transmission line is to integrate antennas along with the components and therefore make the connection through free space.

Several circuits of this type which use microstrip technology are demonstrated. The use of microstrip allows the entire circuit to be manufactured on a single plane and also allows the possibility of conformal circuits. The circuits described in this talk are not only useful at higher frequencies, but also have applications at frequencies below 10 GHz.

DB1-2
1420

ON THE COUPLING OF DIELECTRIC RESONATORS

BY
Xuan Tu and T.Bhattacharjee
Department of Electrical Engineering
New Jersey Institute of Technology
Martin Luther King Blvd.,
Newark, New Jersey 07102

The Dielectric Resonators made from low-loss, high permittivity dielectric material are very useful in miniaturization of high Q microwave circuits. Though the analysis of both the rectangular and the cylindrical dielectric resonators are widely available in existing literatures, the use of the dielectric resonators in practical circuits necessiates the knowledge of the coupling phenomenon between the resonator and the associated microwave circuits. Thus this needs to be investigated in more details.

Generally, the coupling coefficient can be evaluated by using Fourier analysis and from the knowledge of the stored energy and the electric field. Here, in this paper,a simplified method of calculating the coupling coefficient is presented. The assumption of the existence of a single mode in the resonance field has been considered in this paper.Also the elimination of the boundary matching requirements in the boundaries of the shaded regions, shown in the figure below , can be justified from the fact that the fields in the shaded regions of the structure are practically negligibly small. These assumptions are true in practical cases. Based on these assumptions, the theoretical expressions for potential functions in the different regions have been modified. When compared, the results from numerical evaluation with such simplifications show excellent agreement with the results without such simplification (Komatsu and Murakami, IEEE MTT,31,34-40,Jan.1983) and the experimental results. Also, the effects of the substrate thickness on the values of the coupling coefficients are evaluated and discussed.

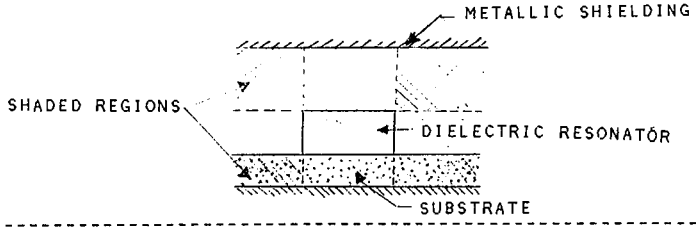

Commission B - Fields and Waves.

DB1-3
1440

ANALYSIS OF LONGITUDINAL/TRANSVERSE COUPLING SLOTS

Sembiam R. Rengarajan
Department of Electrical and Computer Engineering
California State University, Northridge
Northridge, CA 91330

Resonant slot couplers generally find applications in waveguide fed planar slot arrays to feed power from the main waveguide to crossed branch waveguides. A commonly employed coupling slot is longitudinal and offset from the broad wall center line in the main waveguide and centered transverse in the branch waveguide, as shown in the figure. This paper presents a rigorous analysis of the longitudinal/transverse coupling slot by formulating the pertinent integral equations, taking into account finite wall thickness. The integral equations are then solved for the aperture electric field. Coupling slot characteristics are then deduced including resonant length and dominant mode scattering in both waveguides. This coupling slot behaves nearly like a shunt element in the main guide, and as a series element in the branch guide. Since the shunt representation becomes poor under certain conditions, two definitions of resonance in the literature are investigated.

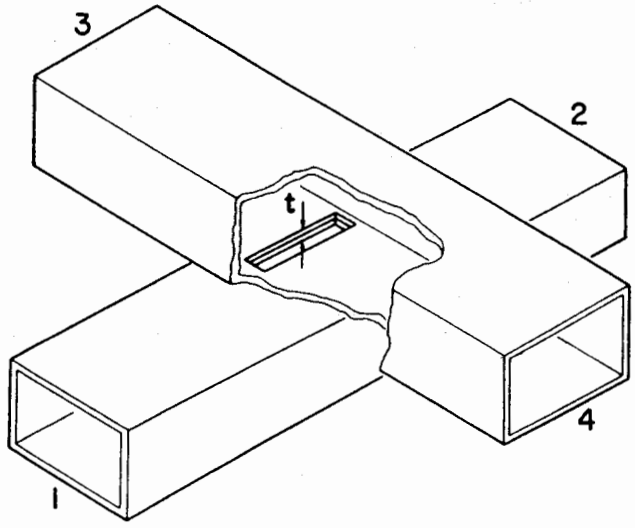

DB1-4
1500

POTENTIAL THEORY FOR MICROSTRIP DISCONTINUITIES

R.E. Collin and S. Toncich
Department of Electrical Engineering and
Applied Physics
Case Western Reserve University
Cleveland, OH 44106

A vector-scalar potential theory for analyzing microstrip discontinuities will be described. The method is a dynamic version of the charge reversal method introduced for calculating quasi-static capacitances of discontinuities.

This new method is computationally more efficient than Jansen's resonant cavity method and can be applied effectively to a variety of discontinuities.

Results for the open-circuit capacitance of a semi-infinite shielded microstrip line will be presented and compared with the results obtained with other methods. A discussion of the numerical convergence in terms of the number of basis functions used in the method of moments implementation of the theory will also be given.

DB1-5
1540

MULTIPLE - POST OBSTACLES IN RECTANGULAR WAVEGUIDE: THEORY AND EXPERIMENT

William P. Johnson
Microwave Filter Corp.
6743 Kinne St., Syracuse, NY 13057

A.T. Adams
Dept. of Electrical and Computer Engineering
Syracuse University, Syracuse, NY 13244

The cylindrical post in a rectangular waveguide is a classical scattering problem first treated during World War II by Julian Schwinger who used variational methods to obtain the equivalent circuit of the post obstacle. He used the zeroth and first order terms of a Fourier series expansion for the post currents. This limited the results to posts which were of moderate size and were distant from the walls and from each other.

Two different moment method techniques have been used to treat the post problem. The first is a multifilament current model with point - matching. The second is a full - domain exponential Fourier series current model with exponential weighting functions (a variational or Galerkin model). The computer results for the equivalent circuit of single - and triple - post configurations from the two dissimilar moment methods agree within a fraction of one percent. The data has also been extended to cover large and closely - spaced posts. Post and wall losses can also be treated.

Recently, experiments have been carried out to verify the computed results for the equivalent circuit elements of the single and triple - post configurations. Arrays of single - and triple - posts have been constructed and the filter center frequency has compared with theoretical results. Precise agreement is observed.

DB1-6
1600

A MICROSTRIP TO GUIDED WAVE TRANSITION

W. N. Klingensmith and J. M. Dunn
Department of ELectrical and Computer Engineering
University of Colorado
Boulder, CO 80309-0425

Future millimeter wave integrated circuits will rely on microstrip technology. However, for certain applications, there are disadvantages to microstrip elements, and these disadvantages become more pronounced at millimeter wave frequencies. In particular, microstrip antenna elements display a narrow bandwidth, and microstrip lines become very lossy. Dielectric wave guiding structures do not share these same problems.

A structure is being studied which may provide a practical transition from microstrip lines to dielectric waveguides. The transition consists of a scattering grid lying at the end of a terminated microstrip line. A dielectric cover layer is placed on top of the microstrip. An incident quasi-TEM mode field underneath the microstrip is converted by the scattering grid to TM modes which are suitable for carrying power in the form of guided waves. The guided wave structure can later be terminated to form a broadband endfire antenna, or a high Q resonating structure.

The two-dimensional version of the transition is currently under study. A moment method solution for the currents on the scattering grid will allow the estimation of the guiding properties of the real device. The next step is the solution of the three dimentsional problem, which will provide a tool for the optimization of the design of the device.

air

DB1-7
1620

THE ELECTROMAGNETIC FIELD DISTRIBUTION WITHIN A MULTIPORT DISK RESONATOR

S.K. JUDAH and M.J. PAGE

Microwave Laboratory,
Department of Electronic Engineering,
University of Hull,
Cottingham Rd.,
Hull,
HU6 7RX
ENGLAND.

Abstract

In the analysis of multiport planar disk resonators it is assumed that the electromagnetic field distribution is identical to the electromagnetic field distribution within a single port edge fed magnetic wall disk resonator. This field variation is assumed as $\cos m\varphi$, m denoting the resonant mode and φ being the angular coordinate in the cylindrical coordinate system (T. Okoshi and T. Takeuchi, 'Planar 3-dB Hybrid Circuit', ECJ, Vol. 58-B, No. 8, 1975), (K.C. Gupta and M.D. Abouzahra, 'Analysis and Design of Four-Port and Five-Port Microstrip Disk Circuits', IEEE Trans MTT, Vol. 33, No. 12, Dec. 1985).

In practice this is not so and the presence of ports will cause the electromagnetic fields to differ from those within an edge fed single port disk resonator due to the fact that the magnetic field now has a non-zero angular component at the periphery of the disk resonator where the ports are connected. Taking this into account an analysis technique is developed which predicts the electromagnetic fields within a multiport disk resonator. The theoretical field predictions are in good agreement with the experimental results for a four-port 3 dB planar disk rat race junction. A knowledge of the electromagnetic fields allows the designer to perturb the fields using a novel technique involving the introduction of pins to the disk resonator in order to modify the fields and hence tailor the electrical characteristics of the device. Theoretical and experimental results for the perturbed fields using this technique will also be presented.

DB1-8
1640

Multiport Network Method for Evaluating Radiation from Discontinuities in Microstrip Circuits

Albert Sabban and K.C. Gupta
Department of Electrical and Computer Engineering
University of Colorado
Boulder, CO 80309-0425

Because of the open nature of the microstrip configuration, hybrid and monolithic microwave circuits suffer from radiation originating at various geometrical discontinuities in these circuits. Two consequences of this radiation phenomenon are: additional signal loss at microstrip discontinuities, and undesired interactions between different parts of the circuit due to spurious external couplings. These parasitic couplings are present even when the circuit is enclosed.

This paper presents a method of estimating radiation losses from microstrip discontinuities. This method can be extended for parasitic coupling calculations and is compatible with CAD approach.

The fields at the edges of a microstrip circuit or component are evaluated using two dimensional planar analysis. The edge voltage distributions are expressed as equivalent magnetic current sources. The total radiation is calculated as the vector sum of fields for individual magnetic current elements. Results have been obtained for radiation from bends, steps and T-junctions. This method can be used for calculating radiation from complicated discontinuity configurations also.

For a 90° bend in 50 Ω line on 10 mil thick substrate with ε_r=2.2 the radiated power at 30 GHz is -15 db below the incident power. This corresponds to a radiation loss of 0.14 dB. For a 10 Ω to 50 Ω step change in width, radiation loss at 10 GHz is 0.63 dB (for 1/32" thick substrate with $\varepsilon_r = 2.2$). For a T-junction 50 ohm line with 35.5 ohm branchline, the radiation loss at 12 GHz is 0.11 dB (again for substrate thickness 1/32" and $\varepsilon_r = 2.2$).

These results are in good agreement with results based on complex Poynting vector method [Lewin, Proc. IEE 1978; M. Abouzahra IEEE Trans. MTT, 1981].

F2-1
1400 CALIBRATION TRANSFER TARGET FOR A MICROWAVE RADIOMETRIC PROFILING SYSTEM

J.R. Jordan
Wave Propagation Laboratory, NOAA
325 Broadway, R/E/WP5
Boulder, CO 80303

Atmospheric temperature and humidity profiles, cloud liquid, precipitable water vapor, and pressure heights have been routinely inferred from ground-based microwave radiometer measurements at Stapleton Airport in Denver, Colorado, since 1981. Precipitable water vapor and cloud liquid are derived from channels at 20.6 and 31.65 GHz. These two channels are calibrated by the tipping-curve method. However, the atmospheric attenuation at the four frequencies used for sensing temperature (52.85, 53.85, 55.4, 58.8 GHz) is too large to allow calibration with tipping curves. Calibration factors for these channels are derived from National Weather Service radiosonde profiles and the radiative transfer equation. The technique provides the necessary calibrations but limits the locations of radiometric profilers to radiosonde launch sites, reducing the usefulness of an operational network. The Wave Propagation Laboratory constructed a temperature-controlled black-body target to test the feasibility of transferring the calibration factors from a radiometer located at a radiosonde launch site to another uncalibrated radiometer. Accuracy of the transferred calibration and construction details of the target will be discussed along with the possibility of extending the technique for generating absolute calibrations.

F2-2
1420

NUMERICAL MODELLING OF PASSIVE MICROWAVE O_2 OBSERVATIONS OVER PRECIPITATION

A.J. Gasiewski and D.H. Staelin
Research Laboratory of Electronics
Massachusetts Institute of Technology
Cambridge, Massachusetts 02139

The microwave scattering and emission properties of precipitation cells are investigated by comparing 118-GHz radiometric observations with a planar-stratified numerical radiative transfer model. Liquid and frozen hydrometeors are modelled as a spherical Marshall-Palmer and Sekhon-Srivastava distributed Mie-scattering polydispersions, respectively, with Henyey-Greenstein phase functions.

Comparisons are made between computed brightness temperatures based on weather radar observations of a convective precipitation cell couplet during COHMEX, 1986 and brightnesses observed coincidentally by the Millimeter-wave Temperature Sounder (MTS) scanning spectrometer aboard the NASA ER-2 high-altitude research aircraft. Agreement between observed and computed brightness perturbations is within ± 10 percent over the mature regions of the cell, although a mean ice particle size 1.5 times larger than the Sekhon-Srivastava distribution size is necessary for agreement over the anvil region.

The sensitivity of the 118-GHz channels to temperature at various levels in the troposphere is exhibited, in the presence of precipitation, through the perturbed temperature weighting functions. Calculations using the perturbed and clear-air weighting functions suggest transparent-channel cell top reflectivities of up to 50 percent in the convective core region and 6 percent in the anvil region.

This work was supported by NASA grant NAG 5-10.

Jan 1989 URSI

F2-3
1440

COMPARISON OF SIMULATED RAIN RATES FROM DISDROMETER DATA EMPLOYING POLARIMETRIC RADAR ALGORITHMS

N. Balakrishnan[1] and Dusan S. Zrnic'
NOAA, Environmental Research Laboratories
National Severe Storms Laboratory
1313 Halley Circle
Norman, OK 73069

Julius Goldhirsh and John Rowland
The Johns Hopkins University
Applied Physics Laboratory
Johns Hopkins Road
Laurel, MD 20707

Disdrometer data collected during three spring days, with moderate to heavy rain in the Norman, Oklahoma region are used with various polarimetric radar algorithms to simulate rain rates. It is assumed that available measurables are 1) reflectivity at horizontal polarization, Z_H, 2) differential reflectivity, Z_{DR} (ratio of horizontal to vertical reflectivity factors in dB), and 3) differential propagation constant, K_{DP}. The accuracies of the simulated rain rates from Z_H, Z_{DR}, and K_{DP} are evaluated and compared. A new algorithm that utilizes both reflectivity factor and differential propagation constant is also examined. In comparing the relative accuracies, the disdrometer derived rain rates are assumed to be the "truth" measurements.

Diameter 2" of distrometer
25 s sampling rate at 25 mm/hr
Samples on three days

$D_{max} = 2.5\, D_0$

Apparently they did not make any radar measurements, just simulated them.

" Serious bias in $R(Z_H, Z_{DR})$ may result from assumed D_{max} "

$R(Z_H)$ optimum for $R < 20$ mm/h
$R(Z_H, Z_{DR})$ 20 to 40
$R(K_{DP})$ 7 to 40

F2-4
1500

DROPSIZE DISTRIBUTIONS IN WATER CLOUDS FROM GROUND-BASED CLEAR-AIR-SENSING DOPPLER RADAR OBSERVATIONS

E.E. Gossard, Cooperative Institute for Research in the Environmental Sciences (CIRES), University of Colorado/NOAA, Boulder, CO 80309; and R.G. Strauch, NOAA/ERL/Wave Propagation Lab, Boulder, CO 80303

With the availability of Doppler clear-air radars for wind-height profiling the way is opened for their use in a variety of other applications. This paper uses knowledge of the clear-air Doppler spectrum from a zenith-pointing radar together with the measured water droplet Doppler vertical velocity spectrum to calculate spectra of drop number density through clouds of droplets having substantial fall velocity. The method has been applied by Japanese scientists to measure dropsize distributions of large precipitation particles from data acquired at the VHF, 7-m wavelength, MU radar facility and by Gossard to data from the 32 cm wavelength, WPL wind profiler at Denver. This report extends the method and describes procedures that allow spectral lines and details to be extracted from the radar data. Spectra measured with a 915 MHz, wind-profiling radar are used as examples and compared with the spectra that would have been obtained if the clear-air information were ignored. From the number density vs. dropsize distribution, the corresponding liquid water distribution can be calculated. Failure to take into account turbulence in the medium can result in large errors in number density and liquid water especially in the neighborhood of spectral lines and large gradients. The advantages and limitations of a radar remote sensing drop spectrometer are described.

F2-5
1540

COMPARISON OF C_n^2 MEASUREMENTS MADE WITH THE FLATLAND VHF RADAR WITH OTHER MEASUREMENT TECHNIQUES AND MODEL ESTIMATES

J.M. Warnock[1], J.H.Brown[2], W.L.Clark[1], F.D. Eaton[3], K.S. Gage[1], J.L. Green[1], J.R. Hines[3], E.A. Murphy[2], G.D. Nastrom[4], T.E. VanZandt[1]

An experimental campaign was conducted at the Flatland radar site (Champaign-Urbana, Illinois) in June 1988 to measure height profiles of the refractivity turbulence structure parameter C_n^2 and related turbulent parameters. Three different techniques were used to measure the height profiles of C_n^2. The 50 MHz pulse Doppler Flatland radar and a stellar scintillometer measured the profile remotely, and high resolution in situ measurements were obtained from over 20 thermosonde balloon flights. Model estimates have been calculated from the balloon data, and compared with these measurements. In addition, measurements were made of the transverse coherence length and of the isoplanatic angle; both these parameters depend on the integrated value of C_n^2 through the atmosphere. The Flatland site was chosen because it is located in very flat terrain far removed from mountains, so that orographic effects are minimized. These unique turbulent measurements made over simple topography by several techniques will be compared and contrasted with previous measurements made over rough terrain. The implications of these results on clear-air radar studies will be discussed.

[1] Aeronomy Laboratory, NOAA/ERL, Boulder, CO 80303.

[2] Air Force Geophysics Laboratory, Hanscom AFB, Bedford, MA 01731

[3] Atmospheric Science Laboratory, White Sands Missile Range, NM 88002

[4] Department of Earth Sciences, St. Cloud State University, St. Cloud, MN 56301

F2-6
1600

SIMULTANEOUS OBSERVATIONS OF THE TROPOSPHERE AND LOWER STRATOSPHERE BY THE FLATLAND AND URBANA RADARS -- INTIAL RESULTS

G. D. Dester[1], J. L. Green [2], G. R. Stitt[1], S. J. Franke[1] and C. H. Liu[1]

[1]Department of Electrical and Computer Engineering
University of Illinois at Urbana, Champaign
1406 W. Green St., Urbana, IL 61801

[2]Aeronomy Laboratory
National Oceanic and Atmospheric Administration
325 Broadway, Boulder, CO 80303

Simultaneous radar observations of the troposphere and lower stratosphere were carried out in August 1988, near Urbana, Illinois, using the Flatland radar and the Urbana radar. The two radar sites are both located in the vast plain area of Central Illinois, separated by approximately 30 kilometers. The geographical and observational configuration for the campaign is considered to be favorable for investigating mesoscale structures in the troposphere/stratosphere region. Some initial results from the campaign will be presented in this paper. Power and reflectivity profiles from the two radars will be compared to examine the horizontal variations of the echo producing structures. Radial velocities observed at the two sites will be studied in terms of special wave events as well as power spectra. In particular, a case of convective storm in the evening of August 18th will be investigated in detail using the data from the two radars.

F2-7
1620

RECENT RESULTS FROM THE FLATLAND RADAR

T.E. VanZandt[1], W.L.Clark[1], J.L. Green[1],
G.D. Nastrom[2], and J.M. Warnock[1]

The Flatland radar is located in very flat terrain near Champaign-Urbana, Illinois. From March 1987 until April 1988 it measured vertical velocities almost continuously every 2.5min with 750m height resolution.

At periods shorter than about six hours the frequency spectra of vertical velocity stratified by background wind speed agree very well with model Doppler-shifted spectra. This agreement shows that in this period range the observed vertical velocity fluctuations are almost entirely due to gravity waves. This result is in sharp contrast to spectra from radars located near rough terrain, where the spectra agree with model gravity wave spectra only when the wind is light.

At periods longer than about six hours the observed spectral density is comparable with that due to large-scale vertical motions. This suggests that clear-air Doppler radars located in flat terrain may be able to monitor large-scale vertical motions, which are critical for the formation of clouds and precipitation.

[1] Aeronomy Laboratory, NOAA/ERL, Boulder, CO 80303

[2] Department of Earth Sciences, St. Cloud State University, St. Cloud, MN 56301

Session G-2 1335-Weds. CR2-6
IONOSPHERIC EFFECTS ON RADAR AND SATELLITE SYSTEMS
Chairman: Dennis L. Knepp, Mission Research Corp.,
26382 Carmel Rancho Lane, Carmel, CA 93923

G2-1
1340

CHARACTERIZATION OF IONOSPHERIC IRREGULARITY ENVIRONMENT FOR PROPAGATION MODELING

Santimay Basu
Air Force Geophysics Laboratory (LIS)
Hanscom AFB, MA 01731
Sunanda Basu
Emmanuel College
400 The Fenway
Boston, MA 02115

An attempt is made to characterize the ionospheric density irregularity environment and irregularity motion at low and high latitudes for use in the modeling of radio and radar propagation through the ionosphere. In order to derive the above characterization, phase and amplitude scintillation data obtained from an analysis of VHF and UHF signals received from stationary, quasi-stationary, and orbiting satellites in the equatorial, auroral oval and polar cap regions have been used. In addition, satellite in-situ data providing information on plasma density and electric field fluctuations have been utilized. Typical examples of electron density irregularity spectra with their spatial and spectral anisotropies in each of these global regions are illustrated. The various forms of the electric field fluctuation spectra and their effect on radio wave propagation are also discussed.

G2-2
1400

PROPAGATION EFFECTS IN EXTENDED RANDOM MEDIA

L. J. Nickisch
Mission Research Corporation
26382 Carmel Rancho Lane
Carmel, California 93923

The mutual coherence function and its fourier transform, the scattering function (or generalized power spectrum) describe the effects of scatter by random irregularities in the propagation medium. Calculation of these functions is usually done in the parabolic approximation, valid for strong forward scatter. To obtain a tractable theoretical solution to the parabolic wave equation one usually assumes that the propagation medium can be approximated by a thin layer or phase screen.

It is shown that an analytic solution to the parabolic wave equation can be obtained which approximates an extended random medium. A phase screen/diffraction method (PDM) is used. The extended medium is collapsed to a number of thin screens with free space between, and an analytic expression for the two frequency - two position - two time mutual coherence function is obtained for an arbitrary number of screens. The electron density and plasma velocity of each screen remains arbitrary in this formulation, allowing the effects of these nonuniform profiles on the delay - doppler power spectra to be studied. The effect of the extended medium on the form of scattering function for typical HF link conditions is shown to be large. Polar data from the DNA HF Channel Probe is compared to the scattering functions obtained in PDM, and it is shown that nonuniform plasma velocity profiles can account for the many varied shapes observed.

G2-3
1420

IMPACT OF IONOSPHERIC SCINTILLATIONS ON SPACE-BASED SURVEILLANCE RADARS

Brian M. Lamb
Lester L. DeRaad, Jr.
R & D Associates
P.O. Box 9695
Marina del Rey, CA 90295

Displaced phase center antenna (DPCA) radar is one of the approaches for moving target detection from space. DPCA depends on precise phase control to achieve a high level of clutter rejection. Doppler processing is also performed, and also requires a high degree of phase coherence over the integration time. Such systems may experience significant performance degradation due to propagation effects in the presence of ionospheric disturbances. In this paper, an analytic model is used to calculate the performance degradation as a function of the strength of the ionospheric disturbances and the radar design parameters. Illustrative examples are also briefly discussed.

The usual three-phase-center DPCA configuration is described, together with an alternative configuration) that is less sensitive to propagation effects. A modified set of radar equations, including different DPCA configurations, anomalous propagation effects, and the various DPCA, delay filtering, and Doppler processing functions, are derived. It is shown that the clutter rejection depends, in general, on the specific DPCA configuration, the interpulse period, and the total round trip travel time; the latter two as measured relative to the pulse-to-pulse signal decorrelation time due to platform motion and propagation effects anomalies.

Degradation of cluter rejection as a function of signal decorrelation length is calculated for two candidate systems, and two alternate DPCA configurations for each candidate system. The first system is a high PRF system operating at L-band, while the second is a low PRF system operating at UHF. A brief discussion is also presented of the relationship between the signal decorrelation time (or length) and the perturbed environments that may be expected due both to nuclear effects and to ambient spread-F or auroral effects.

G2-4
1440

VHF RADAR SCINTILLATION EFFECTS ON ALTAIR

Dennis L. Knepp
Mission Research Corporation
26382 Carmel Rancho Lane
Carmel, California 93923

This paper summarizes some of the results of the Defense Nuclear Agency PEAK (Propagation Effects Assessment - Kwajalein) experiment that was conducted during August 1988 at Kwajalein Atoll, in the Marshall Islands. The principal objective of this experiment was to collect radar data from orbiting targets during severe ionospheric propagation disturbances. This data was collected using the ALTAIR VHF radar and is analyzed to determine the effect of the ambient equatorial ionosphere on radar performance.

Particular areas of interest include radar tracking performance during severe scintillation, the effects of ionospheric induced multipath on the received radar signal, and the effects of fast fading on radar coherent integration performance. Results showing the first radar measurements of frequency-selective scintillation will be presented. Measurements showing the relationship between the signal measured on simultaneous one-way and two-way propagation paths will also be shown.

G2-5
1520

DESCRIPTION AND REMOVAL OF IONOSPHERIC INDUCED PHASE ERRORS IN SYNTHETIC APERTURE RADAR IMAGERY

C. V. Jakowatz, Jr., W. D. Brown, P. H. Eichel
Sandia National Laboratories
Albuquerque, NM 87185

A formalism which relates the degradation of Synthetic Aperture Radar (SAR) performance to the characteristics of the spectrum of ionospheric–induced phase errors is presented. The dependence of the character of SAR performance degradation on spectral parameters is illustrated. Statistics of expected SEASAT performance degradation based on computer simulations are described as a function of ionospheric parameters. We further demonstrate the utility of a new SAR autofocus algorithm for removing phase errors of this type. This new algorithm has been shown to be effective in removing arbitrary low-frequency phase errors (not order–dependent) generated along the synthetic aperture. Several examples of actual SAR imagery degraded by simulated ionospheric phase errors will be presented along with the corresponding autofocused images.

G2-6
1540

SATELLITE RADAR IMAGING WITH IONOSPHERIC PROPAGATION EFFECTS

Morgan K. Grover
Brian M. Lamb
R & D Associates
P.O. Box 9695
Marina del Rey, CA 90295

Using computer simulations of space-based synthetic aperture radar one-dimensional (azimuth) and two-dimensional (azimuth-plus-range) imaging, we examine the effects of ionospheric propagation disturbances on satellite SAR performance. The computer simulations use statistical models for ionospheric refractive index structure and Fresnel-Kirchhoff scattering theory for the propagation effects.

The impacts of propagation effects on SAR imaging are characterized in terms of point images and point spread functions (PSFs), 2-D images of extended scenes, and modulation transfer functions. The propagation effects impacts are shown to be mainly a degradation of azimuth imaging, due to signal phase effects, and related to the ratio of synthetic aperture length to signal phase decorrelation length.

A variety of mitigation techniques are considered and evaluated. Principally addressed is the improvement of performance with increasing radar frequency. Also addressed are optimal choices of flight and viewing geometries to exploit geomagnetic anisotropies in the ionospheric structure. A more general mitigaton technique is also described and evaluated. In this case, multi-sub-look relative image displacements are used to estimate the second derivative of the local phase perturbation; and this estimate is then used to correct for propagation effects in the final imaging.

Additional discussion is given of the problem of constructing a real-time simulator for perturbing real SAR return signals to allow ambient environment testing and validation of propagation-effects-resistant designs. Several alternative simulator concepts are described.

G2-7
1600

AN ASSESSMENT OF IONOSPHERIC EFFECTS ON THE GPS USER

Paul S. Jorgensen
The Aerospace Corporation
P. O. Box 92957
Los Angeles, CA 90009

The single frequency, C/A code GPS user employs a rather simple analytic model of the ionospheric delay of the L1 GPS navigation signal. It is recognized that the model is an approximation and that its use will only partially remove ionospheric effects from the user's navigation solution.

In order to perform an assessment of the residual effects of the ionosphere on navigation accuracy, this paper turns the problem around and uses the ionosphere model in a way it was not originally intended. Let's assume the model represents truth and a hypothetical user does not attempt to correct for its effects. With this approach we have a means for obtaining various statistics of ionospheric effects on a world wide, 24-hour basis. The paper presents results for both horizontal and vertical navigation errors as well as time transfer errors. Time transfer results are given both for when time transfer is part of a three-dimensional navigation solution and for time transfer at a known location.

Some of the results presented in this paper might appear to be quite surprising. The user position errors are low relative to the magnitude of the ionospheric delays. Furthermore, the horizontal errors are only about 1/6 of the vertical. These low errors are at the expense of the time transfer part of the navigation solution. From a known location, time transfer errors are much lower for two reasons. There is no error amplification due to "geometric dilution of precision" and we can limit ourselves to using high elevation angle satellites.

G2-8
1620

ON THE ACCURACY IN CONVERTING MEASURED VALUES OF SLANT TEC TO EQUIVALENT VERTICAL TEC

John Stalker
Physics Research Division
Emmanuel College
Boston, MA 02115
John A. Klobuchar
Air Force Geophysics Laboratory
Hanscom AFB, MA 01731

While many observations of Total Electron Content, (TEC), of the earth's ionosphere have been made over the last three decades, little apparently has been done on studies of the accuracy of converting values of TEC, generally observed along an off-zenith direction, to equivalent vertical TEC_v. This problem is especially important in specifying TEC values from observations at one station, for another location, generally viewing in another direction.

Of course the largest differences between actual TEC_v and equivalent TEC_v occur where there are large geographic gradients observed as a function of elevation angle from a single measurement station. In our computations to determine errors in this conversion, we modeled a deep, narrow trough in ionization, along with an ionization enhancement such those found along the auroral boundary, (E. J. Weber, et. al., J. Geophys. Res., 90, 6497-6513, 1985). As expected, we found that, even at moderate elevation angles, narrow troughs or enhancements in ionization tended to be under-represented by the conversion from slant to equivalent TEC_v. For example, a trough having a one degree half width was underestimated in depth by 50% by TEC observations at 40^o elevation. At lower elevation angles, while the depth of a trough was greatly underestimated, its location, as determined from slant TEC measurements, was not significantly changed from the actual one. Wider troughs or enhancements in ionization, observed at moderate to low elevation angles, are more accurately represented in the conversion from slant measurements to TEC_v.

In the conversion from measured slant values to TEC_v, the choice of mean centroid height of the ionosphere is fairly important. For a model ionosphere in which a zero gradient was assumed, an error in the choice of mean height which differs from the actual one by only 50 km. can produce errors in TEC_v of 15% at elevation angles of 10^o. Similar errors in the conversion to TEC_v can occur when there is a gradient in the mean height of the ionosphere which is not taken into account.

Session H-1 1355-Weds. CR1-46
SPACEBORNE ELECTRODYNAMIC TETHERS AND THEIR EM EMISSIONS INTO NEAR-EARTH PLASMA
Chairman: Dr. Kenneth J. Harker, STAR Laboratory, Stanford Univ., Stanford, CA 94305

H1-1
1400

GENERATION OF CURRENTS AND FIELDS BY A CONDUCTING TETHER MOVING THROUGH A MAGNETOPLASMA

Denis J. Donohue, Kenneth J. Harker and Peter M. Banks
STAR Laboratory, Durand 202, Stanford University,
Stanford CA, 94305

The problem of interest is the generation of currents and associated fields produced by the motion of a long conducting tether in a magnetized plasma. An exact, self-consistent theory based on a surface integral equation formulation is being developed to determine the induced currents and fields satisfying the electromagnetic boundary conditions at the tether-plasma interface. The integral equation is based on the equivalence principle as applied to a moving conducting body excited by a source electric field, in this case the v x B magnetomotive force. The equation is solved using standard method of moments with point-matching techniques.

Included in the theory is a novel approach to formulating the 3-dimensional Green's function in an anisotropic medium using the 3-dimensional inverse Fourier transform of the k-space representation. Under certain approximations valid for the tether problem, the transform is reduced to a 1-dimensional numerical integration. A computer model is being developed to carry out this theoretical regimen. Current results from the model and its application to the shuttle electodynamic tether will be presented.

H1-2 PLASMA CONTACTOR CLOUDS: A COMPARISON OF THEORY AND EXPERIMENT

D.E. Hastings, Dept. of Aeronautics and Astronautics, Massachusetts Institute of Technology, Cambridge, MA 02139; and M.R. Oberhardt, Air Force Geophysics Lab, Hanscom AFB, MA 01731

The use of plasma contactors in space has been increasingly proposed as a means to probe or control spacecraft environments. A plasma contactor is a device acting as a plasma source that provides electrical contact between a space vehicle and the medium through which it travels. The contactor ensures electrical contact by providing a collection area in which ambient electrons may be collected and by providing a means to ionize neutral gas in the surrounding region.

There have been several theories developed to predict the behaviour of current collection through plasma contactor clouds. These theories offer markedly different predictions as to the current amplification properties of these clouds. The key features of each theory and the points of disagreement will be discussed. A new theory will be presented which takes into account the experimentally observed double layers and multi-temperature electron distribution function. This is done by treating the electrons as a fluid composed of two parts; a high temperature and a low temperature part.

The experimental data from contactor experiments at NASA Lewis, Colorado State University and from Frascati will be contrasted with the theory so as to highlight points of agreement and disagreement. The scaling of these results to space in light of the theoretical understanding will be discussed.

H1-3
1440

IONOSPHERIC WAVE PROPAGATION FROM AN ELECTRODYNAMIC TETHERED SATELLITE SYSTEM

R.D. Estes
Harvard-Smithsonian Center for Astrophysics
Cambridge, Massachusetts 02138

Previous studies of wave generation by a tethered system have considered an infinite, uniform cold-plasma medium. This new analysis takes into account vertical variations in the ion-neutral collision frequency and the Alfvén speed as well as the existence of the boundaries between the ionosphere and atmosphere and the Earth and atmosphere. In the model used, vacuum equations are taken to apply in the atmosphere, and the Earth has a complex dielectric constant. The model allows for arbitrary angles between the geomagnetic field lines and the horizontal plane. The Earth and the boundaries are flat. The tether lies along the vertical, and the orbital motion is perpendicular to the meridian plane. The initial incoming Alfvén wave packet is taken to be that generated by an electrodynamic tethered satellite system with a constant or slowly varying current in a uniform medium. This wave packet is reflected at the atmosphere and, in the case of a varying tether current, may be coupled to a fast magnetosonic wave, which is confined to the ionospheric wave guide. Through the use of Budden admittance matrices and boundary conditions at the ionosphere/atmosphere interface, it is possible to solve for the electromagnetic field components at the boundary by numerical integration, thus implying the solutions on the Earth's surface. Details of the numerical methods used and preliminary results will be presented.

H1-4
1500

SPACEBORNE TETHERS AS HIGH-POWER ORBITING RADIATORS OF E.M. WAVES FROM ULF TO VLF

Mario D. Grossi
Harvard-Smithsonian Center For Astrophysics
Cambridge, Massachusetts 02138

The first electrodynamic tether is expected to go into orbit on board a Shuttle flight in early 1991. A firm understanding of the related phenomenology and a reliable assessment of the potential of tethers for practical applications must wait for the conduct of at least this first experiment. However, application systems can be conceptually defined in some detail even prior to the 1991 flight, on the basis of a-priori models of the experiment results. By relying on the correctness of these models, we can state that a one-dimensional vertical electrodynamic tether has the potential of performing as a communication transmitter of practical relevance for special communications in the ULF band, at a frequency of about 1 Hz. A self-powered, drag-compensated configuration could generate a primary power of about 22 KW at 1 Hz, with tether length of 25 Km and tether current of 10 A. This tether, in a 500-to-1000 Km orbit, with an inclination 60^{o}, could be kept within a very limited mass constraint, about 3 Tons. The ohmic losses in the cable could be as low as 5 Kw, and the overall orbiting system, inclusive of solar cells for loss compensation and of chemical batteries in parallel to the cells , would have a mass less than 10 Tons. This mass could be reduced by a factor of two, should progress in high-temperature superconductivity be such that a superconducting tether become feasible. An orbiting antenna as described would make it possible to perform low-data-rate communications, using receivers with a bandwidth of 0.1 Hz.

Two-dimensional tethered structures in Earth orbit, although more complex and more costly, would broaden considerably the applicability of tether technology to E.M. communications. These structures (circles, ellipses, squares, reactangles, triangles, etc.) could function as spaceborne reticles (a sort of very large spider web) made of kevlar wires, capable of providing structural support to arrays of dipoles of unprecedented radiation intensity. For instance, a magnetically-stiffened array of rectangular shape, with dimensions 50 Km x 150 Km, could contain 1,000 loops (magnetic dipoles) and provide at ELF (75 Hz) a magnetic moment as large as 10^{11} $A \cdot m^2$, with a total mass less than 50 Tons. In the VLF band, 3 KHz to 30 KHz, two-dimensional tethered structures could support large arrays of elementary dipoles and make it possible to achieve a gain of 40 dB. Unquestionably, applications of spaceborne tethers to communications represent one of the most promising areas where to find practical uses of tether technology.

H2-1
1600

GROUND LEVEL SIGNAL STRENGTHS OF ELECTROMAGNETIC WAVES GENERATED BY PULSED ELECTRON BEAMS IN SPACE

K.J. Harker, T. Neubert, P.M. Banks, A.C. Fraser-Smith, and D.J. Donohue
Space, Telecommunications, and Radioscience Laboratory
Stanford University
Stanford, CA 94305

A theoretical study has been made of the signal strengths at ground level of waves generated by pulsed artificial electron beams in space. Typically such beams might be generated by pulsed electron guns aboard either a satellite or rocket.

The radiated energy is first calculated by a theory based on coherent spontaneous emission. The theory evaluates the electric and magnetic field strengths and power fluxes in the far field by applying asymptotic expansion techniques in the usual manner. With this information at hand, the power flowing out within a cone whose apex is located at the gun position is calculated. A three dimensional ray tracing code is then used to determine the intersection of this cone with the earth's surface. Finally, wave amplitudes at ground level are found by first assuming conservation of power within the cone, and then correcting for collisional loss.

Ground signal levels are calculated for typical conditions as a function of beam pitch angles and voltages. For short beams, the ground level signal strengths are relatively insensitive to the wave-particle resonance condition, but for longer beams the associated peaking of the signal level begins to be observed. Finally, these results are discussed in light of ambient noise levels to determine under which circumstances these ground signals could be detected.

H2-2
1620

PARAMETERS AFFECTING THE PRODUCTION OF NARROW-BAND RADIATION FROM PULSED ELECTRON BEAMS IN SPACE: SPACELAB-2 PAYLOAD BAY STUDIES

G. D. Reeves, P. M. Banks, T. Neubert,
K.J. Harker, D. A. Gurnett
STAR Laboratory, Durand 202, Stanford University,
Stanford CA, 94305

Active experiments in VLF wave stimulation by electron beam injection were conducted on the Spacelab-2 space shuttle mission. A 1 keV, 100 mA, square wave modulated electron beam was used to stimulate waves in the ionospheric plasma which were measured with a 0-30 kHz, high resolution wideband receiver. The results of the experiments conducted during the free flight of the plasma diagnostics package (PDP) have been reported in the literature. Here we present new results from investigations which took place with the PDP in the orbiter payload bay.

The PDP was located in the space shuttle's payload bay for the majority of the Spacelab-2 mission which allowed over 300 separate electron beam injection sequences to be performed. In addition, command controlled pulsing patterns (sequences of beam pulsings with particular frequencies and durations) allowed the investigation of specific parameters which affect the characteristics of electron beam generated waves in space plasmas.

Pulsed electron beams have been found to produce narrow-band radiation at harmonics of the beam pulsing frequency. Two important beam parameters which were found to affect the amplitude of that radiation were the pulsing frequency and the duty cycle (ratio of beam on time to pulse period). Measured amplitudes are compared to theory and theoretical predictions are presented for parameters which could not be isolated in the measurements.

H2-3
1640

NEUTRAL GAS EMISSIONS DURING AN ELECTRON BEAM MOTHER-DAUGHTER SOUNDING ROCKET EXPERIMENT

B.E. Gilchrist, P.M. Banks, T. Neubert, P.R. Williamson, N.B. Myers, W. J.
Raitt, S. Sasaki, R.I. Bush
STAR Laboratory, Durand 209, Stanford University, Stanford CA, 94305-4055

During the CHARGE-2 sounding rocket experiment of December, 1985, electron beams with energies of 1 keV and currents up to 40 mA were injected from a mother payload. A electrically tethered daughter payload was also propelled out to a distance of 426 m perpendicular to the Earth's magnetic field using a modified neutral gas rate control system (RCS). Substantial vehicle charging, representing approximately 50% of initial beam energy, was observed during many beam emissions. However, during RCS gas injections substantial enhancement to return current collection at the daughter was observed which reduced vehicle potential. This can be interpreted in terms of an electrical discharge in the region near the daughter payload, enhancing current collection from the ionosphere. Further, when a +450 V high voltage bias system was connected between the tether and mother electrical ground, concurrent with RCS and electron beam injections, the mother potential was observed to be driven negative. These results will be discussed and compared with attitude control system (ACS) neutral gas emissions on the electron beam mother platform.

J2-1
1340

WORLD ARRAY VLBI OBSERVATIONS OF M87

J. A. Biretta and M. J. Reid
Harvard-Smithsonian Center for Astrophysics
Cambridge, MA 02138

We present results of the 18 antenna "World Array" Very Long Baseline Interferometry experiment at 18 cm wavelength for the galaxy M87. This unprecedented number of antennas for a VLBI array yields an image with angular resolution 4 milliarcseconds, and a dynamic range exceeding 2000 to 1. Global fringe-fitting, careful editing, and special antenna and baseline self calibration techniques also contributed to the high dynamic range.

This image reveals complicated structures in the nuclear jet not seen before in VLBI images. These include limb-brightening, side-to-side oscillation, and transverse expansion of the jet. These phenomena are suggestive of hydrodynamic processes within the jet and at its surface. Comparison with previous VLBI maps of this source give strong evidence for motion of knots in the nuclear jet at $\beta = v/c \approx 0.3$. Constraints on the the flow speed and its orientation to the line of sight are mutually exclusive in the context of the standard beaming model. This suggests that motions of the knots at the parsec scale are slower than the flow of material in the jet, or that the jet is intrinsically one-sided and has only a mildly relativistic ($\beta \approx 0.3$) flow speed.

World Array results for other sources will be reviewed, and present and future prospects for large array VLBI will be discussed.

J2-2
1400

VLBI POLARIZATION MEASUREMENTS

D. C. Gabuzda
Department of Physics
Brandeis University
Waltham, MA 02254

The technical difficulties encountered in making linear polarization maps at milliarcsecond resolution will be reviewed. VLBI polarization calibration techniques will be described, and recent results presented. A wide range of sources have been mapped; individual VLBI components with polarized flux densities as low as 5–15 mJy have been detected, demonstrating that polarization VLBI can render useful information for sources with relatively low (as well as much higher) polarized flux densities.

VLBI polarization mapping provides a wealth of information not accessible through total intensity mapping alone. Information about the linear polarization structure on milliarcsecond scales is of great interest in itself; in addition, we have found that polarization information can in some cases allow a better determination of the total intensity structure.

J2-3
1420

VLBI OBSERVATIONS AT A WAVELENGTH OF 7 MM

Norbert Bartel
Harvard-Smithsonian Center for Astrophysics
60 Garden Street
Cambridge, MA 02138

A dozen radio sources have been observed with VLBI at a wavelength of 7 mm and with projected baselines with lengths up to $1.4 \times 10^9\lambda$. One of the sources, 3 C84 was imaged. We will discuss the results from three epochs of observations and outline plans for future 7-mm VLBI.

J2-4
1440

VLBI AT 100 GHZ

Melvyn Wright, Radio Astronomy Laboratory,
University of California, Berkeley, CA 94720

We have obtained 50 micro-arcsec resolution using global VLBI at 100 GHz; sufficient to resolve ly-scale structure in nearby quasars. Millimeter observations are required to probe the optically thick synchrotron components seen at longer wavelengths. Seven VLBI experiments have been conducted at 3mm since 1981. We used the MKIII VLBI system with 52 Mhz bandwidth. The techniques developed include simultaneous observations at 5 GHz to determine clock parameters, and phased array interferometer observations. With VLBI arrays of 6 or more telescopes we can use global fringe fitting and self-calibration techniques to obtain hybrid maps with dynamic range of 100:1, sufficient to reliably trace the change in source structure from epoch to epoch. The results on 3C84, associated with the Seyfert-like nucleus of NGC1275, show the evolution of a core-halo structure following a flare in 1980. Observations of 3C273 at 3 epochs have followed flares and show that the source displays superluminal expansion on scales as small as 1 ly. Addition of more telescopes in the next 1-2 years will improve the u-v coverage, especially at low declinations. The techniques and telescopes can be extended to observations at 230 GHz to provide 10 micro-arcsec resolution. Comparison of maps at 1.3, 3, 7, and 1.3 cm to compute the spatial and spectral evolution of the source structure will lead to a much clearer understanding of radio flares and jet formation in radio sources.

INVESTIGATORS

D.C.Backer, J.E.Carlstrom, R.L.Plambeck,
M.C.H.Wright, (U.C.Berkeley), C.R.Masson, S.Padin,
A.C.S.Readhead, D.Woody, A.Zensus, (Caltech),
A.E.E.Rogers, (Haystack), J.M.Moran, (SAO),
C.R.Predmore, R.L.Dickman, (U.Mass.), D.T.Emerson,
J.Payne, (NRAO), L.Baath, A.Kus, B.Ronnang, R.Booth,
(Onsala), H.Hirabayashi, N,Inoue, M.Morimoto,
(Nobeyama).

J2-5
1500

OBSERVATIONS OF H_2O MASER MOTIONS IN W49(N)

C. R. Gwinn, J. M. Moran, M. J. Reid, M. H. Schneps
Harvard-Smithsonian Center for Astrophysics
60 Garden St., MS 42
Cambridge, MA 02138
R. Genzel
Max-Planck Institut für Extraterrestrische Physik
D. Downes
Institut de Radio Astronomie Millimetrique

The outflow of water masers in W49(N) provides an excellent laboratory for studying cosmic masers. Masers consist of many compact spots with different Doppler shifts. W49(N) is the most energetic and populous maser cluster in the galaxy, containing hundreds of maser spots with velocities ranging over 400 km/s over a few square arc sec. We observed the maser cluster at several epochs with intercontinental VLBI networks. Our observations show that the masers expand from a common center, coincident with a compact HII region (Dreher *et al.* personal communication, 1988).

We observe evidence for turbulent motions of ≈ 10 km/s in the masing gas: wander of maser spots about straight-line motion, and differential motions between nearby spots. This speed is comparable to the spread in Doppler shift of nearby spots.

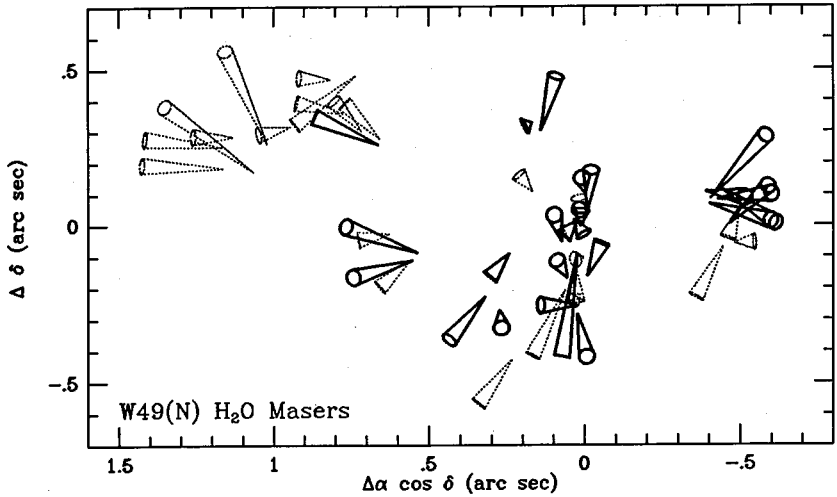

Figure: Motions of H_2O maser spots in W49(N). Spots are at the apexes of the cones; lengths and inclinations show where they would travel in 150 years. Motions of nearby spots have been combined. Dotted cones show receding motions.

J2-6
1520

RADIO SOURCE POSITIONS FROM VLBI

C. Ma, D. Shaffer, J. Russell, K. Johnston, C. deVegt, D. Jauncey, and O. Sovers

Positions of 182 compact radio sources have been estimated from Mark III VLBI data acquired by CDP/IRIS between 1979 and 1988. The average formal error is .00006 sec in right ascension and .0006 arcsec in declination. Mark III observations for reference frame ties made in by NRL in the northern hemisphere have added 54 more sources with typical uncertainties of a few milli-arcsec. 44 sources south of -40 deg declination have been measured with Mark III but using only X-band. A combination of Mark III and Mark II VLBI data from various observing programs yields 294 sources with formal position errors less than 10 mas distributed over the entire sky.

J3-1
1540

RAPID VARIATIONS IN FLUX FROM INTERSTELLAR OH MASERS

Andrew W. Clegg and James M. Cordes
National Astronomy and Ionosphere Center
Cornell University
Ithaca, New York 14853

The 1000′ Arecibo radio telescope was used to monitor seven Galactic interstellar OH (HII/OH) masers from 2 to 14 kpc distant. Interstellar masers, in contrast to masers associated with late-type infrared-bright stars (OH/IR stars), are very compact emission regions located on the periphery of star forming complexes. Interferometric observations have resolved the spots at the milliarcsecond level, although it is not clear whether the observed source size is intrinsic or due to interstellar scattering (c.f., Reid and Moran, *Ann. Rev. Astr. & Astrophys.*, **19**, 231, 1981). If due to scattering, the flux from the masers might be observed to scintillate, in analogy to the scintillations seen in pulsar dynamic spectra.

Our observations revealed that three of the seven masers exhibited significant flux variations on time scales as short as the 16 second integration period. Additionally, the magnitudes of the scintillations generally decreased with increasing distance to the masers, which would result when the scintillation bandwidth decreases to much less than one spectral channel bandwidth as the distance to the maser increases. If the scintillation bandwidth is approximately equal to a channel bandwidth, the shape of the maser line will change with time. This effect was observed in one case.

An OH/IR maser was also monitored and was not observed to undergo flux variations. The emission from OH/IR masers is generally believed to arise in an extended ring or shell about the exciting star, and the large angular size of the region is expected to quench scintillations.

The results are consistent with an interstellar scattering explanation; however, other explanations cannot be ruled out, and further observations are required. If indeed propagation effects are the cause, our observations constrain the intrinsic sizes of the masers. Otherwise, combining our data with light travel time arguments provides a lower limit to the brightness temperature of the emission regions.

J3-2
1600

PHYSICAL MECHANISMS FOR THE GENERATION OF INTERSTELLAR DENSITY IRREGULARITIES

S. R. Spangler
Department of Physics & Astronomy
The University of Iowa, Iowa City, IA 52242-1479

Increased radioastronomical observational activity in the past few years has greatly advanced our knowledge of the spectrum of interstellar density turbulence. The situation is now conducive to theoretical work on the mechanisms for generating these relatively small scale irregularities. In this paper, I discuss the proposals which have been made to date. The suggestions can be categorized as *microphysical* ones, which invoke a plasma instability, and *magnetohydrodynamic* ones, which attribute the fluctuations to fluid-like turbulence. Future theories can probably be accommodated within these two classifications. Depending on the nature of the generating mechanism, the observed fluctuations may be part of very important interstellar processes. The damping of these irregularities may provide an important contribution to the heating of the interstellar medium. As pointed out by Jokipii, the magnetic field fluctuations corresponding to the density perturbations may play an important role in the confinement (and acceleration?) of the cosmic rays. Observational programs in progress should measure or constrain the outer scale of the density turbulence, which might permit identification of the responsible mechanism, or at least the category of generation mechanism.

This research was supported by grants NAGW-806 and 831 from NASA.

J3-3
1620

SPECKLES IN IMAGES SCATTERED BY THE INTERSTELLAR PLASMA

C. R. Gwinn
Harvard-Smithsonian Center for Astrophysics
60 Garden St., MS 42
Cambridge, MA 02138

Radio images of cosmic masers and pulsars, as scattered by the interstellar plasma, are predicted to be made up of many individual subimages, known as speckles. Star images in visible light scattered by atmospheric turbulence show speckles, as do radio sources scattered by the solar wind. Due to limitations on baseline length and signal-to-noise ratio, imaging of speckles in scattering disks in the interstellar plasma is not practical. However, their effects should be observable. I discuss the consequences of speckles for VLBI observations of pulsars and masers, and present limits on their properties obtained from observations.

J3-4
1640

IONOSPHERIC SCINTILLATIONS AT VENUS

R. Woo, W. Sjogren and A. Kliore
Jet Propulsion Laboratory
California Institute of Technology
Pasadena, CA 91109
J. Luhmann
Institute of Geophysics and Planetary Physics
University of California at Los Angeles
Los Angeles, CA 90024
L. Brace
NASA Goddard Space Flight Center
Greenbelt, MD 20771

Although ionospheric scintillations have been widely observed in the case of Earth and the outer planets, they have not been observed at non-magnetic planets such as Venus and Mars. In this paper we present the first S-band (2.3 GHz) radio scintillations detected in the ionosphere of Venus. These were observed by Pioneer Venus Orbiter (PVO), a spacecraft that has been orbiting and returning scientific data on the planet Venus since 1978. The global morphology of the ionospheric scintillations is very different from theat of the terrestrial ionosphere as scintillations occur only in the subsolar region of Venus. Because the PVO spacecraft was *within* the ionosphere when the scintillations were detected, *in situ* fields and particles measurements made by PVO were also available. PVO is, therefore, the first planetary spacecraft for which a comparison of simultaneous plasma and scintillation measurements of the same ionosphere has been possible.

The fields and particles measurements show that the scintillations are caused by disturbed plasma in the topside ionosphere but below the ionopause. The disturbed plasma is associated with the penetration of large-scale magnetic fields into the ionosphere of Venus, and takes place when the solar wind dynamic pressure exceeds the ionospheric plasma pressure. This occurs most frequently in the subsolar region. The disturbed plasma and the resulting scintillations are, therefore, a manifestation of high dynamic solar wind interaction with the ionosphere of Venus.

We also demonstrate that the disturbed plasma produced by the high-dynamic solar wind interaction can be remotely sensed by scintillations during radio occultation measurements, i.e. when the spacecraft is *outside* the ionosphere. Such observations can, therefore, provide useful information on the high-dynamic solar wind interaction of non-magnetic planets such as Venus and Mars when *in situ* measurements are not available. Of particular interest is Venus during solar cycle minimum when there are no *in situ* measurements because of the rise in PVO periapsis altitude. Because the ionosphere is weaker during solar cycle minimum, high-dynamic conditions may be expected to be more prevalent.

0830-Thurs. Duane G0-30
PLENARY SESSION

PS-1 0840 NUMERICAL MODELING OF PASSIVE MICROWAVE O_2 OBSERVATIONS OVER PRECIPITATION: A.J. GASIEWSKI and D.H. Staelin, Research Laboratory of Electronics, MIT, Cambridge, MA

PS-2 0900 EDGE WAVE VERTEX AND EDGE DIFFRACTION: L.P. IVRISSIMTZIS and R.J. Marhefka, ElectroScience Laboratory, The Ohio State Univ., Columbus, OH

PS-3 0920 GAUSSIAN BEAM ANALYSIS OF PROPAGATION FROM AN EXTENDED PLANE APERTURE DISTRIBUTION THROUGH PLANE AND CURVED DIELECTRIC LAYERS: J. MACIEL and L.B. Felsen, Dept. of Electrical Engineering and Computer Science, Polytechnic Univ., Farmingdale, NY

PS-4 1000 HARRY DIAMOND MEMORIAL AWARD PRESENTATION

PS-5 1015 EARLY STUDIES OF THE IONOSPHERE/NEAR-EARTH PLASMA IN THE USSR: Y.L. Alpert, Harvard Smithsonian Center for Astrophysics, Cambridge, MA 02138

PS-6 1100 POLARIMETRIC RADARS FOR REMOTE SENSING: F. Ulaby, Dept. of Electrical and Computer Engineering, Ann Arbor, MI 48109

PS-7 1135 ELECTROMAGNETIC TARGET IDENTIFICATION: D. Dudley, Electromagnetics Laboratory, Dept. of Electrical and Computer Engineering, Univ. of Arizona, Tucson, AZ 85721

PS-8 1210 PRESENTATION OF STUDENT AWARDS

Thursday Afternoon, 5 January, 1355-1700

Session A-2 1355-Thurs. CR1-42
ELECTROMAGNETIC MEASUREMENTS
Chairman: Motohisa Kanda, Electromagnetic Fields Division, National Institute of Standards and Technology, Boulder, CO 80303

A2-1
1400

AN ISOTROPIC, PHOTONIC PROBE FOR MEASUREMENT OF ELECTRIC FIELDS TO 1 GHZ

K.D. Masterson and L.D. Driver + M. Kanda
Electromagnetic Fields Division MS/723.03
National Institute of Standards and Technology
(formerly National Bureau of Standards)
325 Broadway
Boulder, CO 80303

We have developed a passive, all dielectric, isotropic, photonic probe to measure high frequency electric fields. The probe uses 15 cm resistively-tapered dipole elements with Pockels effect electro-optic modulators to convert the electric-field information to optical signals which are transmitted to the signal processing electronics over optical fibers. The frequency response is flat to within 3 dB from 30 kHz to 100 MHz, except for a region between 1 and 10 MHz where acoustic resonances occur in the crystal. Using a 3 kHz detection bandwidth, the noise equivalent field is approximately 7 V/m, thereby giving a calculated linear dynamic range of 68 dB in field intensity. The isotropic response is excellent, and each individual dipole follows the theoretically predicted angular response.

a Hochmann

A2-2
1420

HIGH FREQUENCY CHARACTERIZATION AND APPLICATIONS OF HIGH T_c SUPERCONDUCTORS

Jeffery T. Williams, Stuart A. Long,
David R. Jackson, and Donald R. Wilton

Applied Electromagnetics Laboratory
Department of Electrical Engineering
University of Houston
Houston, TX 77204

The development of superconducting materials with critical temperatures above the temperature of liquid nitrogen ($77K$) has sparked renewed interest in the use of superconductors in microwave and millimeter-wave systems. Previously, superconductors with critical temperatures less than $35K$ proved useful for many high frequency applications; however, the cost and complexity of the systems used to obtain such low temperatures limited their application. For the new high temperature superconductor, simplier and more cost effective cryogenic systems can be used. However, in order to assess the potential microwave and millimeter-wave applications of these high T_c superconducting materials careful electrical and mechanical characterization studies must be undertaken. The Department of Electrical Engineering, in cooperation with the Texas Center for Superconductivity, at the University of Houston has established a program to develop and characterize thin film high T_c superconducting materials for microwave and millimeter-wave applications. We will discuss these experimental and theoretical efforts, and will present results from the high frequency characterization and applications studies. These results will include the electromagnetic absorption and surface resistance of the high T_c thin film superconductors (YBaCuO and BiCaSrCuO) deposited on MgO and ZrO_2 substrates, as a function of temperature and frequency, obtained from measurements in cylindrical cavity and microstrip resonators. In addtion, the results from studies of superconducting microstrip and stripline transmission lines and antennas will presented.

a Hachment

A2-3
1440

COMPUTER-AIDED DATA ACQUISITION SYSTEM FOR EXPERIMENTS ON THE DETECTABILITY OF WEAKLY INTERACTING PARTICLES

Mario D. Grossi
Harvard-Smithsonian Center for Astrophysics
Cambridge, Massachusetts 02138

Experiments on the detectability of the radiation pressure of low-energy neutrinos are underway using intense tritium sources, that produce neutrinos by the beta-decay process. These sources are placed on a large rotating table, right at its edge. The sensors under investigation are distributed all around the table, at fixed stations on the floor, in close proximity to the table's edge. Table rotation causes the neutrino flux that illuminates each sensor to be time-variable (flux modulation by range variation). This time-variable signal is the object of our search. One of the tables that we use in the experiments rotates at 1 RPM; a second one, still under construction, has been designed for 2000 RPM.

Data acquisition with the 1 RPM table is performed by using a LabTech Notebook software package on a PC. For every scan cycle, corresponding to the 60-second table rotation period, the system takes 36 contiguous samples of the sensor's output, each sample being 1.66 seconds long. The samples are recorded on a PC-mounted hard disk, for later reduction and processing. They are also displayed on the PC screen, for real-time visual observation. The display is connected to a printer/plotter for recording on paper the display's content. The system performs in real-time a scan-to-scan time-coherent integration, by adding the amplitudes of the samples that fall on the same x-value of the horizontal coordinate axis, from scan to scan. The expected processing gain of $N^{1/2}$, where N is the number of the samples that have been integrated, has been verified for integration times as long as 168 hours. The processing gain is, in this case, +40 dB.

When an experiment is run with the 2000 RPM table, the search is for a spectral line at 100 Hz, at the output of a sensor that is essentially a mechanical resonator tuned at that frequency, with 10^{-2} Hz line-width. Sampling rate is 600 samples/sec, and in this case data acquisition is performed with a high-speed DiaBase software/hardware approach. The real-time process consists of the spectral analysis of the sensor's output. The real-time display shows the power spectrum of the signal (the FFT is performed with a SKY COMPUTER card mounted on the PC), and this spectrum is periodically updated while the integration goes on. Integration times as long as 168 hours are planned also for this case. Raw data are also recorded, for off-line data reduction and processing at four participating Institutions.

A2-4
1500

EMC Modeling Considerations for Frequency Domain Observations

D.S. Friday, E.J. Vanzura and J.W. Adams
Electromagnetic Fields Division
National Institute of Standards and Metrology
325 Broadway
Boulder, Colorado 80303

Many EMI/EMC related studies involve measurements in which frequency is swept and the response recorded in discrete equally spaced intervals. In some experiments there may be measurable sampling variability and in others it will be insignificant. A more important issue often involves independent factors which when adjusted change the frequency response in a complex manner. Such is the case when a typical electronic box is irradiated from various directions and the induced current is measured at some port or interior point. The question is the interpretation of the results and the determination of bounds for the observed data. Ad-hoc methods are presently used. We will present alternative methodology based on statistical modelling and physical theory and discuss its interpretation.

A2-5
1540

EXPERIMENTAL PERFORMANCE OF A DUAL SIX-PORT ANA INCORPORATING A BIPHASE-BIMODULATION ELEMENT.

S.K.JUDAH and A.S.WRIGHT.

Microwave Lab. Dept Electronic Engineering.
University of Hull.
Cottingham Road. Hull HU6 7RX.
United Kingdom.

Abstract.

The experimental performance of a new technique in Dual Six-Port reflectometry is reported. Recently a new theoretical technique known as Biphase-Bimodulation was introduced. (S.K.Judah and A.S.Wright " A Second Generation Dual Six Port Network Analyser" IEEE MTTS Digest 1988 pp295-296). This methodology has the attractive feature that mechanical phase shifters and attenuators have been eliminated, producing a design free from dynamic mechanical parts.

The diagram illustrates the design of this new reflectometer system. The Biphase-Bimodulation element consists of a Wilkinson power splitter, two PIN diode modulators and a 3db quadrature coupler. This element introduces a microwave carrier to the dual reflectometer that consists of two components. For the LHS reflectometer the microwave carrier consists of a 0^0 phase shift labelled with the audio tone f_1 and a 90^0 phase shift labelled by the audio tone f_2. For the RHS reflectometer the microwave carrier is similarly composed, except the audio tones f_1 and f_2 label opposite phases. This labelling yields a degree of independency that allows the system to be considered as two independant dual six-ports. This in turn allows four pseudo reflection coefficients to be measured from which the scattering parameters of the DUT may be computed.

Experimental results will be demonstrated showing the validity of this technique, especially in regards to speed of measurement.

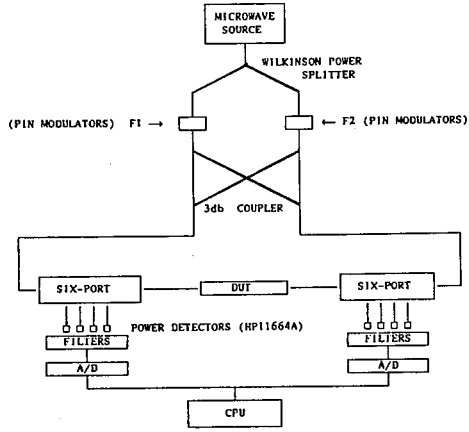

A2-6
1600

TOTAL MILLIMETER-WAVE POWER TRANSMITTED THROUGH UNIFORMLY ILLUMINATED SEMICONDUCTOR PANEL SCANNED WITH A STRIP OF SHADOW

M.H. RAHNAVARD
Electrical Engineering Department
Shiraz University, Shiraz, Iran

One of the needs in air traffic is to know the environmental situation under any weather condition. Visible or IR radar will fail in adverse weather because of high attenuation but there are several windows in millimeter wave region with low attenuation in bad weather condition (Weibel, C.H. and Dressel, H.O. 1967, Proc. IEEE, 55, 497). One of the methods to convert millimeter wave to visible light is by using illuminated semiconductor panel. Semiconductor panels are used as image convertors in both transmission and reflection mode of operation (Jacobs, H. et.al, 1967, J. Opt. Soc. 57, 913). In both cases the response of illuminated semiconductor panel is important. Excess carrier in moving strip illuminated semiconductor panel is obtained by Rahnavard, et. al. (Rahnavard, et. al. J. Applied Physics, Vol. 46, No. 3, March, 1975, pp. 1229-1234). Using the above result attenuation coefficient and reflection coefficient for this case are also studied (Rahnavard, et. al. Sensor and Actuator Journal, vol. 12, No. 4, pp. 367-374 (1987)). Transmission coefficient and local power transmission through uniformly illuminated semiconductor panel scanned with a strip of shadow are also studied (Rahnavard, et. al. Appl. Opt. 26, pp. 1213-1215, April 1987, Rahnavard, Microwave and Optical Technology letters, Vol. 1, No. 6, pp. 211-214). In this paper total transmitted power through uniformly illuminated semiconductor panel scanned with a strip of shadow vs. velocity of the moving shadow strip, width of the moving shadow strip, attenuation etc. are studied.

Session B-3 1355-Thurs. CR0-30
EM THEORY I
Chairman: R. Collin, Electrical Engineering Dept., Case Western Reserve Univ., Cleveland, OH 44106

B3-1 **DUAL SOURCES ON BOUNDARIES**
1400 C.E. Baum
Air Force Weapons Laboratory/NTAAB
Kirtland AFB NM 87117-6008

Duality is an important concept in electromagnetics involving a symmetry in the equations between electric and magnetic parameters. Using the combined field, one has a compact form for stating various electromagnetic theorems. In this paper this is first extended to a dual equivalence principle in which electric and magnetic surface currents are interchanged on a surface with a corresponding interchange of electric and magnetic fields. Then we consider production of electrostatic and magnetostatic fields using electric potential and electric surface current density respectively to make the two fields have the same spatial distribution in a volume.

B3-2
1420

TIME-DOMAIN SOLUTION OF MAXWELL'S EQUATIONS IN FREQUENCY-DEPENDENT MEDIA

A.H. Mohammadian, W.F. Hall, and V.V. Shankar
Science Center
Rockwell International Corporation
P.O. Box 1085
Thousand Oaks, CA 91360

In this work, a method is proposed to modify the recently developed finite-volume scheme for solving Maxwell's equations in the time domain (V.V. Shankar and W.F. Hall, URSI Meeting, Boulder, Jan. 1988) in order to treat frequency-dependent media. The capability to treat frequency-dependent media is particularly important in transient field problems or scattering due to pulse incidence.

To demonstrate the methodology without loss of generality it will be assumed that only the permittivity of the medium varies with frequency of the applied field. The induced polarization due to the applied field may be resolved into a slow and a fast part. While the fast part is very nearly proportional to the instantaneous applied field, the slow part is not. For most materials of practical interest, the slow part of the polarization may be approximated for time-harmonic excitation by the product of a rational function of frequency and the applied field amplitude.

Maxwell's curl equations in the frequency domain and frequency-dependent media are inverse Fourier-transformed to the time domain. This will result in a system of integro-differential equations where the kernel of the integral part is convolutional. To avoid storing the field quantities for all previous time steps, a recursive scheme has been developed to evaluate the convolutional integral. This is always possible if the susceptibility function has the previously stated properties.

The bistatic radar cross-section data for a circular cylinder made of a frequency-dependent material were obtained from a single Gaussian incident pulse. These results are in excellent agreement with those obtained from the series expansion method.

B3-3
1440

A MATRIX INVERSION METHOD OF ORDER $N^{2.5}$ AND APPLICATIONS TO ELECTROMAGNETIC SCATTERING COMPUTATIONS.

D. K. Cohoon and R. M. Purcell
Damaskos, Inc.
Post Office Box 469
Concordville, Pennsylvania 19331

A class of N by N nonsingular, nonsparse, complex, nonsymmetric matrices that can be inverted in a number of operations less than $N^{2.5}$ has been created. Part of this theory is based on the Pan-Reif fast matrix multiplication algorithm. Letting A denote the matrix whose inverse is required, we let $T_0 = (\lambda_0 I - A)$, where λ_0 is a large enough complex number so that $T_0^{-1} = \lambda_0\left(\sum_{k=1}^{\infty}(\lambda_0^{-1}A)^k\right)$. If $\frac{dR_\lambda}{d\lambda} = -R_\lambda^2$, where $R_0 = T_0^{-1}$, and if there exist arbitrarily large circles, C, centered at λ_0 and a constant C_n depending only on n such that

$$\frac{1}{2\pi i}\int_C \frac{R_\lambda}{\lambda - \lambda_0}d\lambda = A^{-1}$$

then A^{-1} can be determined to an accuracy of N digits in less than $N^{2.5}$ steps. The use of computers with multiple processors can further reduce the time of matrix inversion, but R. M. Chamberlain (Hypercube Multiprocessors, 1987, pp 569-575) has reported that considerable time is spent in message passing between processors for LU factorization on a hypercube. If we represent an integral equation whose solution gives the electric vector E or the magnetic vector H induced in a penetrable body, then if this is written in the form,

$$F(p) - F^i(p) = \lambda\int_\Omega G(p,q)F(q)dv(q)$$

where F^i is known and F is being sought, then we can find a resolvent kernel $R_\lambda(p,q)$ such that

$$F^i(p) - F(p) = -\lambda\int_\Omega R_\lambda(p,q)F^i(q)dv(q)$$

where $R_0(p,q) = G(p,q)$ and

$$\frac{d}{d\lambda}R_\lambda(p,q) = \int_\Omega R_\lambda(p,w)R_\lambda(w,q)dv(w).$$

Besides this analogue of the method in Fredholm theory, our matrix inversion method will reduce moment method costs.

B3-4
1500

NEW INTEGRAL EQUATIONS FOR SCATTERING FROM AN INDENTED SCREEN

J.S. Asvestas, M/S A02-26, Corporate Research Center
Grumman Corporation
Bethpage, NY 11714-3580
R.E. Kleinman, Department of Mathematical Sciences
University of Delaware
Newark, DE 19716

Boundary integral equations are derived for the two-dimensional problem of scattering of an harmonic electromagnetic wave by an indentation on an infinite, perfectly conducting, screen. The problem is modeled as a two-dimensional scattering problem for the Helmholtz equation, both polarizations are considered, and the cross section of the indentation is arbitrary. Using the appropriate Green's function for each polarization, integral equations are obtained involving the total field and its normal derivative on the projection of the indentation onto the plane of the screen, as well as the total field (H-polarization) or its normal derivative (E-polarization) on the indentation. The unique solvability of this system of integral equations over finite boundaries is discussed as is the discretization and numerical solution. It is also shown that one of the unknown quantities may be eliminated at the cost of increased complexity. The relative advantages of each formulation are pointed out.

B3-5
1540

COMPUTATION OF ELECTROMAGNETIC FIELD EXTERIOR TO A CLOSED SURFACE SURROUNDING THE SOURCES

R. M. Bevensee
Engineering Research Division, L-156
Lawrence Livermore National Laboratory
Livermore, CA 94550

Well-known formulas yield the field exterior to a closed numerical surface S surrounding the sources. These formulas require knowledge of both tangential E and tangential H on S. This fact is consistent with the Uniqueness Theorem, which states that either tangential E or tangential H on S suffices to determine the exterior field.

Computations of the radiation field determined by the tangential fields on a numerical rectangular parallelopiped surrounding an electric dipole, and also a magnetic dipole pair, prove generally that the external field is not simply related to either tangential E or tangential H on S.

Yet the external field can be obtained directly from either tangential E or tangential H on S, via a Compensation Theorem formula. However, one must solve an auxiliary problem--compute either the tangential magnetic field induced on electrically conducting S or tangential electric field on magnetically conducting S by an external "test" dipole at the field point.

Usually it is more computationally efficient to obtain both tangential E and H on S. For some simple geometries the Green-function solution to the auxiliary problem can be obtained in closed form.

B3-6
1600

USE OF HOMOTOPY METHODS FOR ELECTROMAGNETIC DESIGN

D.K. Cohoon and R.M Purcell
Damaskos, Inc.
P. O. Box 469
Concordville, PA 19331

The basis of our method concerns tracking a homotopy path using the fact that if on the curve $(\lambda(s), x(s))$ $\lambda(s)\epsilon[0,1]$, $X(s)\epsilon\mathbb{R}^n$ if we have for each $X = X(s)$

$$\rho_a(\lambda,X) = \lambda F(X) + (1-\lambda)(X-a)\epsilon\mathbb{R}^n$$

then if it were true that a path $s \to (\lambda(s),X(s))$ were chosen so that

$$\rho_a(\lambda(s),X(s)) = 0 \ \epsilon\mathbb{R}^n$$

that then we would have

$$\begin{bmatrix} \frac{\partial(\rho_a)_1}{\partial\lambda} & \frac{\partial(\rho_a)_1}{\partial X_1} & \cdots & \frac{\partial(\rho_a)_1}{\partial X_n} \\ \vdots & \vdots & & \vdots \\ \frac{\partial(\rho_a)_n}{\partial\lambda} & \frac{\partial(\rho_a)_n}{\partial X_1} & \cdots & \frac{\partial(\rho_a)_n}{\partial X_n} \end{bmatrix} \begin{bmatrix} \frac{d\lambda}{ds} \\ X_1'(s) \\ \vdots \\ X_n'(s) \end{bmatrix} = \begin{bmatrix} 0 \\ 0 \\ \vdots \\ 0 \end{bmatrix}$$

If along the path satisfying these equations, the Jacobian were full, then its kernel would be one dimensional. If we then required that

$$\frac{d\lambda}{ds} > 0$$

and that

$$\left(\frac{d\lambda}{ds}\right)^2 + X_1'(s)^2 + \ldots + X_n'(s)^2 = 1$$

we would uniquely determine, in terms of the above coefficient matrix the values of $\frac{d\lambda}{ds}$, $X_1'(s)$, ... , $X_n'(s)$ as functions of the parameters.

B3-7
1620

A WIDEBAND MODEL FOR ELECTROMAGNETIC INTERFERENCE FROM CORONA ON ELECTRIC POWER LINES

R.G. Olsen and M.D. Wu
Electrical and Computer Engineering Department
Washington State University
Pullman, WA 99164-2752

A new analytical model for predicting electromagnetic interference from corona on electric power lines has been developed. The main contribution of the new model is that it is valid in the frequency range 2-30 MHz for which no other analytical model presently exists. It is also valid for distances and directions from the power line which are essentially unrestricted.

In past calculations, it was necessary to find an expression for the field of a single corona source as an explicit function of the axial coordinate. These fields were then added to obtain an expression for the interference fields from a distribution of corona sources along the power line, This addition is extremely difficult unless the fields are assumed to be those of a quasi-TEM mode. Since this is only valid at low frequencies, only low frequency interference models have been developed using this method. In the new method, only the spatial transform of the single wire source field is needed. The sum can be easily done without the quasi-TEM assumption. The result is a relatively simple expression for the interference field from a distribution of corona sources on a power line.

The model is shown to be in good general agreement with an empirical formula which was developed from the limited experimental data available.

B3-8
1640

A NEW ASYMPTOTIC EXTRACTION TECHNIQUE FOR EVALUATING TWO-DIMENSIONAL SOMMERFELD INTEGRALS

S. L. Dvorak and E. F. Kuester
Electromagnetics Laboratory
Department of Electrical and Computer Engineering
University of Colorado — Campus Box 425
Bouder, CO 80309

Two-dimensional (2-d) Sommerfeld integrals are encountered when the plane-wave spectrum method is used in conjunction with the method of moments to analyze planar/layered structures. Due to the slow convergence properties of these integrals, a large percentage of the total computation time in one of these problems is usually expended on the computation of the integrals in the impedance matrix. Therefore, it is very important to develop efficient techniques for the computation of 2-d Sommerfeld integrals.

In a previous paper (S.L. Dvorak and E.F. Kuester, *National Radio Science Meeting, URSI Abstracts,* pp. 72, 1987), the angular integral, in the polar representation of the Sommerfeld integral, was rewritten in terms of a finite number of incomplete Lipschitz-Hankel integrals. Later, this technique was used to compute the Sommerfeld integrals that are encountered when using Galerkin's method with piece-wise sinusoidal basis functions. Now, in this paper, the incomplete Lipschitz-Hankel integral expansion will be used to obtain an asymptotic form for the integrand of the Sommerfeld integrals, which when integrated from some large limit to infinity, can be represented in terms of special functions. Extracting this asymptotic portion of the integral greatly improves the computational efficiency.

Earlier, Pozar showed how a homogeneous-space term can be extracted from the integrand, thereby improving the convergence of the integral (D.M. Pozar, *Electromagnetics,* pp. 299-309, 1983). Pozar's technique will be compared with the technique presented in this paper. Also, the asymptotic extraction technique will be applied in conjuction with Galerkin's method to the analysis of a printed strip dipole antenna.

B3-9
1700

ELECTROMAGNETIC PENETRATION THROUGH NARROW SLOTS IN CONDUCTING SCREENS AND COUPLING TO A THIN WIRE ON THE SHADOW SIDE

Erik K. Reed and Chalmers M. Butler
Clemson University, Clemson, SC 29634-0915
Ray J. King
Lawrence Livermore National Laboratory, Livermore, CA 94550

Electromagnetic field penetration through arbitrarily shaped narrow slots in a planar conducting surface and coupling to a thin wire located on the shadow side of the slotted surface is determined in the frequency domain by integral equation methods. A coupled integral equation is derived and solved numerically for the slot electric field and the current on the thin wire, from which the field that penetrates the slotted surface is subsequently determined. The validity of the numerical method is established by demonstrating close correlation between data obtained from computations and those determined from measurements.

The integral equation is solved numerically for the slot electric field, or equivalent magnetic current, and the current on the coupled thin wire by a standard technique utilizing a piecewise linear approximation of the unknown currents and equation enforcement by pulse testing. From knowledge of the slot's equivalent magnetic current and the wire's electric current, obtained as the solution of the coupled integral equation, the field which penetrates the slotted surface is calculated at various locations for several cases of plane-wave excitation.

Narrow slots were chemically etched in thin brass sheets and an apparatus was fabricated to measure shadow side electric field and the current at the base of a coupled monopole. The experimentation was conducted at the Lawrence Livermore National Laboratory on a frequency-domain test range employing a monocone source over a large ground plane. Electric field was measured at various shadow-side locations for several combinations of excitation, slot shape, and slot width. Also, current at the base of a coupled monopole was measured for several monopole locations, lengths, and orientations. Data were collected for narrow slots having strait, annular, and rectangular geometry in the range 0.5 to 10.5 GHz. Good agreement exists between the experimental and theoretical results.

Session B-4 1335-Thurs. CR2-28
ANTENNAS
Chairman: R. Pogorzelski, TRW, Space and Technology Group, Redondo Beach, CA 90278

B4-1
1340

A CIRCULAR ARRAY FOR PLANE-WAVE SYNTHESIS

David A. Hill
Electromagnetic Fields Division
National Institute of Standards and Technology
Boulder, CO 80303

In electromagnetic-susceptibility testing of electronic equipment, the ideal incident field is a plane wave. The feasibility of using near-field phased arrays to produce a plane wave has been studied theoretically (D.A. Hill, IEEE Trans., EMC-27, 201-211, 1985) and experimentally with a seven-element array of Yagi-Uda antennas (D.A. Hill and G. H. Koepke, IEEE Trans., EMC-28, 170-178, 1988).

The ability to scan the direction of arrival of the plane electronically and to step or sweep the frequency would be extremely useful in electromagnetic-susceptibility testing and in antenna measurements. In this paper we analyze a circular array of electric line sources to study the feasibility of directional and frequency scanning. This two-dimensional model is idealized, but it contains many of the relevant features of a more realistic three-dimensional array. Some related work with circular arrays has been performed with application to antenna measurements (J.C. Bennett and N.E. Muntanga, Proc. IEE, 129, 229-231, 1982) and hyperthermia therapy (J.R. Wait, IEEE Trans., MTT-33, 647-649, 1985).

The complex weightings of the electric line sources are chosen to approximate a plane wave in the interior region of the array. Identical results for the synthesized element weightings are obtained using matrix inversion or a Fourier series technique. A physical optics approximation for the element weightings is also presented, but it yields a much poorer result for the synthesized field. The angle of arrival of the plane wave can be scanned by recalculating the element weightings, and the quality of the field is maintained. Frequency scanning is also possible, but the number of array elements limits the maximum frequency. Numerical results are presented for the element weightings and the amplitude and phase of the synthesized field.

Near field
Applications?
near field ant. meas, EMC meas, Focused heating

Use $\vec{E} = \vec{E} - \eta \hat{n} \times \vec{H}$ hybrid vector to avoid cavity resonances when applying BC — similar to Harrington and Mautz.

B4-2
1400

DIGITAL MULTIPLE BEAMFORMING BY A PLANAR ARRAY

Takahiko Fujisaka*, Yoshimasa Oh-hashi*,
Michimasa Kondo* and Norio Takeuchi**
*Information Systems and Electronics Development Laboratory
**Communication Equipment Works
Mitsubishi Electric Corporation
5-1-1 Oh-Funa,Kamakura-city,Kanagawa-pref.
247 JAPAN

Digital Beamforming(DBF) technique has lately attracted considerable attention because of its remarkable features (e.g., multiple beams,self-calibration and ultra-low sidelobes)(H.Steyskal,Microwave J.,107-122,JAN-1987). We have experimentally produced and evaluated a DBF antenna(shown in figure 1) with 8x8 antenna elements arranged in an equilateral-triangular grid pattern(A.E.Ruvin,EASCON-78,152-163). Each element has one receiver and two analogue to digital converters,the outputs of which are processed for beamforming by a computer.

The beamforming is the spatial filtering to separate the signal arriving at the antenna from a desired direction θk from the receiver noise and interfering signals. If the wavefront is incident from an angle θ and the received signal at the element i is $s(\theta,i)$, then the output of the spatial filter $Bk(\theta)$ which represents the antenna pattern is given by

$$Bk(\theta)=\sum_i w(i)\frac{s(\theta,i)}{[s(\theta,i)]rms}\frac{s^*(\theta k,i)}{|s(\theta k,i)|}$$

where w(i) represents the sidelobe controlling weight,[ ]rms represents the root mean square in brackets and * denotes complex conjugate.

In figure 2, examples of the antenna patterns with a pointing direction $\theta k=\theta^\circ, \pm 14.4^\circ, \pm 29.7^\circ$ in a horizontal plane are shown, where the weights applied to each element are the product of x-axis and y-axis -40dB Dolph-Chebyshev taper weights.

Fig.1 DBF antenna

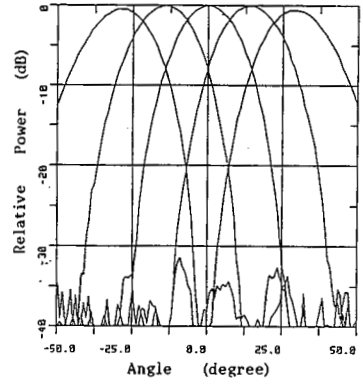

Fig.2 antenna patterns by a 8x8-element array

B4-3
1420

A CONFORMAL MICROSTRIP ARRAY

Albert W. Biggs+, Mark Horton++, and Peter Romine
Electrical and Computer Engineering Department
University of Alabama in Huntsville
Huntsville, AL 35899

This paper describes the design, development, and fabrication of a microstrip antenna array consisting of four rectangular antenna elements. The antenna array will be a source or receiving antenna for evaluating the response of aircraft and missile avionics.

Microstrip feeds were designed with three models (H.A. Wheeler, IEEE Trans. MTT, MTT-13, 171-185, 1965; M.V. Schneider, BSTJ, 48, 1421-1444, 1969; E.O.Hammerstad, Proc European Microwave Conf., Hamburg, Germany, 268-272, 1975). Tabulations were made with characteristic impedances for different copper clad dielectric sheet thicknesses, relative dielectric constants, and ratios of stripline width to sheet thickness.

Transformer sections in the individual antenna feeds and in power dividers were designed to obtain 'equal ripple' VSWR response of a Tchebycheff polynomial, where minima VSWR are achieved with a given bandwidth (or maxima bandwidth with a given VSWR).

Rectangular patch antennas (A.W. Biggs, URSI-APS Joint Mtg., Seattle, WA, 1979) were designed with varying widths and lengths. Antenna radiation patterns were calculated for one element and linear arrays of variable numbers of elements. Theta and phi components of fields were calculated.

+On TDY with the Air Force Weapons Laboratory, Kirtland Air Force Base, NM 87117-6008.
++U.S. Army Missile Command, Redstone Arsenal, AL 35895.

B4-4
1400

MUTUAL COUPLING IN A CLOSELY PACKED ARRAY

A. Kumar
Electromagnetic Canada Consultants
492 Westminster Avenue
Dollard-des-Ormeaux
Quebec
Canada H9G 1E5

A mutual coupling analysis is of importance in the design of phased arrays and array feeds for reflector antennas. Many authors have analyzed mutual coupling between arrays of circular and rectangular apertures. In this paper the effect of mutual coupling between two identical square waveguides has been discussed. The waveguide side length was varied while keeping the distance between their nearest edges constant. One waveguide is excited by a TE_{10} mode, and we consider that the higher modes are generated in the second waveguide for the worst case of E-plane coupling. The analysis has been extended for a large number of elements.

When the elements are arranged in close proximity in the array feed system, mutual coupling can seriously degrade the axial ratio of the individual elements. This occurs because some of the higher order modes generated by mutual coupling are a rich source of crosspolarized radiation. It has been shown that square aperture horns are less satisfactory than circular aperture horns in a circularly polarized array. A detailed discussion on compensation of mutual coupling to improve the axial ratio will be given at the Conference.

B4-5
1500

THE "SSFIP" BROADBAND PLANAR ANTENNA

J.-F. Zürcher, F. Gardiol
Laboratoire d'Electromagnétisme et d'Acoustique
Ecole Polytechnique Fédérale de Lausanne
EL-Ecublens
CH-1015 LAUSANNE, SWITZERLAND

Printed antennas present significant practical advantages like small size and weight, ease of fabrication and potentially low cost, compatibility with printed circuits, that make them very promising for a number of applications ranging from aerospace to direct reception of satellite signals. On the negative side, however, they present less desirable characteristics, among them narrow bandwidth and low efficiency. Surface waves degrade the antenna performance through spurious diffraction and coupling. Many designs combine radiating elements and feed lines on a single dielectric substrate, which provides at best a compromise between ease of fabrication and performance.

Taking into consideration these factors a new concept is proposed : the **S**trip-**S**lot-**F**oam-**I**nverted **P**atch **A**ntenna or in short **SSFIP**. The use of a very low permittivity foam substrate reduces the excitation of surface wave modes and thus their unwanted effects. The radiating patches are deposited on the underside of a thin plastic sheet, that provides a protective cover. The feed line, on a high permittivity material, is located on the underside of the ground plane (feed and radiating elements are clearly separate from one another). Coupling from the line to the antenna is realized through wide slots, whose size was carefully determined to optimize the characteristics of the antenna.

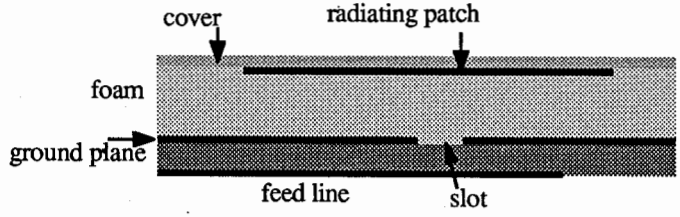

Measured data show significant improvements over more classical realizations. While microstrip antennas typically exhibit frequency bandwidths of a few percents only, a single SSFIP element achieved a bandwidth of 11 % , while a 16-element array even reached a 21.1 % value, in both cases for a SWR less than 2:1. The corresponding antenna gains were respectively 5.8 dB and 16 dB. Further work is in progress to optimize the operation of the antenna and to provide a theoretical model for its accurate simulation on a computer.

B4-6
1520

PLANAR TRANSMISSION LINE EXCITATION OF DIELECTRIC RESONATOR ANTENNAS

Roger A. Kranenburg, Stuart A. Long, and Jeffery T. Williams
Department of Electrical Engineering
University of Houston
Houston, Texas 77204-4793

In 1939 Richtmyer (J. App. Phys., 10, 391-398, 1939) showed that a block of dielectric material in free space would resonate if the dielectric constant of the material was very high. Richtmyer also noted that these resonators exhibited radiation damping. Interest in these resonators were revived in the sixties when they were first used in microwave circuits. The resonant frequencies of the cylindrical resonator were studied with the dielectric-air interface modeled as a magnetic wall. These dielectric resonators are still being used as microwave circuit elements with different feed case, and metal enclosures to reduce the radiation damping. Only recently, however, has the dielectric resonator been investigated as a radiator by McAllister, et al. (IEEE Trans., AP-31, 406-412, 1983), who derived a first-order theory for the radiation patterns and the resonant frequencies of the cylindrical and cubic geometry, and an exact theory for the hemispherical case. An experimental investigation was also undertaken showing the feasibility of these antennas as efficient radiators, using a coaxial probe through a ground plane to excite them.

The purpose of this present work was to examine further the dielectric resonator antenna. More specifically, the approximate theory of a magnetic-walled cavity resonator was extended to obtain the resonant frequency and the far-field radiation patterns of the modes for cylindrical geometry. A broad beam with a maximum normal to the ground plane was obtained for the lowest mode. A more directive beam or a beam with a single sharp null was obtained for the next mode depending on the cylinder geometry. An experimental investigation was then undertaken to show the feasibility of using a microstrip transmission line and a coplanar waveguide as the excitation mechanism for the system. Impedance, coupling, and radiation pattern results are given for various feed positions using dielectric cylinders with radii of 12.7 mm, heights varying from 2.8 mm to 25.4 mm, and relative dielectric constant varying from 8.1 to 20.8. Finally the theoretical resonant frequencies and radiation patterns were compared to experimental results, with resonable correlation resulting.

B4-7
1540

STACKED MICROSTRIP PATCH ANTENNAS

L. Barlatey, J.R. Mosig, F. Gardiol
Laboratoire d'Electromagnétisme et d'Acoustique
Ecole Polytechnique Fédérale de Lausanne
EL-Ecublens
CH-1015 LAUSANNE, SWITZERLAND

Stacked patch antennas, made of two printed antennas located on top of each other and separated by a dielectric sheet, provide an interesting approach to improve antenna performance, of particular interest for the design of monolithic arrays. The two dielectric layers of the structure can have different thicknesses and permittivities, while the patches can take different shapes and dimensions, and thus resonate at different frequencies. The lower patch may be driven and the upper one parasitically excited, or the two patches may be excited by different feeds, for instance to separate emit and receive channels. All these degrees of freedom can be taken advantage of to build higher performance microstrip antennas.

In the simpler case, a printed patch may be inserted between two dielectric layers : this is the case of a patch antenna covered by a protective layer or radome, and the same model can be used to evaluate the effect produced by dirt, ice or snow piling up on top of the antenna.

Dual frequency operation is possible, when two stacked radiating elements are designed to resonate at different frequencies. Wide band operation can be obtained by choosing the two resonant frequencies in the vicinity of each other. An antenna with two stacked patches yields a frequency band increase of two or more, keeping the cross-polarization at a lower level than when reaching the same bandwidthwith a single thick dielectric.

The study of multilayered structures is directly related to the design of monolithic arrays : it is expected that active devices will be integrated directly, on a substrate just below the radiating patches, and then connected to the antennas above them. The active devices require high permittivity substrates, such as GaAs or Silicon, while a high antenna efficiency can only be reached with low permittivity dielectrics. It is therefore important to possess an accurate simulation model for multilayer structures, in order to correctly optimize the overall performance of the assembly.

The present contribution considers the numerical evaluation and the mathematical behaviour of the Green's functions for potentials and fields produced by a Hertzian dipole placed on any one of the dielectric interfaces of the multilayered structure. The resulting mixed potential integral equation (MPIE) is then solved with a method of moments, to determine the current distribution on each metallic patch. The input impedance, or the scattering matrix of the feed assembly are then calculated, together with the radiation pattern of the structure. Theoretical and experimental results will be compared for practical configurations, including a broadband antenna and a dual frequency patch radiator.

B4-8
1600

MULTIPLY-CONNECTED MICROSTRIP DIPOLE ANTENNAS

Ahmad Hoorfar*, David C. Chang** and Elisabeth Penard**
*Department of Electrical Engineering
Villanova University
Villanova, Pennsylvania 19085
**University of Colorado
Campus Box 425
Boulder, Colorado 80309

The development of microwave integrated circuits induces a large demand for monolithic antennas. Microstrip antennas are good candidates for the design of compact systems, but offer a very narrow bandwidth typically 3 or 4% and even less on high dielectric constant substrate like GaAs.

A novel type of antenna is presented in this communication. This new design is based on a multi-resonances technique, where the key idea is to couple n strip-dipoles of slightly different lengths and to overlay the n resonances.

A transmission line model is used as a first approach in the case of two strips. The transmission lines are loaded at both ends by a reflection coefficient due to radiation. This coefficient is obtained by a bi-variational method. An antenna mode (i.e., currents are in phase) and a transmission mode (i.e., currents are out of phase) are excited. The two strips behave as two resonant coupled circuits: the separation between the two resonance frequencies becomes larger as the mutual coupling coefficient increases, and then, in order to get the modes to overlap the distance between the strips must be large.

To overcome this problem the strips are connected together by a short section of line. The connection acts as a short circuit for the transmission mode and provides an additional control on the amplitude and resonance of this mode but it has no effect on the antenna mode. The resonances can be overlapped by adjusting the extra length of the second strip, the position of the connection and the coupling parameters. In that case, the strip separation is very small (~.5 substrate thickness), and then the structure is very compact.

Results will be presented to show that a two-coupled trips structure improves the bandwidth compared with a single strip structure. For more convenience, an air dielectric substrate is considered. We are also planning to use a more accurate method in order to check those first results and also to extend the analysis to more strips.

Jan 1989 URSI Boulder

B4-9
1620

A MOMENT-METHOD/FLOQUET-EXPANSION ANALYSIS OF WIRE MESHES FOR REFLECTOR ANTENNA APPLICATIONS

Y. Rahmat-Samii*, W. Imbriale
and V. Galindo-Israel^

Jet Propulsion Laboratory
California Institute of Technology
Pasadena, CA 91109

Many currently used and planned satellite communication and scientific missions utilize large mesh reflector antennas because of their superb packaging, weight and deployment characteristics. TDRSS, Galileo, Quasat and Mobile Satellite missions are just some examples. To accurately predict radiation performance of these mesh reflectors, it is essential to understand the RF behavior of the mesh surfaces under different operating conditions. The most challenging problem in analyzing mesh surfaces is to carefully incorporate their intricate geometry into an electromagnetic modeling formulation.

Mesh surfaces are typically characterized by their thin periodic structure and their complex "weave" geometry. In the past, the exact nature of the weave was typically simplified in most of the electromagnetic modeling. This simplification ignores some important aspects of the mesh surface, namely, the nature of the weave and the effect of contact points. Experimentally, however, it has been found that severe performance degradation can be attributed to malfunctioning of the junction points and the weave itself.

To properly model the complex nature of the mesh surfaces the authors have recently investigated the development of a scattering model based on a Moment-Method/Floquet-Expansion approach. A very comprehensive computer program has been developed to allow detail description of the mesh geometry including multiple bends, mesh wire conductivity, polarization, wire thickness, etc. Representative numerical results are presented to demonstrate the utility of the computer program and comparisons are made against available numerical and measured data. Useful observations are made to show the effects of mesh weave, conductivity, and thickness on the RF characteristics of the mesh.

* Rahmat-Samii is now with UCLA.
^ The order of listing of the authors is arbitrary.

attachment

B4-10. 1640

ANALYSIS AND DESIGN OF A TRAVELING-WAVE ARRAY OF VERTICAL MONOPOLES IN A SUBSTRATE

S. C. Kwok
Electrical Engr. Dept.
University of Colorado
Boulder, CO 80306-7149

D. R. Jackson
Electrical Engr. Dept.
University of Houston
Houston, TX 77204-4793

An analysis and design technique is given for a traveling-wave array of vertical monopoles embedded within a grounded substrate, fed by a meandering stripline on the opposite side of the ground plane. If the monopoles are electrically short, a traveling-wave structure many wavelengths long may be constructed. In this type of an array the length of the meandering line sections between monopoles primarily controls the interelement phase shift, while the monopole heights primarily determine the monopole feed currents, and hence the array factor of the antenna.

The array is analyzed using a Bloch wave approach, which assumes a quasi-periodic wave propagation on the stripline. Each monopole corresponds to a unit cell of the structure, with the load impedances of the Bloch line being the active impedances of the monopoles. The active impedances in turn depend on the monopole currents, which depend on the Bloch wave propagation constant. Given a specified set of monopole heights and stripline geometry, the resulting nonlinear set of equations for the monopole currents may be solved for iteratively. Alternatively, given a specified interelement phase shift and Bloch wave attenuation constant (which is related to the array efficiency), a set of two nonlinear equations for the stripline section lengths and monopole heights may be solved. This procedure is then generalized to the case of variable attenuation constants for all the unit cells, so that arrays with arbitrary monopole current amplitudes may be designed.

As an example, a 10 element array with a 60° scan angle is designed and built. The measured pattern shows good agreement with the theoretical one.

C2-1
1400

INFORMATION THEORETIC CRITERIA FOR EMISSION COMPUTED TOMOGRAPHY

Alfred O. Hero III

Dept. of Electrical Engineering and Computer Science
The University of Michigan
Ann Arbor, MI 48109

Emission computed tomography (ECT) is a passive object reconstruction procedure which relies on the detection of photons generated randomly from a remote spatial emitter distribution. These photons can be in the form of high energy x-rays, e.g. in positron emission tomography (PET), lower energy x-rays, e.g. in radio astronomy, or rays in the visible spectrum, e.g. in optical astronomy. The spatial distribution of these photons on one of the detector surfaces constitutes an object projection, whose statistics depend on such factors as: system geometry, detector resolution, and the form of ray collimation used at the detector. Traditionally, design of ECT projection geometries has been difficult due to the trade-off between the mutually conflicting goals of high detector fluence and high spatial resolution, and due to poorly understood spatial sampling requirements. In this paper, we apply an information theoretic analysis to evaluate and optimize a set of two-dimensional tomographic projections for a general three-dimensional emitter distribution. The information-optimal projections maximize the inherent mutual information between the emitter distribution and the detection process. The information criterion provides a means for obtaining an optimal tradeoff between detector fluence, spatial resolution and spatial sampling associated with the detection system. The use of information maximization to produce raw data for subsequent imaging tasks can be justified by using results from rate-distortion theory. At the same time, it is important to note that the information-optimal projection geometry may be specified independently of any particular reconstruction, classification or detection algorithm. We will illustrate our approach with applications from single photon emission tomography (SPECT), PET, and other inverse problems.

C2-2
1440

IMAGE RECOVERY FROM LIMITED MEASUREMENTS OF SCATTERED FIELDS

M.A. Fiddy, Dept. of Electrical Engineering, University of Lowell, Lowell, MA 01854

There is considerable interest in the reconstruction of a quantitative image of a scattering object from data collected on the scattered field. This has particular relevance in microwave and acoustic imaging, especially when one is interested in imaging features that have dimensions of the order of the illuminating wavelength, i.e. when scattering effects are most pronounced. The majority of the algorithms developed for this purpose to date are based upon weak scattering approximations such as the first Born and Rytov approximations. These algorithms are computationally attractive because they can be expressed in terms of inversion of Fourier data in order to compute the image distribution.

In practice the Fourier data available, which are determined from the measurements of the scattered field, will be noisy and of limited extent, thus reducing the quality of the reconstructed image. A linear estimation method for signal and image recovery based on the theory of best approximation in weighted Hilbert spaces, known as the PDFT estimator, is briefly described. This paper describes a procedure developed to make use of prior knowledge of the scattering object to recover an optimal estimate for the image from these limited noisy Fourier data.

We go on to show how an inversion method that relaxes the need for weak scattering approximations to be explicitly made, can be formulated in terms of this reconstruction procedure, thus extending the applicability of such quantitative imaging techniques.

C2-3
1540

INVERSE THEORY OF SPECTRUM ESTIMATION

David J. Thomson
AT&T Bell Laboratories, Murray Hill, N.J. 07974

We discuss the estimation of the spectrum of the non-deterministic part of a time series in an inverse-theory framework. Standard inverse theory typically begins with an integral equation of the first kind relating observations to a desired function and builds an approximate solution in terms of the eigenfunctions of the associated homogeneous equation. Here, because we are interested in the second moments of the usual solution instead of the solution itself, it is convienient to introduce a basis for the spectral density function over a finite bandwidth. The coefficients of an expansion of the spectrum on this basis are determined by a components-of-variance like decomposition of the covariance matrix of the coefficients in the basic solution.

Our major result is the existence of a simultaneous orthogonal expansion of both the spectral density and of the induced eigencoefficient covariance matrix. The limiting spectral basis functions are eigenfunctions of a narrow band $sinc^2$ kernel and provide conditions both for unbiased estimation and for a Fisher information to superresolution tradeoff. The corresponding basis matrices are trace-orthogonal so that simple estimation procedures are available.
Examples using geophysical data are given.

C2-4
1620

IMAGE RECOVERY FROM LIMITED FOURIER MAGNITUDE DATA

C. L. Byrne
Department of Mathematics
University of Lowell
Lowell, MA 01854

There are many imaging applications for which Fourier data are collected but the measurement of Fourier phase is frequently difficult or impossible; we cite for example, scattering of higher frequency radiation, whether ultrasound, optical or X-ray.

A linear estimation method for signal and image recovery based on the theory of best approximation in weighted Hilbert spaces, known as the PDFT estimator, is described.From finite complex spectral, i.e. Fourier, data one can construct a continuous object estimate with a given support that is consistent with the data. Given Fourier magnitude data only, one can choose the phases arbitrarily in the above construction. The energy in the extrapolated spectrum is phase dependant and provides a cost function to be used in Fourier phase retrieval. The minimisation is performed iteratively, using an algorithm that can be viewed as an extension of the Gerchberg Papoulis algorithm and the Fienup error reduction procedure. The algorithm has been observed to converge rather than stagnate at a local minimum of the cost function, provided the Fourier magnitude data are sufficiently well over sampled with respect to the Nyquist frequency.

It can be shown also that this minimisation procedure can be implemented entirely in a coefficient domain and does not require iteration between the image and spectral domains; it is thus computationally very fast. Some numerical examples will be shown.

E1-1
1340

ACCOMPLISHMENTS IN THE ELECTROMAGNETICS OF LIGHTNING

Maj. R. L. Gardner
Dr. C. E. Baum
Air Force Weapons Laboratory
Kirtland AFB, NM 87117

Abstract

Electromagnetics plays an important role in lightning research both as a diagnostic of lightning behavior and as a principal means of coupling into modern systems which contain sensitive electronics. A great deal of progress has been made in both of these areas, and the results of much of that progress was recently assembled in a special issue of *Electromagnetics* on the electromagnetics of lightning (*Electromagnetics, Vol. 7*, Nos. 3-4, R. L. Gardner, ed.). Contributions in the following areas are described in this special issue:

1. Models of Fundamental Lightning Processes,
2. Measurements of Lightning Parameters, and
3. Lightning Interaction with Systems

Transmission line models of lightning form the state-of-the-art method for calculating the evolution of lightning currents in space and time. Recent contributions have increased the complexity of such models and their ability to model data on lightning evolution. Other recent models include the means of determining natural frequencies of posts with lightning attached and the motion of ion clouds in air.

Much electromagnetic data on lightning has been gathered recently both in the U. S. and in France. The data improves our understanding of the evolution of lightning discharges and the consequent electromagnetic threat.

Data from lightning interaction with systems forms an important part of the lightning data base. Three separate aircraft test programs have been conducted over the last several years resulting in a large data base that now needs to be reduced into a form that is most useful for systems designers.

Progress in each of the above three categories of electromagnetic research in lightning is described in summary form in this paper. The fundamentals, recent accomplishments, and suggested directions for new research are presented.

E1-2
1400

RADIATION AND DISPERSION EFFECTS FROM FREQUENCY-MODULATED HPM SOURCES

K.F. Casey
JAYCOR
39650 Liberty Street, Suite 320
Fremont, CA 94538, USA

D.G. Dudley
Electromagnetics Laboratory
ECE, Building 104
University of Arizona
Tucson, AZ 85721, USA

With the present advances in the design and development of high-power microwave (HPM) sources, there has occurred a concomitant increase in interest in efficient descriptions of the radiation from structures containing such sources. One such structure is circular waveguide. In this paper, we discuss the far-zone radiation produced by a frequency-modulated HPM source in circular waveguide. Possible multimode effects are included.

We begin with a description of the waveguide modes and the source excitation. We follow with a frequency-domain description of the radiated fields from an equivalent aperture source. We next discuss several methods for producing the time-domain fields through an inverse Fourier transform. Results are given first in terms of standard time and frequency domain plots. We also display representative results using *spectrograms*, a signal representation useful in certain aspects of signal processing. The spectrograms clearly display the effects of the frequency modulation of the source and the dispersion in the wave propagation, as well as multimodal effects which result from modal wave packets traveling at different group velocities.

E1-3
1420

HPM COUPLING IN THE SOURCE NEAR FIELD*

R. J. King and H. G. Hudson
Lawrence Livermore National Laboratory, L-156
Livermore, CA 94550

When testing full systems in HPM simulators, there may be need to conduct the tests in the near-field of the source antenna in order to obtain high incident fluences. In doing so, only a few ports of entry (POEs) may be illuminated at the same time. This leads to the need to address several important issues:

(a) What is the near-field structure (i.e., columnation, spot size and polarization purity) of the source antenna and how does it affect coupling?
(b) Are there significant mutual interactions between the source antenna and the test system? Between the POEs within the test system?
(c) Does near-field receiving cross-section have meaning, and if so, how does it compare with the far-field cross section?
(d) Can near-field tests on individual POEs be superimposed to predict the coupling response to plane wave (far-field) illumination of multiple POEs?
(e) Which are the most important POEs and at what frequencies are they important?
(f) How does the phase front of an incident wave contribute to coupling via multiple POEs?
(g) How do the angle and polarization of the incident wave effect coupling for one vs several open POEs?

This paper gives an overview of many of these issues and sites examples. It is part of an on-going effort to investigate all aspects of the phenomenology of HPM interactions with systems (King & Hudson, LLNL UCID-21493, Aug. 1988). Experimental results are given for near-field coupling into generic test systems. While we do not exhaustively answer all of these questions, certain trends are observed. From these, some general conclusions are drawn to guide the use of HPM simulators for testing full systems.

*Work performed under the auspices of the U.S. Department of Energy by the Lawrence Livermore National Laboratory under contract number W-7405-ENG-48.

E1-4
1440

FOCUSED APERTURE ANTENNAS

C.E. Baum
Air Force Weapons Laboratory/NTAAB
Kirtland AFB NM 87117-6008

The electromagnetic fields from aperture antennas can be represented as integrals over the aperture electric field. Maximizing the fields at an observer defines a focused aperture. In this case, the integrals simplify and the spatial and frequency parts conveniently separate. This makes the results also conveniently expressible in time domain.

E1-5
1520

BOUNDS AND TRENDS OF MICROWAVE COUPLING

K.S.H. Lee
Kaman Sciences, Dikewood Division
2800 28th Street, Suite 370
Santa Monica, CA 90405

Absorption cross section is perhaps the best measure of coupling. It directly yields the power or energy delivered to a load, given the characteristics of the incoming wave. In this paper we briefly review the derivation of the absorption cross-section formulas from a field-theoretic consideration, and discuss how bounds can be obtained from first principles. Analytical and experimental results will be presented for certain classes of front doors (antennas) and back doors (apertures).

E1-6
1540

SLOW WAVE TRANSMISSION LINES

Albert W. Biggs+ and Raymond W. Lemke
Air Force Weapons Laboratory
Kirtland Air Force Base, NM 87117-6008

This paper describes the development of a periodic transition structure which couples a slow wave (J.R. Pierce, Traveling Wave Tubes, Van Nostrand, 1950).transmission line to a fast wave transmission line. The slow wave transmission line is a coaxial transmission line with periodic square wave corrugations on the outer coaxial connector and a smooth wall for the inner coaxial conductor. The fast wave structure is a coaxial transmission line with smooth walls for the outer and inner conductors.

The periodic transition structure is a succession of abrupt steps in characteristic impedance spaced by equal electrical lengths of uniform line. For a given number of steps, bandwidth is maximized for given VSWR, or VSWR is minimized for given bandwidth. With the VSWR 'equal-ripple' response of a Tchebycheff polynomial, this optimum-stepped transformer is also known as a Tchebycheff transformer (S.B. Cohn, IRE Trans. MTT, MTT-3, 16-21, 1955, C.L. Doplh, Proc. IRE, 34, 335-348, 1946).

Comparisons of Tchebysheff and Binomial transformer designs give better performance with the former. Results are presented for different bandwidths in the form of inductance and capacitance per unit length along the line.

Simulations of power transmission with and without these transition sections indicate a significant increase in power transfer from slow to fast wave structures.

+On TDY from Electrical and Computer Engineering Department, University of Alabama in Huntsville, AL 35899.

E1-7
1600

REALIZATION OF SUBLAYER RELATIVE SHIELDING ORDER IN ELECTROMAGNETIC TOPOLOGY

L.H. Clark
University of New Mexico
Department of Mathematics and Statistics
Albuquerque, NM 87131
C.E. Baum
Air Force Weapons Laboratory
Kirtland AFB
Albuquerque, NM 87117

A fundamental problem in qualitative electromagnetic topology is the construction of the interaction sequence diagram given a preassigned shielding between all pairs of primary sublayers. Idealizing this into one of relative shielding order makes this problem amenable to graph theoretic treatment. A constructive characterization of the relative shielding order matrix for the primary sublayers, subject to various constraints, of an electromagnetic topology defined to the level of layers and sublayers is given.

E1-8
1620

SHIELDING PROPERTIES OF AN ENSEMBLE OF PARALLEL WIRES OVER A LOSSY HALF SPACE

Jeffrey L. Young
James R. Wait
Electromagnetics Laboratory
Department of Electrical and Computer Engineering
University of Arizona
Tucson, Arizona 85721

We determine the total electric field produced by an ensemble of thin wire scatterers over a flat lossy half space when illuminated by a plane wave whose polarization is parallel to the wires and the interface. By invoking the thin wire idealization, a matrix equation is given to determine the currents on each wire, from which the total electric field is obtained. Several plots are given to show how the wire's radii, the earth's conductivity, the incident angle and the total number of wires effect the shielding for a semi-circular shell. In many cases we demonstrate that the shielding effectiveness can be as much as 70 dB; for other cases, when the structure is of resonant dimensions, the shielding can be degraded to 20 dB. We show close agreement of our results with those furnished by a moment method code for the continuous perfectly conducting structure of similar dimensions.

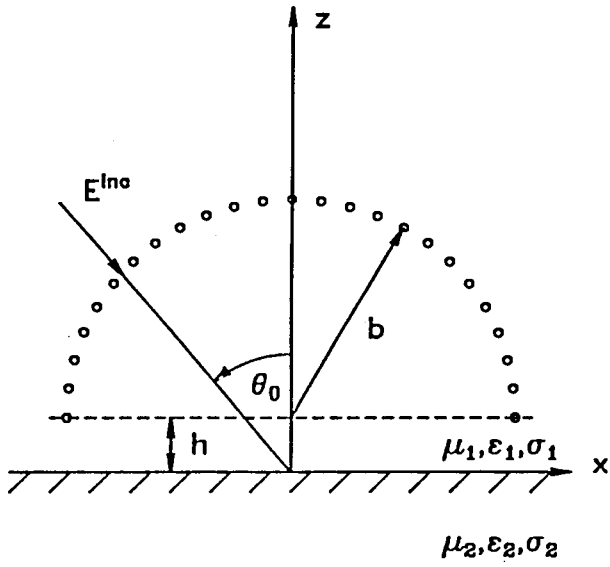

E1-9
1640

ENERGY NORMS AND 2-NORMS

C.E. Baum
Air Force Weapons Laboratory/NTAAB
Kirtland AFB NM 87117-6008

This paper defines an energy norm or e-norm based on the energy delivered to some port in a system. It is expressible as a weighted 2-norm. Criteria are developed for the frequency spectrum of time-domain excitation waveforms to bound the 2-norms and e-norm at the port. Canonical incident waveforms are introduced to give convenient bounds.

Session F-3 1355-Thurs. CR1-9
MILLIMETER-WAVE PROPAGATION
Chairman: J. Richter, Naval Ocean Systems Center, 444 Casitas Street, San Diego, CA 92107

F3-1
1400

94 GHz PROPAGATION IN THE EVAPORATION DUCT

K.D. Anderson
Ocean and Atmospheric Sciences Division
Naval Ocean Systems Center
San Diego, CA 92152-5000

One-way, low-altitude radio propagation measurements at 94 GHz and simultaneous surface meteorological measurements were made on a 40.6 km over-horizon, over-water path along the southern California coast to assess the effects of the evaporation duct on signal propagation. More than 2000 hours of received signal power--sampled approximately twice a second and averaged (rms) in ten minute intervals--were recorded in eight measurement periods from July 1986 to July 1987. The average received power was 63 dB greater than expected for propagation in a nonducting, or standard, atmosphere; 90 percent of the measurements were at least 55 dB greater than the standard atmosphere.

Predictions of transmission loss based on the observed surface meteorology compare favorably to the measured transmission loss; on the average, the predictions underestimate the transmission loss by 10 dB. In addition, transmission loss predictions based on an independent climatology of evaporation duct heights for the area also compare favorably to the observations. The reliability and reasonable accuracy of the model provide a strong justification for utilizing the technique to assess millimeter wave communication and radar systems operating in many, if not all, ocean regions.

Jan 1989 URSI

F3-2
1420

A POLARIMETRIC MILLIMETER-WAVE PROPAGATION MEASUREMENT SYSTEM

K.C. Allen, D.N. Haupt, R.J. Achatz, and D.L. Jones
National Telecommunication and Information Administration
Institute for Telecommunication Sciences
325 Broadway
Boulder, CO 80303

A fully polarimetric measurement system for millimeter-wave propagation studies has been developed. A single local oscillator (LO) is used for all frequency sources at the transmitter, so that the system is fully coherent. The receiver LO is phase locked to the lowest frequency transmitted, 9.6 GHz. Thus, the receiver LO is phase coherent with the transmitter LO, except for the propagation delay at 9.6 GHz. This enables the propagation delay of all higher frequency signals to be measured with respect to the delay at 9.6 GHz.

A vertically polarized signal at 28.8 GHz and a horizontally polarized signal at 28.815 GHz are transmitted from one antenna using an orthomode transducer. At the receiver, vertically and horizontally polarized components are received on one antenna, again using an orthomode transducer. After mixing with an LO frequency of 28.785 GHz, the signal components received using vertical polarization produce two intermediate frequencies (IF's) at 15 and 30 MHz, corresponding respectively to co- and cross-polarized signals. The horizontally received signal is treated similarly resulting in two IF's.

Each IF corresponds to one of the elements of the transmission matrix. By measuring the phase and amplitude of all four IF's the complete complex value of the transmission matrix can be measured.

Similarly, vertically and horizontally polarized signals are transmitted and received at 96.1 and 96.15 Ghz, enabling the measurement of the transmission matrix at this frequency.

By using separate frequencies for each polarization, instead of switching polarizations, extremely rapid changes in the transmission matrix can be measured.

Jan 1989 URSI

F3-3
1440

MEASUREMENTS OF MULTIPATH WITH A WIDE-BAND DIGITAL MILLIMETER-WAVE PROBE ON A PROBLEM PATH

D.L. Jones and K.C. Allen
National Telecommunication and Information Administration
Institute for Telecommunication Sciences
325 Broadway
Boulder, CO 80303

Measurements were made in March and April 1988 on an operational AT&T path (Salton-Brawley, CA) known to suffer from frequent multipath. Fading was studied on narrow-band CW links at 11.4 and 28.8 GHz, and on a wide-band, 500 Mb/s, BPSK link using a pseudo-random data word at 30.3 GHz. The wide-band link was also used as a channel impulse-response probe using the classical correlation technique.

The results are compared with fading measurements made in the operational bands at 4 and 6 GHz. Factors affecting the relative performance of centimeter- and millimeter-wave systems on paths for which multipath is a severe problem are discussed.

wideband links performed better; presumably due to smearing of reflecting ray in frequency - destructive interference will be narrowband.

Up to 60 dB fades were measured

Hogg says may be refractive rather than reflective

Jan 1989 URSI

F3-4
1500

MEASUREMENTS OF ATTENUATION IN RAIN ON A SHORT PATH IN HAWAII

K.C. Allen, R.O. DeBolt, and D.L. Jones
National Telecommunication and Information Administration
Institute for Telecommunication Sciences
325 Broadway
Boulder, CO 80303

Measurements of attenuation in rain on a 1-km path have been made in Hilo, Hawaii from February through September 1988 at 9.6, 28.8, 57.6, and 96.1 GHz. The rain rate was measured at a point while attenuation was measured over the propagation path. Because the sampling regions are not identical, the correlation between the instantaneous values of rain rate and attenuation are decreased. This decrease in correlation is in addition to that which results from variations in rain temperature, drop-size distribution, and noise.

Rain rate and attenuation are both approximately log-normally distributed. Therefore the log was taken of both, so that the analysis of the data could be made on approximately jointly normally distributed random variables. Two methods of analysis were explored to find the relationship between rain rate and attenuation.

In the first method, sample cumulative distributions of rain and attenuation rates were computed and values exceeded equal percentages of time were paired. This method mitigates the effects of any time delay differences in the measured rain rate and attenuation over the propagation path.

In the second method, sample distributions of attenuation, conditional upon rain rate, were examined. This permitted the computation of confidence intervals for attenuation values as a function of rain rate. Narrow confidence intervals are needed to determine if there are significant climatological or geographical differences in attenuation rates due to rain.

A comparison of the results of the two methods is made.

This is 4th set of similar measurements to determine location effects on specific attenuation (how does DSD change?)
Used laser rain gauge & tipping bucket
6.3 feet of rain in 9 months
at 96 GHz The four sites, slopes were close, but curves were offset. at 30, climate differences were smaller - scatter was an order of scatter computed for different DSDs (MP, L-P, ...)
Goldhirsh says use a disdrometer and calculate

F3-5
1540

PC SOFTWARE FOR ESTIMATING PROPAGATION EFFECTS ON SYSTEMS FROM 1 TO 1000 GHZ IN VARIOUS OPERATIONAL SCENARIOS

R.O. DeBolt and K.C. Allen
National Telecommunication and Information Administration
Institute for Telecommunication Sciences
325 Broadway
Boulder, CO 80303

Highly structured software for the IBM PC and compatibles has been developed to analyze propagation effects on systems in a wide variety of scenarios for frequencies from 1 to 1000 GHz. The software consists of three principal parts.

The first part is a user data base of equipment types, specifications, installations, and deterministic meteorological conditions. Software is provided to create and maintain this data base. The second part is a world climatological data base and a library of propagation subroutines for computing propagation effects and their statistics.

The third part is the analysis software, which uses the user supplied data base of equipment and installation specifications, the library of propagation subroutines and the climatological data base or deterministic meteorological conditions to predict propagation effects and system performance.

The user chooses a scenario type such as ground-to-satellite, aircraft-to-satellite, ground-to-aircraft, etc. Then the scenario is created by specifying the equipment and/or installations to be used in the scenario. A selection of analyses is available for each scenario type. For example, for a ground-to-aircraft scenario, the RSL can be computed as a function of flight path for a deterministic atmospheric profile and horizon around the ground station, the cumulative distribution of RSL for a fixed aircraft location can be found based on the climatology, etc.

Because the software is so highly structured, new scenario types and types of analysis can easily be added.

F3-6
1600

A MODEL FOR THE PERMITTIVITY OF ICE FROM 0 TO 1000 GHZ

G.A. Hufford
National Telecommunication and Information Administration
Institute for Telecommunication Sciences
325 Broadway
Boulder, CO 80303

To understand the reaction of radio waves to naturally occurring ice and snow, we need to know the permittivity as a function of frequency and temperature. While the general properties of ice are well known, there are important gaps of detail where existing data are both sparse and inconsistent.

The formulas given here seem to provide a good compromise between theory and the several sets of available data. For frequencies below 1 MHz a Debye form is used. The formula below are meant to be valid from 1 MHz to 1000 GHz and from 0 to -40°C. The real part, ϵ', and the imaginary part, ϵ'', of the permittivity are

$$\epsilon' = 3.15$$

and

$$\epsilon'' = \alpha(t)/\nu + \beta(t)\nu$$

where t is the temperature in degrees Celsius, ν is the frequency in GHz,

$$\alpha = (50.4 + 62(\theta-1))\times 10^{-4}\exp(-22.1(\theta-1)),$$

$$\beta = (-.131+.633/\theta)\times 10^{-4} + [7.36\times 10^{-4}\theta/(\theta-.9926)]^2,$$

and

$$\theta = 300/(273.15 + t).$$

F3-7
1620

A MODEL FOR ANISOTROPIC PROPAGATION IN THE MESOSPHERE CAUSED BY THE ZEEMAN EFFECT OF OXYGEN MICROWAVE LINES

H.J. Liebe and G.A. Hufford
National Telecommunication and Information Administration
Institute for Telecommunication Sciences
325 Broadway
Boulder, CO 80303

About 40 spectral lines of molecular oxygen are positioned in the 50 to 70 GHz band and at 119 GHz. At high-altitude (30-100 km) pressures, the O_2 lines appear as isolated features where, due to the geomagnetic field, their spectral signature is influenced by the Zeeman effect. Each line splits into three groups of Zeeman components, spread over a range of a few megahertz. These groups make up an anisotropic medium which can be described by a 3-dimensional matrix of complex refractivity.

The angle between the geomagnetic field vector and the direction of propagation for a plane radiowave determines a 2-dimensional matrix representing the changes of the field components within their plane of polarization. This 2x2 matrix has two complex eigenvalues with corresponding eigenvectors, each defining a *characteristic* wave. Generally, a radiowave, defined as a linear combination of these characteristic waves, changes its polarization state and amplitude with distance and, in the limit, approaches the polarization of the characteristic mode which has the lower attenuation rate.

Software was developed for the IBM-PC and compatibles which analyzes the behavior of a plane, polarized radiowave propagating at frequencies within a few megahertz of O_2 line centers through a spherically stratified mesosphere (U.S. Std. Atm.76). The program calculates for given latitude, longitude, and height (30-100 km) the matrix elements of refractivity. Next, the direction and elevation angle of the radiowave determine the eigenvalues of the characteristic modes, which are used to compute polarization state and amplitude versus distance. Propagation effects are accumulated along a slant path by accounting for changing atmospheric and geomagnetic conditions. A model of the geomagnetic field is included in the model.

G3-1
1400

UV IMAGE, SCINTILLATION AND RADAR STUDY FROM SONDRE STROMFJORD

Sunanda Basu[1], Santimay Basu[2], R.W. Eastes[2], R.E. Huffman[2], R.E. Daniel[3], C. Valladares[1], J.F. Vickrey[4], and R.C. Livingston[4]

[1] Emmanuel College, Boston, MA 02115
[2] Air Force Geophysics Laboratory, Hanscom AFB, MA 01731
[3] Computational Physics, Newton, MA 02164
[4] The SRI International, Menlo Park, CA 94025

We present a co-ordinated study of VUV images from Polar Bear together with TEC, phase and amplitude scintillations obtained from the same spacecraft supported by incoherent scatter radar observations to determine the origin of the perturbations on the beacon signals. Conclusive evidence was obtained for the E-region origin of these perturbations during fairly quiet auroral arc events observed during winter, sunspot minimum conditions when the F-region peak densities are much lower than the E-region peak densities created by the auroral ionization. The phase spectra were found to be rather steep with spectral indices on the order of -4. The electron density profiles expected from the Polar Bear emissions at 1356 Å and 1596 Å were computed using an auroral model and compared with the simultaneous radar profiles. Surprisingly good agreement was observed when spatial and temporal coordination was achieved between satellite and radar fields of view. The linear growth rate of the $\vec{E}x\vec{B}$ gradient drift instability in the $\vec{E}$ region was computed using the simultaneously measured neutral winds by a Fabry-Perot interferometer and the electron drifts measured by the radar.

G3-2
1420

MULTITECHNIQUE OBSERVATION OF THE POLAR CUSP/CLEFT AT SONDRE STROMFJORD

C.E. Valladares[1], R.E. Sheehan[2], F.J. Rich[3] and R.J. Niciejewski[4]

[1] Emmanuel College, Boston, MA 02115
[2] Boston College, Chestnut Hill, MA 02167
[3] Air Force Geophysics Laboratory, Hanscom AFB, MA 01731
[4] University of Michigan, Ann Arbor, MI 48109

We report 5 multitechnique measurements of the polar cusp/cleft region which were performed during February and August 1988. We obtained co-ordinated data from the Sondre Stromfjord incoherent scatter radar and from the HiLat and DMSP satellites orbiting at 800 km. The interplanetary magnetic field conditions were monitored by the IMP-8 satellite during these measurements. At times when HiLat and DMSP observed a large flux of cusp/cleft-type soft electrons, the radar detected enhanced electron temperatures and regions of enhanced and depleted plasma densities. The high density part consists of plasma that has been exposed to soft precipitation during times longer than about 5 minutes, in accordance with calculations of density production due to particle precipitation. The low number density region seems formed by fresh plasma rapidly convecting toward the cusp region. We discuss the variation of the cusp/cleft parameters (Te, Ne) depending on season, B_z and magnetic activity for these 5 case studies. We wish to point out that most of the features in our data can be explained in terms of cleft precipitation, consequent higher exospheric temperatures and convection.

G3-3
1440

CORRELATING POLAR CAP PLASMA DRIFT WITH THE IMF

B.W. Reinisch[1], J. Buchau[2] and C. G. Dozois[1]
[1]University of Lowell
Center for Atmospheric Research
450 Aiken Street
Lowell, Massachusetts 01854
[2]Air Force Geophysics Laboratory
Hanscom Air Force Base, Massachusetts 01731

More than one year of polar cap drift data of the F region have been analyzed. The measurements were made at Qanaq, Greenland (87°N CGL) with a Digisonde 256 operated by the Danish Meteorological Institute. Drift velocities between 150 and 900 meters per second were observed. For February 1988, interplanetary magnetic field (IMF) data were available and the direction of the F region was compared with the north-south component Bz of the IMF. For Bz negative, the drift is antisunward; for Bz positive, it is irregular and often sunward. The response time of the ionosphere to sign changes in Bz is fast. Although fluctuations in Bz and the drift directions make it difficult to define a precise time, one can see a response generally within less than 30 minutes.

G3-4
1500

CONJUGATE OBSERVATIONS OF PLASMA CONVECTION NEAR THE DAYSIDE CLEFT: RESPONSE TO IMF B_y VARIATIONS

R. A. Greenwald[1], K. B. Baker[1], J. M. Ruohoniemi[1], J. R. Dudeney[2], and M. J. Pinnock[2]

[1]Johns Hopkins University/Applied Physics Laboratory
Johns Hopkins Road
Laurel, MD 20707

[2]British Antarctic Survey
National Environmental Research Council
Madingly Road
Cambridge, CB3 OET, England

Since January 1988, HF radar systems located at Goose Bay, Labrador and Halley Bay, Antarctica have been making conjugate observations of plasma irregularities and their convective motions in the auroral zone and polar cap. Many of these conjugate measurements have been made in the vicinity of the high latitude cleft near local noon where complex IMF B_y-dependent plasma flows are known to exist. In this paper we present examples of temporal variations in large scale two dimensional flow patterns observed in this region as a consequence of temporal changes in the IMF B_y-component. The responses in the conjugate ionospheres are delayed by the sum of the propagation time of the solar wind to the magnetopause and the Alfven propagation time to the conjugate ionospheres. In general, for non-zero IMF B_y, this leads to a differential response time in the two hemispheres. The convection patterns observed are similar to the B_y-dependent Heppner-Maynard models.

G3-5
1540

FIRST RESULT FROM HF OBLIQUE BACKSCATTER SOUNDINGS TO THE NORTHWEST OF COLLEGE, ALASKA, USING A MODIFIED DIGISONDE 256

Robert D. Hunsucker and Brett S. Delana
Geophysical Institute
University of Alaska Fairbanks
Fairbanks, AK 99775-0800

During September 1988 K. Bibl and D. Kitrosser of the University of Lowell Center for Atmospheric Research (ULCAR) assisted by UAF personnel, modified an ULCAR Digisonde 256 to obtain HF oblique backscatter soundings. The addition of two log-periodic antennas, plus two power amplifiers, an antenna switching unit and software modifications now permit us to obtain several oblique HF backscatter soundings per hour without interfering with the regular vertical soundings. Since both amplitude and phase of the echoes are recorded, direct backscatter and groundscatter are fairly easily identified. Examples of echoes from aurorally-associated irregularities and "normal" groundscatter for Fall 1988 are presented.

G3-6
1600

THE DAYTIME F-LAYER TROUGH AND ITS RELATION TO MAGNETOSPHERIC CONVECTION

J.A. Whalen
Ionospheric Effects Branch (LIS) Air Force Geophysics Laboratory
Hanscom Air Force Base, MA 01731

The daytime trough is a fundamental and prominent feature of the winter ionosphere frequently resulting in depletions of solar produced electron density at the F-layer maximum by an order of magnitude near midday. As viewed by a world-wide array of Northern Hemisphere ionospheric sounders at solar maximum, this trough is observed to be spatially continuous in latitude and longitude and to be present on every day of a continuous 31 day period. During quiet conditions the trough seen in the afternoon contracts so as to be confined to magnetic latitudes above 70°, but during disturbed conditions it expands so as to extend continuously from polar cap to mid-latitudes.

The relation of the daytime trough to ionospheric-magnetospheric convection is seen in the fact that trough is very similar to the convection pattern in both morphology and dynamics. In addition two troughs are observed, one in the AM and one in the PM, which correspond to the two convection cells, dawn and dusk. The troughs appear in regions where sunward convection can displace high density daytime plasma with low density nighttime plasma. Furthermore there are enhancements of plasma within the nighttime polar cap which are consistent with antisunward convection displacing nighttime plasma with daytime plasma.

These trough and polar cap features vary in extent and magnitude from day to day but are such a common occurrence that they are visible in the monthly medians of foF2 throughout a large range of latitude and longitude. These features are particularly evident at stations near 75° MLat which are in sunward convection in daytime but in anti-sunward convection in nighttime, and as a result detect both daytime trough components as well as the nighttime polar cap enhancement in their individual diurnal distributions.

G3-7
1620

MODELING TOTAL ELECTRON CONTENT VARIATIONS ASSOCIATED WITH POLAR CAP F LAYER IONIZATION PATCHES OBSERVED AT LOW ELEVATION ANGLES

G. J. Bishop and J. A. Klobuchar
Ionospheric Effects Branch (LIS)
Air Force Geophysics Laboratory
Hanscom AFB, MA 01731

Total electron content (TEC) variations associated with large ionospheric structures can be dramatically affected by varying the angle or velocity at which the line of sight transits the structure. Attempts to correlate TEC measurements from satellites at greatly differing altitudes, or to apply TEC data from one such measurement to a system with differing geometry must take these geometric effects into account.

TEC variations have been observed associated with patches of enhanced F region plasma in the polar cap ionosphere (E.J. Weber et al, JGR 91, 121-12, 129, 1986). These variations, that more than double background values in less than ten minutes, were generally dominated by the drift velocity of the patches since they were obtained using signals from satellites at 20,000 km altitude typically observed above 45 degrees elevation. Were these same patches to be observed using satellites at 1000 km altitude, for example, the variations would be dominated by the velocity of the ionospheric penetration point (IPP) of the line of sight and would not show the same temporal TEC gradients. If the same observations were to be made at low elevation angles, such as below 20 degrees, the IPP velocity would be further increased and the TEC values would result from a significantly different set of integration paths through the structure.

Results will be presented from a simplified analytical model of a 1000 km patch (after Weber et al, JGR 89, 1683-1694, 1984), showing TEC variation that would be observed when the line of sight is fixed and drift dominates compared with holding the patch stationary while the line of sight moves in elevation. Effects varying the elevation angle of the fixed line of sight and varying the position of the stationary patch will be discussed.

G3-8
1640

A PORTABLE IONOSONDE FOR STUDY OF THE HIGH LATITUDE IONOSPHERE

D. Mark Haines, D. F. Kitrosser and B.W. Reinisch
University of Lowell
Center for Atmospheric Research
450 Aiken Street
Lowell, Massachusetts 01854

The temporal and spatial variations in the high latitude ionospheric structure have been difficult to quantify. The limited successes often required large scale, labor-intensive campaign efforts and lack the broader base of understanding that can result from routine measurements obtained from a network of instruments. The University of Lowell Center for Atmospheric Research has developed a low power, miniature, portable version of its Digisonde sounders. The system will open new opportunities for comprehensive measurements of the high latitude ionosphere. The system compensates for the lower transmitted power by employing intrapulse phase coding and digital pulse compression. The data acquisition, control, signal processing, display, storage and automatic data analysis functions have been condensed into a single multi-tasking, multiple processor computer system while the analog circuitry has been condensed and simplified by use of reduced transmitter power, wide bandwidth devices, programmable logic devices, and commercially available expansion cards which are installed in the main computer.

The new technology incorporated into this system will be discussed. The major operating modes will be presented and examples shown to illustrate the potential for high latitude ionospheric studies. The system may be operated as a vertical or oblique sounder with the possibility for bistatic oblique forward scatter or backscatter configurations. The system is a combination of narrow frequency steps, long integration times (fine Doppler resolution), low power (reduced interference), lower cost and portability.

Session GH-1 1355-Thurs. CR1-46
ELECTROMAGNETIC ANALYSIS FOR IONOSPHERIC PROPAGATION
Chairman: J. Huba, Naval Research Laboratory, Code 4780, Washington, DC 20375-5000

GH1-1
1400

NUMERICAL FULL-WAVE SOLUTIONS TO THE MAXWELL EQUATIONS APPLIED TO PROPAGATING THROUGH AN IONOSPHERIC MEDIUM

P. A. Minthorn, C. H. Liu, and V. Sparrow
Department of Electrical and Computer Engineering
University of Illinois at Urbana-Champaign
1406 W. Green St.
Urbana, IL 61801

The study of electromagnetic wave propagation through an ionospheric medium, which is time-varying, inhomogeneous, anisotropic, and lossy, traditionally has been approached using methods which are derived by making fundamental assumptions about the solution, such as algorithms based on the stationary phase approximation, ray tracing for example, or algorithms derived from the parabolic wave equation, such as the use of phase screens. Many effects cannot be considered easily with these methods (backscatter, for example) and under certain conditions the underlying assumptions of these methods are not valid. An alternate approach is the solution of the Maxwell curl equations in the time domain using a finite-difference technique to solve for the fields. The advantage of this type of algorithm is the simple system of equations which describe the propagation and the medium. Any medium effects that can be described with a differential equation can be implemented using this technique. In addition, the solution is an exact one, within the limits of the numerical effects. The disadvantage has been the computationally intensive nature of this type of approach, but the new generation of supercomputers has made possible investigations of problems sufficiently realistic to be of interest to the propagation community.

The time-domain finite-difference algorithm has been implemented on a Connection Machine and the results are compared to cases which can be solved analytically or numerically using an established technique. Cases were chosen to demonstrate that the propagation code was working and that the representation of the dispersive, anisotropic medium was also correct.

GH1-2
1420

APPLICATION OF COMPUTERIZED TOMOGRAPHY TO THE INVESTIGATION OF IONOSPHERIC STRUCTURES

J. R. Austen
Department of Electrical Engineering
Tennessee Technological University
Campus Box 5004
Cookeville, TN 38505

T. D. Raymund, S. J. Franke, and C. H. Liu
Department of Electrical and Computer Engineering
University of Illinois at Urbana-Champaign
1406 W. Green St.
Urbana, IL 61801

J. Klobuchar
Trans-ionospheric Propagation Branch
Space Physics Division
Air Force Geophysics Laboratory / LIS
Hanscom Air Force Base, MA 01731-5000

J. Stalker
Physics Research Division,
Emmanuel College
Boston, MA 02115

Ionospheric Total Electron Content (TEC) measurements can be processed using Computerized Tomography (CT) to obtain two-dimensional images of ionospheric electron density (Austen, J. R., S. J. Franke, C. H. Liu, Ionospheric imaging using computerized tomography, *Radio Science, 23*, 299-307, 1988). The CT technique uses simultaneous measures of an integrated parameter (one-dimensional information) to generate a two-dimensional image in the region of the measurements. Using TEC data, CT reconstructs an image of the electron density structures in a vertical slice above the receiving stations. We successfully applied this technique to realistic simulations of ionospheric density variations over several tens of degrees and a height range of one hundred to one thousand kilometers, and also used a method, which is discussed, for approximating the peak height of the electron density profile. Also the potential quality of reconstructions is considered for various geometries and image resolutions. In particular, the image of a mid-latitude trough with background horizontal density gradient and large scale irregular structures has been reconstructed from TEC data which was generated from a model based on an incoherent scatter radar observation. The CT reconstructed image was compared with the contour map obtained by incoherent scatter rader. Good agreements have been achieved.

GH1-3
1440

SIGNAL INTENSITY STATISTICS UNDER NON-RAYLEIGH FADING CONDITINS

Lester L. DeRaad, Jr.
Morgan K. Grover
R & D Associates
P.O. Box 9695
Marina del Rey, CA 90295

Under strong scattering and multipath conditions, the intensity statistics of transionospheric radio signals saturate at the Rayleigh-fading limit. Intensity statistics under weaker scattering conditions are less well established. Empirical studies using satellite data have given conflicting results, but have tended to favor Nakagami-m as the better fit among those models tested.

This paper describes a numerical study of intensity statistics under weak scattering, and as a function of the spatial power spectral density (PSD) of the ionospheric structure. For different PSD parameterizations, numerical realizations of the ionospheric propagation medium are generated. The Fresnel-Kirchhoff scattering equation is then numerically evaluted to determine the received signal intensity statistics.

The results show that non-Rayleigh intensity statistics depend strongly on the PSD of the scattering structure, but in a fairly systemmatic manner. For a three-dimensional refractive index PSD of the form k^{-n} (k is the spatial wave vector), the probablility of very deep fades is found to decrease continuously with increasing n. For $n \lesssim 3.0$, Rice intensity statistics provide an excellent fit. For $n \simeq 4.0$, Nakagami-m statistics provide the better (but less perfect) fit, in apparent agreement with the sattelite experiments. The results demonstrate that no existing simple model (e.g., Rice, Nakagami-m, Gaussian, log-normal) can be accurate in general. However, Rice statistics give a useful "worst case" model which bounds the depths of fading under almost all cases of interest, including both weak and strong scattering conditions.

GH1-4
1520

THE FRACTAL DIMENSIONS OF IONOSPHERIC SCINTILLATION

Paul F. Fougere
AFGL/LIS
Hanscom AFB
MA 01731-5000

The power spectrum of ionospheric scintillation, especially phase scintillation, is often describable as a simple power law process over a large range of frequencies. A recent paper (Fougere,P.F.,J.Geophys.Res.90,4355,1985) has shown that the maximum entropy method (MEM),applied to ionospheric scintillation data ,produces very smooth power spectra with easily derivable spectral index. Such spectra are also characteristic of fractal noises with non-integral (fractional) dimensions.

The power law index derived by MEM will be compared with the fractal dimension derived by using a program suggested in (Grassberger and Procaccia ,Phys. Rev. Lett. 50,346,1983) over a large range of spectral indices from 0.5 to 5.0 using both simulated power law processes and real ionospheric scintillation data from the HiLat and Polar Bear satellites.

GH1-5
1540

INCOHERENT RADAR BACKSCATTER ENHANCEMENTS IN THE TOPSIDE IONOSPHERE

K. M. Groves, M. C. Lee
Plasma Fusion Center
Massachusetts Institute of Technology
Cambridge, Massachusetts 02139

J. C. Foster
M.I.T. Haystack Observatory
Westford, Massachusetts 01886

Intense ($\simeq$ 20 dB) enhancements of the incoherent radar backscatter spectrum from the topside ionosphere have been observed with the Millstone Hill UHF radar (Foster, et. al, *GRL, 15*, 160, 1988). Many of the observed enhancements occur at the local ion acoustic frequency producing large asymmetries in the measured ion line. A theory combining current-driven processes and nonlinear Langmuir wave interaction is investigated as the source of intense ion acoustic turbulence resulting in the enhanced UHF radar cross sections. The generation of Langmuir waves by suprathermal electrons associated with field-aligned currents is investigated.

GH1-6
1600

THEORETICAL AND SIMULATION TECHNIQUES APPLIED TO HIGH LATTITUDE IONOSPHERIC TURBULENCE

J.D. Huba, Plasma Physics Division, Naval Research Lab, Washington, DC 20375-5000

The high lattitude ionosphere is an exciting and dynamic region of near-earth space in which a variety of interesting plasma phenomena occur. In this talk we will present a basic overview of the theoretical and simulation techniques used to understand and model one of these phenomena: plasma turbulence. A brief discussion of the important physical parameters will first be presented in order to identify the relevant spatial and temporal scales. Based on these scales it is argued that turbulent density and field fluctuations can be described by either fluid theory or kinetic theory. The theoretical and simulation techniques for each type of theory will then be described for both linear and nonlinear applications. In addition to a general description of the various issues, specific examples will be given to illustrate the usefulness of each technique. Finally, a discussion of the outstanding problems remaining in the high latitude ionosphere will be presented.

Session J-4 1355-Thurs. CR2-26
SOLAR AND STELLAR RADIO BURSTS
Chairman: Timothy S. Bastian, National Radio Astronomy Observatory, Socorro, NM 87801

J4-1
1400

SOLAR AND STELLAR ACTIVITY AT RADIO WAVELENGTHS

George A. Dulk
Department of Astrophysical, Planetary and Atmospheric Sciences
University of Colorado
Boulder, CO 80309-0391

During the past decade there have been major advances in observing the radio emissions from the Sun and stars, thanks largely to the sensitivity of Arecibo and the VLA and the confidence given by the VLA that observed emissions are actually associated with particular stars. As a result, some ten categories of stars are known to be radio emitters, ranging from cool, dwarf flare stars to hot, giant, wind-emitting stars. The more recent of the observing techniques and observations, ranging from millimeter waves to kilometer waves, will be reviewed.

Four emission mechanisms are known to be important, two are incoherent (thermal bremsstrahlung and gyro-synchrotron), and two are coherent (plasma and cyclotron maser emission). It is often difficult to distinguish the former two, similarly the latter two. On the other hand the coherent mechanisms are distinguishable from the incoherent by their high brightness tempertures ($\gg 10^{12}$ K) and/or high degrees of circular polarization ($\gtrsim 50\%$). From theory, there has been significant progress in accounting for the high brightness and polarization of the coherent radiation, but little progress in elucidating the solar and stellar environments in which the emissions arise. This work will also be reviewed, emphasizing what new observations are needed to motivate and guide the theory.

J4-2
1440

RADIO STUDIES OF THE SUN USING THE CLARK LAKE RADIO TELESCOPE

N. Gopalswamy and M. R. Kundu
Astronomy Program
University of Maryland
College Park, MD 20742

We review some recent results from 2-dimensional imaging observatins of the Sun suing the Clark Lake multifrequency radio heliograph. The radio heliograph routinely mapped the Sun's corona on a daily basis at several frequencies within the range 20-125 MHz during 1982-87. We studied both large scale structures as well as transient phenomena such as bursts. Both bright (streamers) and dark (holes) sources are seen on the disk and limb. These features have been analyzed quantitatively to provide information about their 3-d structure and their rotation. Comparing radio heliograms with ray tracing maps we have derived some realistic parameters such as brightness temperatures and plasma levels in the streamers. One important result of this study is that the radius of the streamer does not change with increasing height.

Type III bursts, especially during low solar activity provide a wealth of information about the magnetic field structure along which they propagate. Using Clark Lake data and coronagraph images aboard P78-1 and SMM satellites we were able to show that the type III electrons propagate along open magnetic field lines contained in the coronal streamers. Preflare activity in the form of type III bursts were observed some tens of minutes before flares. The characteristics of type III emitting electrons were obtained from radio and hard x-ray data from SMM-HXRBS instrument. Simultaneous type III burst emission can occur from sources separated by distances as large as 10^6 km which indicate that accelerated electrons have access to widely separated magnetic field lines.

Radio signatures of both fast and slow CMEs were observed at Clark Lake. Using temporal and spatial analysis of moving type IV bursts, type II bursts and CMEs (from SMM-C/P) we found that the type II and CME need not have a direct cause and effect relationship. Instead, the type II seems to be generated by a "decoupled shock", probably due to an associated flare. We show an interesting example of a high speed type II shock occurring minutes before a slow moving type IV associated with a slow CME. Since the slow CME can produce only a slow shock, this provides severe constraints on the origin of energetic particles because slow shocks cannot accelerate particles. Based on our observations, we have tried to constrain the emission mechanisms of moving type IV bursts.

J4-3
1520

VLA OBSERVATIONS OF SOLAR AND STELLAR RADIO BURSTS

Kenneth R. Lang and Robert F. Willson
Department of Physics and Astronomy
Robinson Hall
Tufts University
Medford, MA 02155

Very Large Array (VLA) observations at 20 cm wavelength specify the temperature and magnetic structure of coronal loops within solar active regions. Snapshot maps at intervals as short as 3 seconds indicate that explosive radio bursts originate at the apex of these loops, and that the bursts may be triggered by preburst heating within coronal loops or magnetic interaction between the loops.

VLA observations at 90 cm wavelength specify closed and open magnetic structures in the low solar corona. Large-scale magnetic loops are often associated with filaments or coronal streamers rather than active regions. Type I radio bursts, that occur during solar noise storms, originate near the apex of large-scale magnetic loops that connect active regions with more distant regions on the solar surface. Successive Type I bursts can originate in the same source. Successive components of other 90-cm bursts originate in the widely-separated legs of magnetic loops. The large-scale 90-cm loops may interact with the smaller-scale 20-cm ones, giving rise to solar bursts within an underlying active region. Similar VLA observations will provide new insights to the unknown initiating source of coronal mass ejections observed by satellite coronagraphs.

VLA observations of dwarf M flare stars indicate narrow-band emission (for YZ Cmi), while Arecibo observations indicate rapid variations, small source sizes and high brightness temperatures ($T_B \geq 10^{12}$ K for AD Leo and EQ Peg). Coherent radiation mechanisms are required, placing constraints on the stellar magnetic fields and coronal electron densities . We have not detected evidence for frequency drifts during radio bursts on stars other than the Sun, suggesting that electron beams and shock waves may not play a dominant role in the radio bursts form dwarf M flare stars.

J4-4
1540

RECENT RESULTS IN SOLAR MICROWAVE BURST SPECTROSCOPY

D.E. Gary, G.J. Hurford
Solar Astronomy 264-33
California Institute of Technology
Pasadena, CA 91125

Theoretical considerations indicate that the shape of solar microwave burst spectra for homogeneous sources can be used to uniquely identify the emission mechanism. The peak frequency and maximum flux density of the spectrum depend on the effective temperature and number of the radiating electrons, the source size, and magnetic field parameters. Such parameters can be obtained directly from the spectrum when the source is homogeneous or is spatially resolved.

Observationally, however, it is rare to spatially resolve a burst at a large number of frequencies, and there is considerable evidence to indicate that unresolved sources are usually not homogeneous. Such evidence includes previously reported two-frequency VLA observations and observations from Owens Valley that show microwave spectra with multiple spectral components.

We discuss a case in which a rare simple burst was observed and illustrate how the information inherent in the microwave spectrum can be extracted when the source is homogeneous. The method can also be applied to bursts dominated by single sources which need not be homogeneous provided that the burst can be resolved and located at each frequency. In this case, information regarding the spatial gradients in the source parameters can be obtained. We discuss this expectation in the light of new 3-element observations obtained during the summer of 1988 at OVRO. These observations give the first true brightness temperature spectra obtained with high frequency resolution.

J4-5
1600

DYNAMIC SPECTRA OF RADIO BURSTS FROM FLARE STARS

J. Bookbinder
Smithsonian Astrophysical Observatory
Cambridge, MA

T.S. Bastian
National Radio Astronomy Observatory, Socorro, NM

G.A. Dulk
Department of Astrophysical, Planetary and Atmospheric Sciences
University of Colorado, Boulder, CO

and
M. Davis
National Astronomy and Ionosphere Center, Arecibo, PR

Abstract

Intense, highly circularly polarized radio bursts from dMe flare stars were recorded as *dynamic spectra* with 20 ms resolution using the autocorrelator at the Arecibo 305 m telescope. We report on observations of AD Leo at 1.4 GHz with a bandwidth of 40 MHz and of YZ CMi at 430 MHz with a bandwidth of 10 MHz. Because man-made radio frequency interference (RFI) can mimic stellar emissions when observed with a single-dish telescope, we have employed several methods to distinguish between them based on their temporal characteristics, spectral characteristics, off-source monitoring, and the antenna response function.

Those bursts identified as stellar in origin display a rich variety of structure in the frequency-time domain, including spikes of rise time less than 20 ms and duration less than 50 ms that attained flux densities up to 940 mJy; the corresponding brightness temperature is 1.2×10^{16} K. In addition, quasi-periodic pulsations were observed with an amplitude greater than 50% and a period of about 0.7 s, and "sudden reductions" of flux density. Some of these properties are similar to those of certain solar bursts at decimetric wavelengths.

We interpret the emission in terms of coherent emission processes driven by a loss-cone anisotropy. Two regimes are possible: i) if the ratio of the electron plasma frequency ω_p to the gyrofrequency Ω_e is such that $\omega_{pe}/\Omega_{Be} \lesssim 3$, then electromagnetic waves are amplified at low harmonics of the gyrofrequency, i.e., a cyclotron maser; ii) if $\omega_{pe}/\Omega_{Be} \gtrsim 3$ upper hybrid waves are amplified and plasma radiation is produced near the fundamental and/or second harmonic of the plasma frequency. We suggest that the quasiperiodic pulsations observed during one event were caused by MHD oscillations in a magnetic loop.

J4-6
1620

PROPAGATION AND ABSORPTION OF ELECTRON CYCLOTRON MASER EMISSION DURING SOLAR AND STELLAR FLARES

Michael E. McKean
Department of Astrophysical, Planetary and Atmospheric Sciences
University of Colorado
Boulder, CO 80309–0391

The electron cyclotron maser is believed to be the source of microwave spike bursts often observed during solar and stellar flares. There are reasons to believe that large amounts of energy are involved in the cyclotron maser radiation, that very little escapes from the flaring region, and that most is reabsorbed and heats a large volume of the plasma surrounding the flare region. Subsequently, the bulk of the energy escapes as soft X-ray radiation. In this talk, the propagation and absorption of the maser radiation during solar flares are examined through linear theory and electromagnetic particle simulations. It is shown using linear theory that strong absorption of the radiation should occur as it propagates towards the second harmonic layer where the magnetic field is half as strong as in the emission region. Particle simulations are used to evaluate the nonlinear response of the plasma as the maser radiation propagates through the absorption layer. It is shown that some of the maser radiation is able to escape through a process of absorption below the second harmonic of the local gryofrequency and reemission above it. The fraction able to escape is much higher than that predicted by linear theory, although the amount of escaping energy is only a small fraction of the incident energy. The bulk of incident energy goes into the perpendicular heating of the ambient electrons. A few electrons are accelerated to several tens of keVs as a result of the heating.

J4-7
1640 THE OWENS VALLEY FREQUENCY-AGILE INTERFEROMETER

G.J. Hurford, D.E. Gary
Solar Astronomy 264-33
California Institute of Technology
Pasadena, CA 91125

The Owens Valley Radio Observatory (OVRO) frequency-agile interferometer can make solar observations at up to 86 frequencies in the range 1-18 GHz. The system is based on a pair of 27 m antennas and occasionally incorporates a 40 m diameter antenna for 3-element interferometry with baselines up to 1.25 km. By observing at up to 25 frequencies per second, the system functions effectively as a microwave spectrometer for the study of solar bursts and active regions.

We briefly describe the present instrument and emphasize its unique capabilities as a solar instrument. We show some recent results, including our experiences with broad band frequency synthesis as a technique to enhance spatial information. Finally, we discuss our plans to expand the instrument by adding 3 small (2 meter) elements, which, in conjunction with frequency synthesis, will substantially enhance the imaging capability.

J4-8
1700 THE NEW HIGH TIME RESOLUTION PROCESSOR AT THE VLA: M. McKinnon, New Mexico Institute of Mining and Technology, Socorro, NM 87801

Session B-5 0835-Fri. CR0-30
EM THEORY II
Chairman: Ross Stone, Stoneware Ltd., 1446 Vista Clarida, La Jolla, CA 92037

B5-1 0840

A SYSTEMATIC ANALYSIS OF STRAIGHT-WIRE ANTENNAS BY MEANS OF THE MODIFIED DIAKOPTIC THEORY

Chalmers M. Butler, Robert G. Kaires,
and William A. Walker
Clemson University, Clemson, SC 29634-0915

A systematic method, based on the modified diakoptic theory, is developed for analyzing straight-wire antennas of specified length and radius. The theory incorporates the exact kernel throughout so is applicable to cylindrical-tube antennas of any radius, provided the excitation is circumferentially invariant. In the modified diakoptic theory, zero-order and first-order currents are obtained from a simple integral equation scheme which necessitates only the determination of currents on short segments of the antenna, with the approximate current on each segment computed as if it were isolated from all other segments of the diakopted antenna. The open-port impedance matrix employed in the diakoptic theory is subsequently determined from these zero-order and first-order currents in a variational expression. For computational convenience, the approximate currents are represented in terms of basis functions and it is demonstrated that the open-port impedance matrix can be expressed as a matrix function involving the usual moment method impedance matrix. Much research has been devoted to the efficient and accurate computation of the elements of the moment method impedance matrix, which is utilized to great advantage in the calculation of the open-port impedance elements. Numerical results (currents and open-port impedances) are presented for straight wires, or cylindrical tubes, which are "diakopted" into P+1 segments, giving rise to P ports. For comparison, currents and open-port impedance matrices are obtained using a MoM solution for the entire wire. Excellent agreement is observed for all cases considered. It is pointed out that, in the modified diakoptic theory, wire current results from solving a system of linear equations which is far smaller than is necessary in the MoM technique applied to the same problem. For example, currents of comparable accuracy have been determined for various length wires by the two methods and one finds that the rank of the diakoptic matrix is typically less than one-tenth that of the MoM matrix.

B5-2
0900

AN EXTENDED FREQUENCY-DERIVATIVE MODEL FOR ADAPTIVE SAMPLING OF ELECTROMAGNETIC TRANSFER FUNCTIONS

E. K. Miller, Rockwell International Science Center, PO Box 1985, Thousand Oaks, CA 91360
G. J. Burke, Lawrence Livermore National Laboratory, Livermore, CA 94550
S. Chakrabarti, University of Kansas, Lawrence, KS 66045

A method was previously reported for estimating an electromagnetic transfer-function response by computing samples of the response and its first D - 1 derivatives at a single frequency to obtain the D coefficients of a rational-function model [G. J. Burke, E. K. Miller, S. Chakrabarti, and K. R. Demarest (1988), "On Reducing the Number of Frequency Samples Needed to Reconstruct an Electromagnetic Transfer Function", National Radio Science Meeting, Boulder, CO, January 5-8]. Besides reducing the computational cost by decreasing the number of samples required over the bandwidth of interest, an additional advantage arises because the number of operations needed to obtain the derivative information grows in proportion to N^2 for an N-unknown model compared with the N^3 cost of the frequency sample itself. In this presentation, we report on two extensions of that work: (1) use of two (or more) sampling frequencies for a single rational-function model; and (2) use of two (or more) models to develop the numerical uncertainty of the estimated transfer function in their region of overlap.

A potential advantage of using more than one sampling frequency for a given model is that derivatives of lower order can then be employed, albeit at some loss of computational efficiency. But using lower-order derivatives might compensate for decreased efficiency by increased computational robustness of the estimation process. The use of multiple models based on sets of data which differ by one or more of their samples also provides an error estimate in the region of model overlap which could be useful for developing a strategy for adaptive sampling. These issues are explored using simulated and moment-method data and the tradeoff between efficiency and accuracy in determining a transfer function is assessed. The basic idea is to develop a strategy for selecting the fewest samples and achieving the least computational cost while satisfying some error criterion over a bandwidth for which the transfer function is sought.

B5-3
0920

AN OVER-RELAXATION METHOD FOR THE ITERATIVE SOLUTION OF INTEGRAL EQUATIONS IN SCATTERING PROBLEMS

R.E. Kleinman
Center for the Mathematics of Waves
University of Delaware
Newark, DE 19716, U.S.A.

G.F. Roach
Department of Mathematics
University of Strathclyde
Glasgow G1 1XH, Scotland

L.S. Schuetz, J. Shirron
Acoustics Division
Naval Research Laboratory
Washington, D.C., U.S.A.

P.M. van den Berg
Laboratory for Electromagnetic Research
Department of Electrical Engineering
Delft University of Technology
The Netherlands

Abstract

A simple iterative method for solving many of the integral equations arising in scattering problems is presented. By introducing a relaxation parameter the equation is changed to one which may be solved as a Neumann series. An explicit choice of the relaxation parameter is proposed which does not require detailed knowledge of the spectrum nor does the method require the symmetrization of the, in general, non-selfadjoint integral operators that occur. Convergence of the method is demonstrated in examples where the Neumann series for the original equation either diverges or converges at a much lower rate.

B5-4
0940

EXACT FORMULAS FOR THE REACTIVE INTEGRALS OF THE ELECTROMAGNETIC SCATTERING PROBLEM FOR NONHOMOGENEOUS, ANISOTROPIC BODIES OF REVOLUTION

D.K. Cohoon and R.M. Purcell
Damaskos, Inc.
P. O. Box 469
Concordville, PA 19331

ABSTRACT

Three novel exact formulas and one novel numerical method, involving a Runge Kutta step adjusting integration around a Branch cut, have been developed to evaluate reactive integrals associated with the temperate, rotationally--invariant fundamental solution of the free-space Helmholtz operator. These integrals arise in the discretization of the integral equation of electromagnetic scattering describing scattering by an aniostropic, inhomogeneous body of revolution with the size of the matrix representing a discretization of the associated integral operator being reduced by Fourier analysis of the induced electric and magnetic fields. There is one integral to be evaluated associated with each coefficient in the expansion with the coefficient of $\exp(im\psi)$ being called the mth order mode. With the three exact methods, there is no increase in computational complexity as the mode index m increases. The integrals which we have evaluated have the form,

$$I^{(c)}_{(\ell,m)} + iI^{(s)}_{(\ell,m)} = \int_0^{2\pi} \frac{e^{i\xi}}{\xi^{\ell}} \cos(m\psi)d\psi = -i \oint_C \frac{e^{i\xi}}{\xi^{\ell}} \zeta^{m-1}\, d\zeta$$

where C is $\{\zeta \varepsilon \mathbf{C} : |\zeta| = 1\}$

$$\xi^2 = (A - 2B\cos(\psi))$$

$A^2 > 4B^2$, $A > 0$, $\ell = 1, 2, 3, \ldots$ and $m \varepsilon \{0, 1, 2, \ldots\}$ and $I^{(c)}_{(\ell,m)}$ and $I^{(s)}_{(\ell,m)}$ are real valued functions of m and ℓ.

Our exact Mie-like determination of the radiation scattered by a multi-layer anisotropic sphere was used for benchmarking.

B5-5
1020

ELIMINATION OF SPURIOUS RESONANCES FROM THE UNAUGMENTED ELECTRIC AND MAGNETIC FIELD INTEGRAL EQUATIONS

David A. Ksienski
Electrical Engineering and Applied Physics
Case Western Reserve University
Cleveland, Ohio 44106

The electric and magnetic field integral equations are sometimes used in an augmented form to avoid difficulties with spurious internal resonances. In this paper it is shown that these resonances are a result of the method of application of the boundary conditions. A formulation will be presented which eliminates the internal resonances without requiring augmentation. This formulation will be compared to augmentation, and scattering from a metal sphere will be presented as an example.

B5-6
1040

CARTAN ALGEBRAS AND PROJECTIONS OF SOLUTIONS OF HIGHER DIMENSIONAL ELECTROMAGNETIC PROBLEMS ONTO THREE DIMENSIONAL SPACE

D.K. Cohoon and R.M. Purcell
Damaskos, Inc.
P. O. Box 469
Concordville, PA 19331

ABSTRACT

The use of Cartan algebras to decompose vector fields has been carried out. The curl operation is given by

$$\text{curl}(E) = \sum_{i=1}^{7} \left[\left[\frac{\partial E_{i+3}}{\partial X_{i+1}} - \frac{\partial E_{i+1}}{\partial X_{i+3}} \right] + \left[\frac{\partial E_{i+6}}{\partial X_{i+2}} - \frac{\partial E_{i+2}}{\partial X_{i+6}} \right] + \left[\frac{\partial E_{i+5}}{\partial X_{i+4}} - \frac{\partial E_{i+4}}{\partial X_{i+5}} \right] \right] \vec{e}_i$$

where $\vec{e}_i$ = the unit vector in the direction of the ith coordinate axis, $\vec{E} = E_1\vec{e}_1 + E_2\vec{e}_2 + E_3\vec{e}_3 + E_4\vec{e}_4 + E_5\vec{e}_5 + E_6\vec{e}_6 + E_7\vec{e}_7$ and $E_{i+7} = E_i$ and $X_{i+7} = X_i$ for all $i\varepsilon\{1,2,\ldots,7\}$.

A calculation shows that

$$\text{curl}(\text{curl}(\vec{E})) = \text{grad}(\text{div}(\vec{E})) - \Delta\vec{E}.$$

This implies that if $C^\infty(\Omega,\mathbb{C}^7)$ denotes the infinitely differentiable functions from the open set Ω of $\mathbb{R}^7$ into C^7, complex 7 dimensional space, that then every vector field is a curl plus a gradient. This follows from the fact that $\Delta\vec{G} = \vec{F}$ has a solution $\vec{G}$ in $C^\infty(\Omega,\mathbb{C}^7)$ for each $\vec{F}$ in the same space. Integral equations describing interactions with 7 dimensional heterogeneous anisotropic material have been formulated and exact finite rank integral equations (EFRIE) relate these to arbitrary projective approximation schemes so that the solution of the EFRIE is the projection onto the space of approximates of the solution of the original infinite rank integral equations. Resolvent kernel methods and exact solutions are obtained in the higher dimensional space, and provide an inverse integral equation by obtaining a Dyadic function space valued solution of an ordinary integrodifferential equation. Computer algorithms describing projected solutions have been obtained.

B5-7
1100

2D GREEN'S FUNCTION FOR A ROTATIONALLY INVARIANT ANISOTROPIC MEDIUM

J. Cesar Monzon
Damaskos, Inc.
P. O. Box 469, Concordville, PA 19331

A material that is anisotropic and rotationally invariant is in general inhomogeneous, possesses a center and does not admit ordinary plane waves as solutions. Here we obtain the 2D Green's function for a ten parameter material specified in cylindrical coordinates by:

$$\bar{\bar{\varepsilon}} = \begin{bmatrix} \varepsilon_{\rho\rho} & \varepsilon_{\rho\theta} & 0 \\ \varepsilon_{\theta\rho} & \varepsilon_{\theta\theta} & 0 \\ 0 & 0 & \varepsilon_{zz} \end{bmatrix}; \quad \bar{\bar{\mu}} = \begin{bmatrix} \mu_{\rho\rho} & \mu_{\rho\theta} & 0 \\ \mu_{\theta\rho} & \mu_{\theta\theta} & 0 \\ 0 & 0 & \mu_{zz} \end{bmatrix}.$$

For this specific choice of parameters, both polarizations decouple and only one of them needs to be treated explicitly since the other is obtainable via duality. Only the case of periodicity in 2π is treated explicitly. The Green's function representation is initially obtained in the form of a model angular spectrum which is not very convenient for numerical calculations. Via the use of suitable integral representations, the series is transformed into an integral representation wherein the anisotropy manifests in a discrete spectrum of filamentary sources plus an infinite sheet of sources; all sources being located in complex space, at a real radius but forming a complex angle with the observation point. Numerical results are presented and the implications of these new results discussed.

B5-8
1120

TIME-DOMAIN FIELD ANALYSIS FOR VERTICAL DIPOLE SOURCES ABOVE DIELECTRIC INTERFACE

Keijo I. Nikoskinen, Ismo V. Lindell
Electromagnetics Laboratory,
Helsinki University of Technology,
Otakaari 5A, 02150 Espoo, Finland

In the present analysis problem involving vertical magnetic or electric dipole above the planar interface of two lossless and dispersionless dielectric media is studied. Many attempts have been made to solve time-domain field equations mostly for VED source in this geometry during last decades, but these analyses appear to be rather complicated and final solutions cannot be applied easily to the field computation. In the present study this difficult task has been approached from a new direction by exploiting the time-harmonic results of the recently introduced exact image theory (EIT). It is shown that EIT is valid in the whole frequency range $-\infty < \omega < \infty$ and thus, its results can be Fourier transformed to obtain the time-domain field arising from a dipole source with $\delta(t)$ time dependence.

The problem is seen to split into two different cases depending on which medium is electrically denser with respect to the location of the source. If the medium containing the dipole has greater permittivity the reflected field is given as originating from a semiphysical image current located in the opposite side of the interface. Hence, the reflection field is a simple but exact integral expression, from which the well-known diffraction effect (the bow wave) can be directly seen, for example. In the converse case of refraction indeces the reflected field is given in the form of an infinite stable integral, from which the field can be integrated rapidly with a simple routine. In these both cases the derivation of the field expressions is mathematically less involved than the conventional time-domain studies in this geometry and the practical computation of the fields appears to be an easy task which is demonstrated with examples. As a special case of the present theory the lateral radiation from VED dipole on the boundary between the two dielectrics is evaluated and a numerical comparison to the results obtained elsewhere is made.

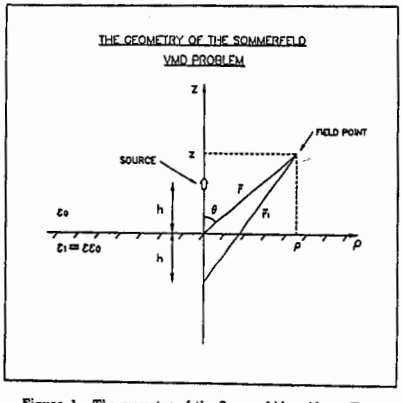

Figure 1. The geometry of the Sommerfeld problem. The media are nondispersive dielectrics with real permittivities ϵ_0 and $\epsilon_1 = \epsilon\epsilon_0$.

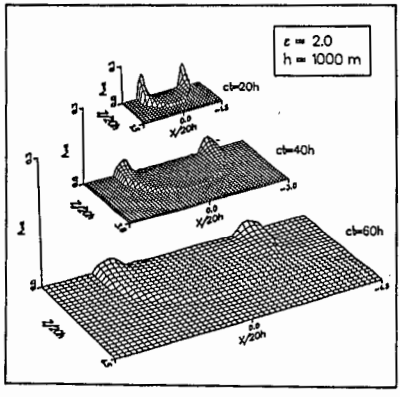

Figure 2. The evolution of the time-domain magnetic vector potential $A_{m3}(\bar{r}, t)$ due to the reflection. $h = 1000$ m and $\epsilon = 2.0$. The delta wavefront is not shown.

B5-9
1140

EDGE WAVE VERTEX AND EDGE DIFFRACTION

L. P. Ivrissimtzis, R. J. Marhefka
The Ohio State University, ElectroScience Lab.,
1320 Kinnear Rd.,
Columbus, OH 43212

The diffraction of an edge guided wave by the vertex and the edge of a perfectly conducting trihedron is studied asymptotically, as shown in the figure.

The edge wave is excited by a dipole radiating in the close vicinity of one of the edges of a semi-infinite wedge. Analytically, it is represented by the leading term in the power series expansion of the Green's dyadic for an infinite wedge. It is a ray optical wave singular at the edge.

The radiation integral of the surface current induced by the edge guided wave, which is then truncated, is evaluated asymptotically, resulting into vertex and edge diffracted ray contributions to the total pattern. A fringe current effect due to the terminating edges is superimposed to the previous result. The final asymptotic solution remains uniform across the shadow boundary of the edge diffracted edge wave.

The uniform asymptotic analysis is validated via comparisons with moment method computations and measurements for a dipole or monopole radiating in the close vicinity of one of the edges of a polygonal plate.

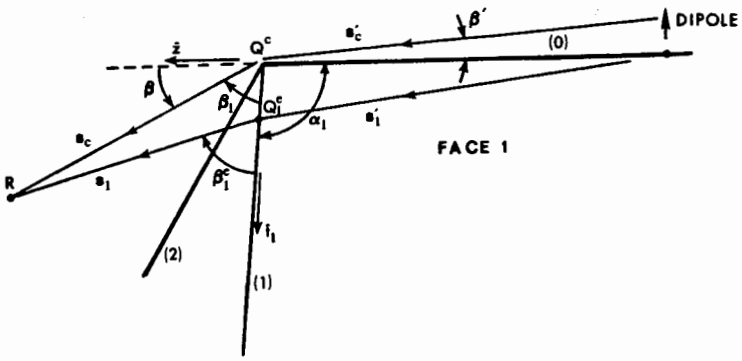

C3-1
0840

PERFORMANCE ANALYSIS OF SIGNAL MODE IDENTIFICATION ALGORITHMS

Richard J. Vaccaro
Department of Electrical Engineering
University of Rhode Island
Kingston, RI 02881

This talk presents theoretical analyses, which are appropriate for both high and low signal-to-noise ratios (SNR's), for algorithms which identify signal modes from noisy data. The analyses are verified by numerical simulation. The algorithms of interest are subspace-based methods which use the singular-value decomposition. An example of such an algorithm is low-rank linear prediction.

The performance of such nonlinear estimation algorithms can be classified as "above threshold" (for high SNR) or "below threshold" (for low SNR). At high SNR, the performance of a good algorithm should be close to the Cramer-Rao bound, and this performance can be predicted using some type of linearized analysis. Two such analyses are presented in this talk: one based on matrix approximation, and the other on Taylor series. These analyses are used to predict the high-SNR performance of a low-rank linear prediction algorithm for identifying signal modes.

At low SNR, the performance of an algorithm can no longer be predicted using linearized analysis, and other techniques must be used to predict threshold behavior. The threshold effect is characteristic of non-linear parametric estimation algorithms. When the SNR is below a critical threshold value, the variances of the estimated parameters is much larger than that predicted by the Cramer-Rao bound. In this case, the performance of an algorithm can be predicted by calculating the probability of an outlier occurring, and determining the threshold effect based on this calculation.

C3-2 0920 **Wavelets and applications.**

Ingrid Daubechies
A.T.&T. Bell Laboratories
Murray Hill NJ 07974

The wavelet transform of a function f is given by $\phi(a,b) = |a|^{(-1/2)} \int dx h\left[\frac{x-b}{a}\right] f(x)$, where h is the basic wavelet. The parameters a, b can be chosen to vary either continuously (a, $b \in R$, with $a \neq 0$), or in a discrete way ($a = a_0^m$, $b = nb_0a_0^m$, with m, $n \in Z$, and $a_0 > 1$, $b_0 > 0$). This transform is an alternative to the windowed Fourier transform; it allows for "zoom-in" on short-lived high frequency phenomena. For special choices of h, a_0, and b_0, the $h_{mn}(x) = a_0^{-m/2} h(a_0^{-m}x - nb_0)$ constitute an orthonormal basis of $L^2(R)$. The decomposition of a function with respect to such bases can be done extremely fast (faster than FFT!).

C3-3
1000 MAXIMUM LIKELIHOOD ESTIMATION OF PARAMETERS IN THE PRESENCE OF NON-GAUSSIAN NOISE
C.G. Constable, Institute of Geophysics and Planetary Physics, Scripps Institution of Oceanography, University of California, San Diego, La Jolla, CA 92093.

Least squares (LS) is a time honored technique for the estimation of model parameters. If the data errors are Gaussian and independent the LS estimators will be maximum likelihood (ML) estimators and will be unbiased and of minimum variance. However, if the noise is not Gaussian, e.*g.*, if the data are contaminated by extreme outliers, LS fitting will result in parameter estimates which may be biased or grossly inaccurate. When the probability distribution of the errors is known it is possible, using the maximum likelihood method, to obtain consistent and efficient (minimum variance) estimates of parameters. In some cases the distribution of the noise may be determined empirically, and the resulting distribution used in the ML estimation. A procedure for doing this will be described. Hourly values of geomagnetic observatory data contain a number of periodic components, whose amplitudes and phases are geophysically interesting: these will be used to illustrate the technique. Geomagnetic storms and other phenomena in the record make the noise distribution long-tailed, asymmetric and variable with location. Using an iterative procedure, one can model the form of these distributions using smoothing splines. For these data ML estimation yields quite different results from standard robust and LS procedures. A bootstrap technique is used to assess the usefulness of the uncertainty estimates obtained in both the ML and LS procedures. The technique has the potential for widespread application to other problems involving the recovery of a known form of signal from non-Gaussian noise.

C3-4
1100 EXPERIMENTAL MULTIFREQUENCY RESULTS ON ANGLE OF ARRIVAL ESTIMATION IN THE PRESENCE OF MULTIPATH: S. Haykin and V. Kezys, McMaster Univ., Hamilton, ONT L8S4K1

C3-5
1140

Spatial filtering of helioseismic data: Accurately retrieving modal amplitudes and frequencies

Michael H. Ritzwoller (Deptartment of Earth and Planetary Sciences, Harvard University, 20 Oxford St., Cambridge, MA 02138)

Timothy M. Brown (High Altitude Observatory, NCAR, Box 3000, Boulder, CO 80303)

Like the Earth, the interior of the Sun undergoes an intricate set of global oscillations with the patterns of motion resulting from interference among 10^7 resonant modes. The observed solar spectrum is very rich, with periods of clearly observed modes ranging from three to ten minutes and with horizontal wavelengths of a few thousand kilometers to global scales. Each mode resides in a cavity beneath the surface whose depth and extent depend on the geometry of the mode. Modal frequencies are a function of the stratification and dynamics of that portion of the sun where their amplitudes are appreciable. Modal amplitudes depend on the location, strength, and nature of the excitation process as well as the means of damping each excited mode. The accurate determination of modal frequencies affords remarkable ways of probing the solar interior. In particular, helioseismology holds the promise that models of differential rotation with depth and latitude can be refined sufficiently to give substantial guidance to the formulation of models of convection and the magnetic dynamo. In addition, amplitude information permits testing and discriminating between theories of the excitation and damping of the solar oscillations.

On a global scale, the sun is very nearly an axially symmetric object. Global scale features such as large scale magnetic fields and giant cell convection certainly exist but are believed to have a rather subtle expression in helioseismic data. However, on short spatial scales sunspots and solar granulation break the symmetry. Therefore, at least for the long wavelength components of the oscillation field, spherical harmonics Y_l^m form a natural basis set and each Y_l^m should be associated with a small set of dominant frequencies ${}_n\omega_l^m$ where n indexes the radial variation of the mode. Traditional methods for projecting the solar velocity field onto a Y_l^m have been based on Legendre transforms, whose success is dependent on the orthogonality of spherical harmonics. Unfortunately, spherical harmonics are not orthogonal when integrated over the domain accessible to observation (i.e., the sun's visible hemisphere), and these traditional methods of spatial filtering fail to isolate the single targetted Y_l^m. Rather, in a deterministic way, they retrieve a linear combination of spherical harmonics. This effect is known among helioseismologists as modal cross-talk.

In theory, modal cross-talk can be entirely eliminated by solving a simple least-squares problem in which the matrix is composed of all spherical harmonics within a given frequency band. This approach has been applied with success to geoseismological data at low frequencies since low frequency modes are often isolated in frequency and, hence, the matrix can be quite small . The solar spectrum is much more dense than its terrestrial counterpart and modes are never isolated. For example, in the 50 μHz band around 3 mHz approximately 4300 individual Y_l^m's contribute for $l \leq 150$. Fortunately, any specifed Y_l^m is significantly nonorthogonal only to a small set of other $Y_{l'}^{m'}$. Thus, to estimate the Y_l^m component we need also include in the matrix only the $Y_{l'}^{m'}$. In doing so, we have attempted to orthogonalize the basis functions on a subspace of the space spanned by spherical harmonics and, therefore, call this technique subspace orthogonalization.

We discuss the application of subspace orthogonalization to synthetic helioseismic data and compare results of its application to results of application of traditional spatial filtering techniques. We also discuss the application of both of these techniques to real helioseismic data.

Session DB-2 0855-Fri. CR0-36
WAVE GUIDING STRUCTURES
Chairman: J.B. Davies, University College, London, England

DB2-1
0900

HIGH-FREQUENCY PROPAGATION ON NONUNIFORM MULTICONDUCTOR TRANSMISSION LINES IN UNIFORM MEDIA

C.E. Baum
Air Force Weapons Laboratory/NTAAB
Kirtland AFB NM 87117-6008

This paper considers the asymptotic form for high frequencies of the equations of propagation on a nonuniform N-conductor transmission line. By considering the case of perfect conductors in uniform, isotropic media all N propagation velocities are the same, but the characteristic impedance matrix is allowed to vary with position along the line. Closed-form solutions are obtained for some cases of interest.

DB2-2
0920

TM WAVE EXCITATION AND SCATTERING ON ASYMMETRIC PLANAR DIELECTRIC WAVEGUIDE

Dennis P. Nyquist
Department of Electrical Engineering
Michigan State University
East Lansing, MI 48824

An asymmetric planar dielectric waveguide is formed by the typical tri-layered substrate/film/cover configuration in an integrated circuit environment. The structure supports surface waves when the film-layer guiding region has positive index contrast relative to its surround. An electric dyadic Green's function is constructed for the TM field maintained in the cover layer by currents immersed in that region. A direct complex-analysis approach leads to a source-point singularity contribution not present in conventional eigenfunction expansions for the electric field. The electric Green's dyad is exploited to study scattering of TM surface waves by dielectric obstacles in the cover layer.

If the x-axis is normal to the layer interfaces and the waveguiding z-axis is parallel to them, then y-invariant TM fields having x and z components are excited by similar components of current. Spectral analysis in the axial transform domain leads to

$$E_\alpha(x,z) = \int_{LCS} \sum_\beta G_{\alpha\beta}(x,z|x',z')J_\beta(x',z')dx'dz' \quad ...(\alpha,\beta)=x,z$$

where LCS indicates the longitudinal cross section of the source region and Green's dyad components $G_{\alpha\beta}$ have spectral integral representations. Subsequent to complex transform-plane analysis, the $G_{\alpha\beta}$ are decomposed into the superposition of a discrete surface wave contribution, arising from pole singularities, and the radiation field arising from integrations about substrate/cover branch cuts. The source point singularity leads to a term in G_{xx} proportional to $\delta(x-x')\cdot\delta(z-z')$, i.e., E_x proportional to J_x at that point.

If a dielectric discontinuity having index contrast $\delta n^2(x,z) = n^2(x,z)-n_c^2$ is immersed in the cover layer, then its induced field satisfies the system of EFIE's

$$E_\alpha(x,z) - j\omega\varepsilon_0 \sum_\beta \int_{S'} \delta n^2(x',z')G_{\alpha\beta}(x,z|x',z')dx'dz' = E_\alpha^i(x,z)$$

for $\alpha=x,z$, where S is LCS where $\delta n^2\neq 0$ and E_α^i is the incident surface-wave field. A pulse-Galerkin's solution leads to the induced field, from which scattering coefficients are calculated. Numerical results for reflected, transmitted and radiated power are obtained.

DB2-3
0940

EFFECTS OF CHIRALITY ON GUIDED EM WAVES

Nader Engheta and Philippe Pelet
The Moore School of Electrical Engineering
University of Pennsylvania
Philadelphia, Pennsylvania 19104

Electromagnetic chirality embraces both optical activity and circular dichroism. Optical activity refers to the rotation of the plane of polarization of optical waves by chiral media, whereas circular dichroism indicates a change in the polarization ellipticity of optical waves by such media. These phenomena are due to the presence of two unequal characteristic wavenumbers corresponding to two circularly polarized eigenmodes with opposite handedness. An isotropic chiral medium, which exhibits electromagnetic chirality, can be described electromagnetically, for time-harmonic fields, by the constitutive relations $\mathbf{D} = \varepsilon \mathbf{E} + i\xi_c \mathbf{B}$ and $\mathbf{H} = i\xi_c \mathbf{E} + (1/\mu)\mathbf{B}$ where ε, μ, ξ_c are, in general, complex and represent the dielectric constant, permeability and chirality admittance of the chiral medium, respectively.

We have shown that when cylindrical waveguides are filled with homogeneous isotropic chiral materials, novel and unique features are observed. This type of waveguides, we name *chirowaveguides*. In this talk, the theory of electromagnetic wave propagation in chirowaveguides will be presented and discussed. It is shown that the Helmholtz equations for the longitudinal components of electric and magnetic fields in such waveguides are always coupled, and consequently these waveguides cannot support individual TE, TM or TEM modes. The coupling coefficient is shown to be proportional to the chirality admittance ξ_c of the chiral material inside the waveguide. A general method for solving these coupled Helmholtz equations and obtaining dispersion relations will be given. As an illustrative example, the case of parallel-plate waveguide filled with a homogeneous isotropic chiral material will be presented and analyzed in detail and the corresponding dispersion relations, cut-off frequencies, propagating and evanescent modes will be given. It is observed that, for this chirowaveguide, there exist bifurcated modes which have common cut-off frequencies and unequal propagation constants for any given frequency. We have also observed that the dispersion (Brillouin) diagram for a chirowaveguide has three regions: the *fast-fast-wave* region, the *fast-slow-wave* region and the *slow-slow-wave* region. For each of these regions the electromagnetic field components in a parallel-plate chirowaveguide will be shown. Potential applications of chirowaveguides in integrated optical devices and communication systems will be addressed.

DB2-4
1000

ENTIRE-BASIS MOM ANALYSIS OF COUPLED MICROSTRIP TRANSMISSION LINES

C.-H. Lee, J.S. Bagby
Department of Electrical Engineering
University of Texas at Arlington
Arlington, Texas 76019

Y. Yuan, D.P. Nyquist
Department of Electrical Engineering and System Science
Michigan State University
East Lansing, Michigan 48824

A system of exact dyadic integral equations is utilized in the analysis of propagation in uniform coupled integrated microstrip transmission lines. Axially-transformed natural mode surface currents on N coupled microstrip transmission lines satisfy the homogeneous coupled dyadic integral equations:

$$\hat{t}_j \cdot \sum_{i=1}^{N} \int_{\ell_i} \overleftrightarrow{g}^{e}(\rho \,|\, \rho'; \zeta) \cdot \vec{k}_i(\rho')\, d\ell' = 0, \quad j = 1, \ldots, N$$

where $\vec{k}_i$ is the transformed surface current on the i^{th} strip, $\overleftrightarrow{g}^{e}$ is the electric Green's dyad of the background structure, ζ is the unknown propagation constant of the coupled mode, $\hat{t}_j$ is a unit tangent to the j^{th} strip, and ℓ_i is the cross-sectional contour of the i^{th} strip.

The above integral equation is solved by the method of moments. Longitudinal and transverse currents are expanded in entire basis functions consisting of Tchebyshev polynomials of the first and second kind with multiplicative factors incorporating the proper edge behavior. This formulation is shown to converge to accurate results in as few as three terms.

Numerical results in the form of dispersion curves and surface current distributions are presented for the dominant and first three higher order modes, both even and odd, for the case of two identical coupled lines.

DB2-5
1040

EFIE-BASED PERTURBATION APPROXIMATION FOR COUPLED MICROSTRIP LINES

Yi Yuan and Dennis P. Nyquist
Department of Electrical Engineering
Michigan State University
East Lansing, MI 48824

To solve the eigenvalue problem of coupled microstrip lines, a full-wave analysis based on an electric dyadic Green's function is developed. The electric field integral equations (EFIE's) are solved, by a Galerkin's MoM technique with Chebychev polynomial basis functions, for both isolated and coupled microstrip. The direct numerical solution becomes very time consuming for a coupled microstrip system, consequently an approximate coupled-mode perturbation formulation is pursued.

In this paper, we present an EFIE-based perturbation approximation to solve for the system eigenmodes of N coupled microstrip lines. In solving the coupled EFIE's, the eigenmode current of the isolated line (which is obtained by a Galerkin's MoM solution to the isolated EFIE in a convenient Chebychev polynomial series) is used as a first-order perturbation approximation for nearly-degenerate eigenmode currents of the loosely-coupled system. The EFIE's yield a matrix equation

$$\bar{C}_{mm} a_m [\zeta - \zeta_{mp}^{(0)}] + \sum_{n \neq m} C_{mn} a_n = 0 \quad \text{... for } m=1,2,\ldots,N$$

where ζ is the unknown propagation eigenvalue, $\zeta_{mp}^{(0)}$ is that eigenvalue for the p'th mode on the n'th isolated microstrip, a_n is the current amplitude, and the C_{mn} are coupling coefficients involving field/current overlap integrals. ζ is that value which leads to a non-trivial solution for the a_n. Since the C_{mn} are ζ-independent, the numerical procedure is relatively efficient. For the special case of two-line coupling, it is found that the propagation eigenvalues split and shift symmetrically away from their isolated limit as the two microstrip become closely spaced.

A numerical implementation of the perturbation method is developed. The numerical results of the perturbation approximation are compared with those of the MoM numerical solution. Computation times are also compared, and the validity range of the perturbation approximation is investigated.

DB2-6
1100

FREQUENCY DEPENDENT PROPAGATION CHARACTERISTICS OF MICROSTRIP STRUCTURES ON INHOMOGENEOUS SUBSTRATES

M.A. Thorburn and V.K. Tripathi
Department of Electrical and Computer Engineering
Oregon State University
Corvallis, Oregon 97331-3202

A. Agoston
Tektronix Laboratories
P.O.Box 500
Beaverton, Oregon 97077

Planar propagation structures with inhomogeneous substrates have been analyzed in recent years for both the quasi-static and freqency dependent characteristics by various techniques such as the method of lines and the mode-matching technique (Diestel, PhD Dissertation, Hagen 1984., Thorburn & Tripathi, URSI, 1988., Pregla, Koch, & Pascher, EMC 1987., Young & Itoh, MTT-35, #9, 1987.). The ability to accurately compute parameters such the propagation constant, current distribution, and field configuration for such structures with inhomogeneous substrates is important for a variety of applications including the design of optimized electro-optic modulators, determining the effects on a microstrip line as it nears the substrate edge, or designing ridge substrate and microslab waveguides. The problem was also among those identified as requiring attention in order to improve MMIC CAD modeling (Pucel, Proc. 16th European Microwave Conference, Sept 1986.).

In this paper the method of lines is extended to analyze the full wave electromagnetic propagation problem with general structures having inhomogeneous layers and then is applied to study the frequency dependence of the propagation characteristics of these structures. In order to illustrate the technique first a microstrip near the edge of a chip is examined and the effects of the substrate inhomogeneity on quantities such as the propagation constant, modal impedance, current distribution, fields, and attenuation constant are calculated. Next some dielectric slab waveguides and electro-optic modulators are examined and their phase velocities, losses, and impedances are computed.

The propagation constants of several microstrips near a substrate edge were measured as a function of the distance from the edge and the frequency by using the standard resonance measurement technique. The experimental results are found to be in excellent agreement with the computations. For our computations, we have used several machines ranging from a 386 based personal computer to a Cray supercomputer. The results and cpu times are compared and presented in the paper.

DB2-7
1120

ANALYSIS OF TRANSMISSION LINE STRUCTURES SUSPENDED BETWEEN INFINITE PARALLEL PLATES USING A NUMERICALLY EFFICIENT IMAGE-MODE GREEN'S FUNCTION

R. L. Olesen
Mission Sciences Corp.
6090 Jericho Tpke.
Commack, NY 11725

I. Tai Lu
Polytechnic University
Department of Electrical
Engineering & Computer Science
Webster Research Institute
Route 110
Farmingdale, NY 11735

A numerical analysis is developed for application to arbitrary structures suspended between infinite parallel ground planes. A Green's function that consists of numerically accelerated image-mode terms is presented. Transmission lines of arbitrary cross section, and number are analyzed using Moment method expansions with point matching. To further accelerate convergence for multiple conductors, a Gauss-Jacobian iteration solution is presented. Several configurations are studied, and compared with work given in the references where possible.

DB2-8
1140

VARIATIONAL AND FINITE ELEMENT SOLUTIONS OF TE MODES IN WAVEGUIDES WITH NONLINEAR MATERIAL

B.Davies*,R.Ettinger,A.Fernandez,A.Rahman,R.Souza
University College
Department of Electronic and Electrical Engineering
London WC1E 7JE, England
*Currently Visiting Professor at:
Department of Electrical Engineering
University of Colorado
Boulder CO 80309-0425

An alternative method is presented of solving for the TE modes in a uniform waveguide containing non-linear material. The method relies on an iterative scheme converging to a self-consistent solution. Solutions are obtained for stable and bi-stable modes.

Computer programs have written based on two methods for solution of the waveguides. Firstly, use of finite elements involving both 1st degree triangular elements and "infinite elements". Secondly use of Gauss-Hermite complete polynomials over the infinite domain. Both methods use a full 3-vector H-field, and apply the Rayleigh-Ritz procedure to yield a standard matrix eigenvalue problem.

As the refractive-index profile is field-dependent, an iterative procedure is used to determine a stable and consistent modal solution for a given power level. An initial calculation is performed with assumed negligible power level,- as though the waveguide contained only linear material. The resulting field is then scaled to the required power level, used to calculate the associated refractive index profile, and the problem is solved again. This iterative scheme is repeated until a consistent solution is obtained. The computer programs can analyze materials with Kerr or quite arbitrary forms of nonlinearity.

Symmetric and asymmetric step-index waveguides with Kerr-type nonlinearity have been analyzed. Results have been obtained and compared with analytical and other solutions in the literature. Agreement has been very good. A feature of this approach appears that ONLY physically stable solutions emerge.

Session G-4 0835-Fri. CR2-6

COMPUTATIONALLY FAST IONOSPHERIC MODELS AND THEIR APPLICATIONS

Chairman: David Anderson, Air Force Geophysics Laboratory, Ionospheric Physics Division, Hanscom AFB, MA 01731

G4-1 0840 STATUS OF URSI WG G.3 IONOSPHERIC MODELING EFFORTS

Charles M. Rush and Frank G. Stewart, National Telecommunications and Information Administration, U.S. Dept. of Commerce, 325 Broadway, Boulder, CO 80303-3328

URSI Working Group G.3 is responsible for the development of improved models of the ionosphere that can be used for telecommunications applications. The activities of the Working Group involve empirical ionospheric modeling, improving the global representation of ionospheric parameters, developing models of particular ionospheric phenomena, and putting together a data base that can be used to verify available ionospheric models. The status of this international effort will be reviewed and activities planned for the next year will be discussed.

G4-2
0900

IMPROVING THE INTERNATIONAL REFERENCE IONOSPHERE

D.Bilitza
National Space Science Data Center
GSFC, code 633
Greenbelt, MD 20771

We review the present status of the International Reference Ionosphere (IRI) model and discuss future plans. A new analytical description of the electron density in the region between E and F peak has been implemented into the IRI model. The improvement of IRI is shown in comparisons with satellite and incoherent scatter measurements. The new profile is based on Epstein functions and is determined by several characteristic parameters including the F1 density, the height of the half-F-peak-density point, and the E valley depth and width. A larger and better data base of these parameters is needed to further improve the IRI model in the middle ionosphere.

A similar formalism will be applied for the region below the E peak. In this region, however, conflicting results exist from ground-based and rocket measurements. The extension of incoherent scatter measurements to these low altitudes may help to resolve this problem and could considerably enlarge the data base for the lower ionosphere.

Finally, we discuss the accessibility of the IRI codes and the spectrum of IRI applications and users. We also indicate how real-time data can be used to enhance the reliability of the IRI predictions.

G4-3
0920

AN UPDATE OF IONOSPHERIC MODELS

M. Singh
Sachs/Freeman Association, Inc.
M. Reilly
Naval Research Laboratory
Ionospheric Effects Branch
Space Science Division
Naval Research Laboratory
Washington, DC 20375-5000

Ionospheric climatological models (e.g., IONOCAP, IRI-79,ICED) are based on monthly median values of ionospheric parameters with corrections for solar flux. Maximum day-to-day differences between the observations and modelled values can range from 30% during low solar activity to 40% during high solar activity at all local times. In this paper, we compare different ionospheric models and profiles produced by different models. In an attempt to improve upon the present models, observing stations are divided into geomagnetic latitude bins of about 2 degrees (e.g., Wallops Island (USA), Kiev (USSR), Tomsk (USSR), Sverdolsk (USSR) are in one bin). The analysis shows that the addition of a universal component, as inferred from data for a geomagnetic bin, to the IONCAP model yields fof2 values which are closer to observed data. It has been shown by previous workers that spatial correlation for either fof2 or TEC at a given local time is very low in an east-west direction after few thousand kilometers. However, if the universal component is first subtracted from the observed fof2 data for Kiev and Sverdolsk, the correlation results for the modified data show an improvement. Moreover, mid-latitude correction due to geomagnetic variations for ionospheric climatological models for fof2 is directly related to Kp, but present analysis indicates that a component for the variation in geomagnetic conditions (Kp or Dst) should be added to the fof2 corrections.

Furthermore, prediction of basic ionospheric parameters (e.g., fof2, hmf2, etc.) does not necessarily mean accurate prediction of profiles. Model profile results are compared with observed values of TEC at Sagamore Hill and Goose Bay. Results show that Elkin and Rush profiles are better not only for high-latitudes but also can out-perform the other profile models at mid-latitudes with a small modification.

G4-4
0940

AN ALTERNATE APPROACH TO THE DEVELOPMENT OF A foF2 MODEL

D.B. Sailors
Naval Ocean Systems Center
Ocean and Atmospheric Sciences Division, Code 54
San Diego, CA 92152-5000

The usual approach for developing a foF2 model is to develop a numerical map representing its global variation. This usually results in a large number of coefficients. In recent years another approach has been the development of models suitable for running on microcomputers. Although this has met with great success, it has been recently proposed that these models along with ionospheric measurements from a network of ionospheric oblique sounders be used to update sunspot number or solar 10.7 cm flux (M.H. Reilly and M. Daehler, Radio Science, 21, 1001-1008, 1986). This pseudo-sunspot number is then used to predict MUFs on paths throughout the region. Because the foF2 models used do not have adequate global variations of their parameters, sounder updating may produce extraneous sunspot numbers.

The approach taken here was to determine the parameters of the foF2 model in the MINIMUF algorithm from a data base of foF2 data measured at 175 sites. For the mid-latitudes supplementary data produced using model data from Rush et al. (Radio Science, 19, 1083-1097; Radio Science, 18, 95-107, 1983) was used in ocean areas to fill gaps. For the low-latitude region gap filling a semi-empirical model due to Anderson et al. (Radio Science, 22, 292-306, 1987) was used. The advantage of this approach is that the model would have the accuracy of the former models and the speed of the later model and would be suitable for sounder updating.

The parameter foF2 in MINIMUF (R.B. Rose and J.N. Martin, Naval Ocean Systems Center TR 186, February 1978) is modeled as a response of a dynamic system "driven" by a function of cos χ and based on an analog to a RC circuit. The solution to the differential equation for cos χ is a function of four parameters. The first parameter A_0 is the square of the foF2 at sunrise. The second parameter A_1 is a function of both the daytime variation of foF2 squared and the cos χ_{eff} at maximum foF2 during the day. The final daytime parameter τd represents the risetime of foF2 from sunrise. The parameter τn represents the decay of foF2 from sunset. To determine A_0, A_1 and τd it was necessary to develop an algorithm for solving a non-linear equation using foF2 data values at each hour during a month at each site for sunspot numbers 0 and 100. The algorithm was tested on the theoretical data points from 65°S to 65°N and only failed to find a solution 0.6% of the time. Having found A_0, A_1 and τd, τn was found using linear regression on the nighttime foF2 values. Contour plots of these four parameters for the theoretical data points indicate that the detail in geographic variation will likely require numerical mapping and that the geographical variation is a function of magnetic coordinates.

G4-5
1000

AIR WEATHER SERVICE SPACE ENVIRONMENTAL SUPPORT

Capts. C. R. Tschan and K. F. Havener
Aerospace Physics Division
Directorate of Aerospace Development
HQ AWS/DNXP
Scott AFB, IL 52225-5008

Air Weather Service (AWS) provides operational space environmental support to the entire Department of Defense over a wide range of altitudes. Although the space environmental support mission is constantly expanding, ionospheric support remains an important facet of AWS current and future operations.

Space environmental support is currently provided by Air Force Global Weather Central (AFGWC) at Offutt AFB NE. In the near future, all space environmental support operations will be transferred to the new state-of-the-art Space Forecast Center at Falcon AFB CO.

AWS is improving and expanding its space environmental support through the acquisition of several numerical models whose domains will extend from the Earth all the way to the Sun. In addition, AWS is studying and fielding new ground- and space-based instruments to gather the real-time data required to drive these models.

G4-6
1040

STREAMLINING THEORETICAL IONOSPHERIC MODELS FOR PRACTICAL APPLICATIONS

R. W. Schunk
Center for Atmospheric and Space Sciences
Utah State University
Logan, Utah 84322-4405

The ionosphere is a complex medium that displays a marked variation with altitude, latitude, longitude, universal time, season, solar cycle and geomagnetic activity. To a large degree, this variation is a consequence of the effects that the magnetosphere, neutral atmosphere and geomagnetic field have on the ionosphere. As a consequence, a rigorous numerical model of the ionosphere must allow for both molecular (NO^+, O_2^+, N_2^+) and atomic (O^+, N^+) ions, photochemical reactions, field-aligned diffusion and thermal conduction, ion-neutral energy and momentum exchange, magnetospheric and dynamo electric fields, production and heating due to particle precipitation, and other processes. Furthermore, in the numerical integration, discrete ionospheric features, such as the main trough, require a fine spatial resolution (10–100 km), and rapid auroral fluctuations require fairly small time steps (10–100 sec). It is no wonder that supercomputers are required for comprehensive ionospheric models. However, depending on the parameters desired and the accuracy needed, simplified numerical models of the ionosphere can be developed for practical applications. The limitations associated with such models will be discussed.

G4-7
1100

ICED-89: A LARGE-SCALE REGIONAL MODEL OF AN INSTANTANEOUS IONOSPHERE

H.W. Kroehl, C.D. Wells, T.F. Tascione,
D.N. Anderson and A.D. Richmond
National Geophysical Data Center
325 Broadway
Boulder, Colorado 80303

The Ionospheric Conductivity and Electron Density (ICED) model was designed to construct a three-dimensional ionosphere from available data, statistical data bases and empirical (and theoretical) algorithms for a given instant in time in a near-real time operational environment. High priority was assigned to the critical frequency of the F2 layer and to supporting ray tracing techniques. It was initially decided to construct a gridded ionosphere from layers and a profiler which were continuous functions in latitude, local time and altitude. Since an instantaneous ionospheric model must include the electrodynamics of magnetosphere-ionosphere coupling, different regions were identified which were characterized by different plasma processes, including magnetospheric convection, precipitating particles, neutral winds, diffusion, magnetic merging, etc. Statistical data bases were modified in each region by empirical or theoretical algorithms which utilize incoherent scatter radar data, topside sounder data, precipitating electron data and the MSIS model of neutral densities and temperature to reflect these effects. Vertical profilers were constructed from the same data sources and all the pieces were merged with care.

ICED was first formally presented at the 1988 Ionospheric Effects Symposium (Tascione et al., Radio Sci. 23, 3, 211, 1988). That version, ICED-86-II, covered the area from 20°N to 80°N geographic. Since ICED-86-II, a new model, ICED-89, has been built which contains the following changes: 1) Dave Anderson's Semi-Empirical Low-Latitude Ionosphere Model (Anderson et al., AFGL-TR-85-0254, Air Force Geophysics Lab, Hanscom AFB, MA, 1985) which allows us to add an equatorial region, 2) the use of the URSI-adopted foF2 numerical coefficients prepared by Matthew Fox, Leo McNamara, Frank Stewart and Charlie Rush (Fox and McNamara, IPS-TR-86-03, 1986) and 3) the replacement of the auroral oval with our Precipitating Electron Model which covers auroral, polar cusp and polar cap precipitation (Kroehl et al., EOS, 69, 1988).

During this presentation we will demonstrate the model characteristics for quiet and active, solar and auroral conditions and we will compare both the critical frequencies and regional profiles from this instantaneous model with other statistically-based, monthly models, e.g., IRI-85 and a modified Chiu model, and compare both with IS radar data.

G4-8
1120

A PARAMETERIZED, ANALYTIC MODEL OF THE HIGH LATITUDE IONOSPHERE

R. E. Daniell, Jr. and L. D. Brown
Computational Physics, Inc.
385 Elliot St.
Newton, MA 02164
D. N. Anderson
AFGL, Hanscom AFB, MA 01731
J. J. Sojka and R. W. Schunk
Utah State U., Logan, UT 84322

We are developing a real-time specification model for the high latitude ionosphere with the support of the Air Force Air Weather Service (AWS). The model is intended to be incorporated into ICED and will consist of two components: (1) a parameterized model of the high latitude ionosphere, based on the Utah State University (USU) Global Ionospheric Model, and (2) a real time system which adjusts the ionospheric model to match all available real time ionospheric data as closely as possible. This paper describes the parameterized version of the USU model.

The parameterized ionospheric model is being developed with emphasis on an accurate representation of the mid-latitude trough and auroral oval, but will include statistical description of polar cap features. When completed, it will be parameterized in terms of geomagnetic and solar activity indices and IMF orientation. The analytic representation is based on a series of standard runs of the USU model for a range of environmental parameters (e.g., season, solar activity, etc.) The result of each run is a database containing O^+, O_2^+, and NO^+ concentrations as a function of altitude, magnetic latitude, magnetic local time, and universal time. Each ion species is represented by a modified Chapman function (supplemented by a Gaussian function in the case of the molecular ions). The analytic representation of the electron density altitude profiles is obtained by summing the analytic representations of the individual species.

The parameters of the analytic altitude profiles are, in turn, represented by analytic functions of magnetic latitude and local time. We distinguish between the E-region (where the molecular ions dominate the electron density) and the F-region (where O^+ dominates). In each case, we recognized several subregions (e.g., the diffuse aurora, the convection dominated polar cap, etc.) characterized by the dominant physical processes which create or control the electron density. In each subregion, the analytic representation is tailored to its unique features with the further requirement that the representation be continuous and smooth across subregion boundaries.

G4-9
1140

THE NCAR THERMOSPHERE/IONOSPHERE GENERAL CIRCULATION MODEL AS A FORECASTING MODEL

R.G. Roble
High Altitude Observatory
National Center for Atmospheric Research*
P.O. Box 3000
Boulder, CO 80307-3000

The NCAR thermosphere general circulation model (TGCM) has been extended to include a self-consistent aeronomic scheme and a coupled global ionosphere. The time-dependent model calculates global distributions of electron, ion and neutral gas temperatures, zonal, meridional and vertical neutral winds, height of constant pressure surfaces, neutral composition O, O_2, N_2, $N(^4S)$, $N(^2D)$, NO, He, Ar and ion composition O^+, O_2^+, NO^+, N^+ and NO^+ as well as electron density. Mutual couplings between the thermospheric neutral gas and ionospheric plasma occur at each model time step and each point of the geographic grid. The self-consistent model requires only specifications of external sources, such as solar EUV and UV fluxes, aurora particle precipitation, ionospheric convection pattern, and the amplitudes and phases of semi-diurnal tides from the lower atmosphere. The use of this model for forecasting global thermospheric and ionospheric conditions will be described.

*The National Center for Atmospheric Research is sponsored by the National Science Foundation.

Session H-3 0835-Fri. CR1-46

WAVES IN IONOSPHERIC AND MAGNETOSPHERIC PLASMAS—RECENT THEORETICAL AND EXPERIMENTAL DEVELOPMENTS

Chairman: Delia Donatelli, RADC/EEP, Hanscom AFB, MA 01731

H3-1
0840

COHERENT AND TURBULENT 3-WAVE INTERACTIONS

Crockett L. Grabbe, Dept. of Physics and Astronomy, University of Iowa, Iowa City, IA 52242

Wave-wave interactions are a source of many phenomena observed in plasmas, such as turbulent cascades, stabilization of growing instabilities, anomolous resistivity, solitons, and recurrence. When the waves are phase-dependent 3 coupled equations of the wave amplitudes describe the 3 wave interaction, whereas for weak turbulence (random phase approximation) the 3 kinetic equations for the "occupation number" describe the state. Solutions and their behavior are presented for the weak turbulence state for the case that these numbers are treated as a square wave in k-space. The case of 3 interacting positive energy waves and the case that 1 wave is negative energy are shown to be 2 solutions of a transformed second order nonlinear differential equation. In the state of 3 coherent wave interactions the conservation laws, selection rules and methods of solution are reviewed. These exhibit recurrence and soliton solutions. Effects of diffraction and dispersion of these waves is discussed. A comparison is made of the similarities and differences in the turbulent and coherent states in the interaction.

H3-2
0900

Active Experiments in Bound(ed/less) Plasmas

William J. Burke
Space Physics Division
Air Force Geophysics Laboratory
Hanscom AFB, MA 10731-5000

A two-day workshop on active experiments in space, cosponsored by Northeastern University and the Air Force Geophysics Laboratory addressed the problem of injecting electromagnetic waves into space plasmas. The most direct way involves injection from ground and/or space based antennas. Plans for upgrading the HIPAS facility to ERPs in the multi-gigawatt range could significantly raise exploration thesholds for ionospheric excitation. ISIS sounder data has provide our main source for understanding in situ injection with monostatic and bistatic diagnosis. Though cold plasma dispersion theory explains many observations, it does not predict the observed generation of intense electrostatic waves. Laboratory observations of near field effects, like emitted wave modes becoming trapped in the antenna's sheath remain to be addressed in space. Intense waves in the sheaths of properly configured antennas offer intriguing possibilities for accelerating local electrons. An indirect method of wave injection using modulated, high-current electron beams to stimulate coherent VLF signals was also addressed. Theoretical models of coherent emissions from electron beams, developed at Stanford University were critically examined and the alternative of using modulated ion beams was explored. Uncertainties in electron beam coherence arising from vehicle charging and distributed space charge effects may be minimized using energetic ion beams that tend to drag vehicle neutralizing, cold electrons with them from their sources.

H3-3 0920 ACTIVE: A MULTINATIONAL PLASMA WAVE EXPERIMENT

William W.L. Taylor, TRW, Redondo Beach, CA

In February, 1989, the USSR will launch their space plasma wave laboratory, ACTIVE (ACTIVINY) to do the first high power plasma wave transmission and propagation experiments in space. ACTIVE will consist of the two satellites, a transmitter spacecraft and receiver spacecraft, in a 500 by 2500 km altitude orbit, inclined at 83°, and associated ground stations. The transmitter will deliver 5 kW to a 20 m diameter loop antenna at eight frequencies between 9.0 and 10.2 kHz. Both spacecraft will have extensive diagnostic instrumentation. The scientific objectives include antenna characteristics, propagation, wave-particle interactions, and nonlinear effects. ACTIVE has been planned under the leadership of IKI, who also provided the transmitter satellite, in Moscow with cooperating scientists from Czechoslovakia providing the receiver subsatellite. Scientists from Bulgaria, Cuba, GDR, Hungary, and Poland are also participating. Recently, the USSR has invited additional participation from U.S., Canada, and Japan. The U.S. effort is being lead by the WISP team and hopes to fully participate in planning, data gathering (from satellites and ground stations), and data analysis. The U.S. and USSR have agreed to fully share their data. ACTIVE promises to be a very valuable project for plasma physics and for international scientific cooperation.

H3-4
0940

ROCKET EXPERIMENT TO STUDY ELECTRON BEAM WAVE GENERATION

D.E. Donatelli, Electromagnetics Directorate, Rome Air Development Center, Hanscom AFB, MA 01731-5320

The CHARGE-2B rocket experiment, scheduled for a Jnauary 1990 flight, will carry a 9 kW electron beam system to study wave excitation and propagation at VLF frequencies. The beam will be modulated at 5, 10 and 20 kHz using currents up to 3 A with energies of 1 kv and 3 kv. By emitting the beam so as to achieve the proper resonance conditions, waves should be generated at the modulation frequency and its harmonics. The frequencies most likely to propagate lie between the lower hybrid and the ion plasma frequency. Wave receivers will be deployed from the rocket on a separate payload to detect radiation along geomagnetic field lines up to several kilometers from the beam-emitting payload. A network of ground-based receivers will detect radiation transmitted through the ionosphere into the earth-ionosphere waveguide.

H3-5 1020 ISEE Observations of Long-lasting Diffuse Electromagnetic Emissions in the Geomagnetic Tail

R. R. Anderson
Dept. of Physics and Astronomy,
University of Iowa, Iowa City, IA 52242

In the University of Iowa ISEE Plasma Wave Experiment data we have observed several examples of long-lasting diffuse electromagnetic emissions in the geomagnetic tail. Unlike the bursty electromagnetic emissions frequently observed near boundaries in the tail, these emissions have relatively long durations (from 30 minutes to 2 hours) and have a diffuse hiss-like spectral structure. They have a sharp upper cutoff usually in the range 500 Hz to 1 kHz and a more diffuse lower cutoff. The bandwidth is typically a few hundred Hz. Although they have both electric and magnetic components, the magnetic components are very weak. The emissions have been observed from 21 MLT to 3 MLT and from 12 to 19 R_E in the tail. Each observance was coincident with an abrupt increase in the AE index and with an abrupt decrease in energetic particles indicative that the spacecraft had moved out of the plasmasheet. The emissions ended when the spacecraft re-entered the plasmasheet. It is possible that we are seeing an extension of auroral hiss propagating deep into the geomagnetic tail.

H3-6
1040

VLF BEAMFORMING BY A PHASED ARRAY IN AN IONIZED MEDIUM

H.C. Han and J.A. Kong, Dept. of Electrical Engineering and Computer Science, Massachusetts Institute of Technology, Cambridge, MA 02139, and T.M. Habashy, Schlumberger-Doll Research, Old Quarry Road, Ridgefield, CT 06877-4108

In this paper we present several designs for a two dimensional phased array consisting of electric current loops (magnetic dipoles) whose axes are perpendicular to the plane of the array. The operating frequency is in the VLF regime to achieve a long range of coverage. The elements of the array are phased in order to achieve a beam that can be electronically steered over 360° in the plane of the array. Several phasing schemes are employed and their performances are compared. We also compare between the different designs and discuss the tradeoffs between the beamwidth, the sidelobe level, the transmitted power and the size of the array.

H3-7
1100

SHOCK-DELAYED EMISSION OF TYPE-III SOLAR RADIO BURSTS

W. Calvert
Department of Physics and Astronomy
The University of Iowa
Iowa City, Iowa 52242

Cane, et al. [*Geophys. Res. Lett.*, 8, 1285-1288, 1981] have proposed shock acceleration as the source of the energetic electrons causing certain kilometric-wavelength type-III solar radio bursts; whereas Steinberg, et al. [*Astron. Astrophys.*, 140, 39-48, 1984] have reported timing discrepancies of up to eight minutes in the type-III bursts observed in different directions with Voyager and ISEE-3. Inexplicable as a propagation effect, these timing discrepancies could be explained by shock-delayed acceleration on field lines remote from the flare and the subsequent beaming of emissions perpendicular to the field, since that would produce type-III bursts at different times in different directions with the correct emission geometry and delays. Although differing from previous conclusions about the spiral structure of the type-III burst source, this interpretation also accounts for the pairs of bursts which are frequently observed having spacings of up to an hour or more, by emission from field lines on opposite sides of the sun.

It is thus proposed that the source of kilometric type-III bursts is not necessarily limited to flare field lines, but also occurs over much larger regions, sometimes extending to the opposite sides of the sun. Adopting Cane's concept for all such bursts, it is further suggested that the energetic electrons causing these bursts must originate from shocks in the lower solar atmosphere, and hence with various delays depending upon the distance from the flare. And finally, it is noted that the observed shape of these bursts would then be determined not only by the electron time-of-flight and energy dispersion, but also by the shock delays and the beaming, with obvious implications to the determination of heliospheric plasma densities from the type-III burst measurements.

H3-8
1120

SELF-FOCUSING OF A RADIO WAVE BEAM DURING THE TRANSIONOSPHERIC PROPAGATION

H.C. Han and J.A. Kong, Dept. of Electrical Engineering and Computer Science and Research Lab. of Electronics, Massachusetts Institute of Technology, Cambridge, MA 02139

During the transionospheric propagation of a high power radio wave beam, the nonuniform electromagnetic field interacts with the background plasma and gives rise to a ponderomotive force and a thermal pressure force. Both of the two nonlinear forces mainly act on the electrons, but eventually will have an effect on the ions through the ambipolar diffusion process. The spatial redistribution of the plasma density caused by the actions of these forces will change the local plasma permittivity along the beam path and consequently lead to the focusing of the radio wave beam.

In this paper, we examine the self-focusing phenomena by taking into account both the ponderomotive force and the thermal pressure force as the two primary mechanisms. The threshold power intensity is determined by balancing the natural diffraction and the nonlinear focusing effects of the wave beam. The focal length for the concerned process is then estimated after solving the nonlinear wave equation.

To illustrate the self-focusing process, we carried out a series of numerical simulation for high frequency beams with various initial beam widths propagating in the ionospheric plasmas. The peak field intensity and the electron temperature along the beam path are calculated numerically. It is also shown that the thermal pressure force is predominant over the ponderomotive force in large incident beam width cases; however, the ponderomotive force is more significant if the beam width is small.

H3-9
1140

THE IMPACT OF SPACECRAFT ENVIRONMENT ON SPACE SCIENCE

J.A. Joselyn, NOAA Space Environment Lab
325 Broadway, Boulder, CO 80303
E.C. Whipple, Center for Astrophysics and Space Science, University of California at San Diego, La Jolla, CA 92093

A spacecraft's environment can affect its operational lifespan and the reliability of its sensor data and telemetry signals. In particular, natural populations of charged particles and plasmas can cause command and control errors and general deterioration of exposed satellite surfaces. Particle sensors may be susceptible to the details of electrically charged satellite structures and materials, and could produce contaminated data even though the spacecraft itself is functioning normally. In addition, optical sensors and cameras must contend with glinting from sunlit orbital debris and degradation of optical surfaces. In this talk, the variety of possible effects on data reliability are illustrated and both scientists and operational agencies depending on satellite data are reminded that these effects can be insidious and pernicious.

Session B-6 1515-Fri. CR2-28
SCATTERING II
Chairman: R. Kleinman, Dept. of Mathematics, Univ. of Delaware, Newark, DE 19711

B6-1 1520 **A REVIEW OF ROUGH SURFACE SCATTERING APPROXIMATIONS BASED ON INTEGRAL EQUATION ITERATES**

Gary S. Brown, Dept. of Electrical Engineering, VPI & SU, Blacksburg, VA 24061-0111

There are a number of well known approximations for estimating the scattering of electromagnetic waves from randomly rough extended surfaces. While these are all well understood from a physical point of view, their analytical derivations do not share a common mathematical formulation as a starting point. This diversity in starting points leads one to believe that there is no single formulation capable of producing all of these results. The purpose of this paper is to demonstrate that one can obtain *all of these classical approximations* from a single integral equation for the current induced on the rough surface by the incident field.

For demonstration purposes, we consider the problem of scattering of an incident electromagnetic field by a randomly rough, perfectly conducting surface. (For a rough dielectric interface, the essential elements of the analysis carry over but one must deal with coupled integral equations for electric and magnetic surface currents). The equation for the electric current is the Magnetic Field Integral Equation (MFIE). Once the MFIE is solved, the Fourier transform of the resulting current yields the scattered field. Thus, there are two essential elements to determining the scattered field - solving the MFIE for the current and then transforming this result. We then proceed to show that all of the classical approximations follow from the zeroth and first order iterations of the MFIE coupled with either exact or approximate evaluations of the Fourier transform to obtain the scattered field. We also show that these approximations group very naturally into low and high frequency asymptotic forms which result from an asymptotic evaluation of the Fourier transforms. Where asymptotic methods are not used to evaluate the transforms, one obtains a form of the composite surface scattering approximation. This latter result is particularly interesting because of the difference between the use of zeroth and first order iterates.

B6-2
1540

TE SCATTERING FROM A RIGHT INTERIOR CORNER LOADED BY A SLOT IN ONE CONDUCTING FACE

John W. Silvestro and Chalmers M. Butler
Clemson University, Clemson, SC 29634-0915

Scattering from a right interior corner (270° wedge) loaded by a slot in one of it's conducting faces is considered. The cases of a slot in a conducting surface seperating two different dielectric regions or backed by a parallel plate waveguide are treated. These configurations are being studied for the purpose of determining how a slot affects the scattering from a right angle corner. The basic problem is a two-dimentional solution of a plane wave incident upon an interior corner with an aperture in one of the conducting faces. Equivalent models, incorporating unknown surface magnetic currents placed on the two sides of the shorted aperture, are developed for the two regions. These models are then used as aids in formulating expressions for the magnetic field intensities in both regions. Subsequently, continuity of the tangential components of these field terms is enforced, which results in an operator equation that is solved by the methods of moments. Pulse basis functions and point matching are used in the numerical solution procedure. Once these solutions are known the coupling into a waveguide (for the slot backed by a waveguide) or the scattered fields can be easily determined. A computer code that implements the numerical procedure has been developed, and numerical data are presented. Where available comparisons against published data for related scattering problems will also be discussed.

EM DIFFRACTION BY DIELECTRIC-COVERED SLOTS IN A CONDUCTING CYLINDER OF ARBITRARY CROSS SECTION: TE CASE

B6-3
1600

Ali Sadigh and Ercument Arvas
Department of Electrical and Computer Engineering
Syracuse University, Syracuse , NY 13244.

Fahrettin Arslan
Istanbul University, Istanbul, Turkey.

A simple moment solution is given to the problem of electromagnetic transmission through a dielectric-covered slot in a perfectly conducting cylinder of arbitrary cross section. The cylinders are excited by a TE plane wave. The surface equivalence principle is used to represent the scattered field in terms of equivalent surface electric and magnetic currents. Application of the boundary conditions results in a set of coupled integral equations involving the surface currents. The method of moment with pulse expansion and point matching scheme is used to solve the integral equations numerically. Both E-field and H-field formulations are used. The computed results include the aperture field, the internal field and the scattering cross section of the structure. These are in very good agreement with available published data.

B6-4
1620

ELECTROMAGNETIC SCATTERING FROM CONDUCTING AND/OR DIELECTRIC CYLINDERS OF ARBITRARY CROSS SECTION ABOVE A GROUND PLANE

A. Rahhal-Arabi, Y. Qian, and E. Arvas
Department of Electrical and Computer Engineering
Syracuse University, Syracuse , NY 13244.

A simple moment solution is given for the problem of electromagnetic scattering by a system of perfectly conducting and/or lossy dielectric cylinders. The cylinders are assumed to be placed above (or on) an infinite conducting plane, and have arbitrary cross section. The system is illuminated by either a TM or a TE plane wave. The surface equivalence principle is used to replace the cylinders by equivalent surface currents radiating in an unbounded medium. The boundary conditions on the tangential component of the fields yields a set of coupled integral equations for the surface currents. For the TM case the E-field formulation was used and for the TE case the H-field formulation was employed. The moment method with pulse expansion and point matching scheme is used to solve the integral equations. Computed results include the induced and/or equivalent current distributions, and the bistatic and monostatic cross sections. Computed results are in excellent agreement with exact or otherwise available data.

B6-5
1640

RADAR TARGET DISCRIMINATION IN A FREE-FIELD ENVIRONMENT

P. Ilavarasan, W. Sun, E. Rothwell, K. M. Chen, D. Nyquist
Department of Electrical Engineering
Michigan State University
East Lansing, MI 48824

Recent work (K. M. Chen, et al., IEEE AP-34, 896-904, 1986) has demonstrated the feasibility of discriminating scale model radar targets using measured time domain data. In that work, the scattered field response of a target measured above a conducting ground plane is convolved with an E-pulse waveform to produce a signature based on the target natural resonances. By use of this unique signature, the target can be discriminated from others. Reproducing these results in a free field environment would greatly enhance the viability of radar target discrimination using natural target resonances.

A time domain anechoic chamber recently built at MSU provides an opportunity to extend radar target discrimination using the E-pulse technique into the free field regime. A travelling-wave V-wire antenna is used to illuminate the 12' x 12' x 24' chamber with a nanosecond pulse excitation waveform, and the field scattered from a radar target is measured using a long wire receiving antenna. Using the long wire for receiving eliminates the exteraneous natural antenna resonances which might be confused with target natural modes in the discrimination process. It is felt that this antenna system is a unique application of the properties of wire antennas.

Measurements of the scattered field response of various aircraft targets performed in the free-field range have been made, and are used with the E-pulse scheme to perform target discrimination. The results are given in this paper, and compared to those obtained using the ground plane range.

B7-1
1340

SYMBOL ANALYSIS AND THE CONSTRUCTION OF ONE-WAY FORWARD AND INVERSE WAVE PROPAGATION THEORIES IN OCEAN SEISMO-ACOUSTICS

Louis Fishman
Center for Wave Phenomena
Department of Mathematics
Colorado School of Mines
Golden, Colorado 80401

The analysis and fast, accurate numerical computation of both forward and inverse wave propagation models in ocean seismo-acoustics are often complicated by the extended, variable, three-dimensional channeling environments encountered. Even for the zeroth-order picture of a transversely inhomogeneous environment, the domain of interest is entirely within the scattering regime, with the subsequent absence of an "asymptotically free" , or homogeneous, region. For both forward modeling and ocean tomographic and bore-hole experiments, then, this situation is quite different from the usual formulations of obstacle and quantum scattering theory. While there are numerous methods for attacking the one-way forward calculation, most approaches to the corresponding inverse (tomographic) problems essentially rely on a linearization about a well-chosen zeroth-order model. Phase space and path integral techniques, which extend homogeneous Fourier methods to inhomogeneous environments, lead to comprehensive mathematical and computational forward models, in addition to providing the framework for the exact solution of the transversely inhomogeneous refractive index profile reconstruction problem. These pseudo-differential and Fourier integral operator methods are largely based upon the properties and interrelationships of the corresponding operator symbols.

This talk will present the most recent developments and applications of the phase space and path integral methods, as applied to the scalar Helmholtz equation, for one-way forward and inverse modeling. Exact, numerical, and uniform perturbation constructions of the Weyl symbol and their subsequent application to the phase space marching computational algorithm will be addressed. The relationship between macroscopic and microscopic (infinitesimal) symbols as the basis for the exact inversion method will also be examined.

B7-2
1400

WAVE PROPAGATION IN RANGE DEPENDENT INHOMOGENOUS MEDIA

Y. L. Li, C. H. Liu, and S. J. Franke
Department of Electrical and Computer Engineering
University of Illinois at Urbana-Champaign
1406 W. Green St.
Urbana, IL 61801

A new method based on the path-integral technique to study wave propagation in a three-dimensional inhomogeneous medium will be presented in this paper. It will be shown that exact, analytical solutions for Green's functions can be obtained for a medium where the square of the refractive index is of a general three-dimensional quadratic form. These exact solutions are compared with numerical and approximate solutions. They are also used to investigate the effects of inhomogeneity on the propagation of waves. In the case where turning points exist in one or two dimensions, the Green's function can be expressed in terms of normal modes. The exact analytical solutions obtained for several interesting cases will be used to study the effects of range dependent refractive index on the propagation of these normal modes. It will be shown that depending on the range variation of the refractive index, a given propagating mode may become evanescent and another evanescent mode may become propagating as the wave propagates along a given direction. Applications of these solutions to other interesting problems such as scattering, arrays, etc. will also be discussed.

B7-3
1420

GEODESICS OVER AIRFRAMES TECHNIQUE (GOAT)

Brenton P. Campbell
IIT Research Institute
185 Admiral Cochrane Drive
Annapolis, MD 21401

For frequencies above mid-VHF band, the calculation of the coupling loss between antennas co-located on an airframe is dependent on accurately determining the geodesic path between the antenna terminals. Previous techniques for calculating the geodesic path were applicable to a relatively restricted set of simple geometrical shapes that frequently did not realistically represent the actual aircraft structure. The Geodesics Over Airframe Technique (GOAT) was developed to calculate geodesic paths using a more general geometrical description. In the GOAT technique, the fuselage cross section may be modeled as any smooth, convex, but otherwise arbitrary cross section. The fuselage is modeled using a cylinder of constant cross section terminated at both ends by independently tilted cones that may be arbitrarily truncated. An iterative technique based on the calculus of variations was developed to compute the geodesic path over the complex structures specified. GOAT along with general techniques for computing surface diffraction loss over surfaces with varying curvature (discussed in the following paper by P. Hussar) were implemented in an electromagnetic propagation program to calculate coupling loss for antennas located on aircraft.

B7-4
1440

SURFACE DIFFRACTION OVER GEODESICS-OVER-AIRFRAMES-TECHNIQUE (GOAT) TYPE SURFACES

Paul E. Hussar
IIT Research Institute
185 Admiral Cochrane Drive
Annapolis, MD 21401

The Geodesics Over Airframes Technique (GOAT) (B. Campbell, preceeding paper) permits computation of geodesic paths over cylinders and (tilted) cones of arbitrary convex cross section. The implementation of the technique within a coupling-loss-prediction computer program applicable to antennas mounted on aircraft surfaces involves the calculation of surface-diffraction effects over surfaces of greater generality than have previously been considered by computer models. The basis for this calculation has been developed from standard geometrical theory of diffraction (GTD)/uniform GTD (UTD) techniques (S. W. Lee, IEEE Trans. AP-26, 768-773, 1978; Pathak and Wang, IEEE Trans. AP-29, 911-922, 1981). Since the program is designed as a cull model to determine potential cases of electromagnetic interference, a simplified far-field, worst-case-polarization approximation is acceptable. The computation of the Fock parameter applicable to paths over GOAT-type cylindrical and conical surfaces requires determination of the geodesic curvature along such paths. The GOAT cross-section is defined by a number of discrete cross-sectional points, and these are used to compute a cross-sectional curvature. Expressions for the geodesic curvature in terms of the cross-sectional curvature have been developed from differential geometry. Comparison of program predictions with monopole coupling measured at frequencies between 2 and 18 GHz over a set of circular, elliptical, and composite-elliptical conducting cylinders indicates excellent agreement.

B7-5
1500

GENERALIZED IMPEDANCE BOUNDARY CONDITIONS FOR DIELECTRIC SURFACES AND LAYERS

John L. Volakis and Thomas B. A. Senior
Radiation Laboratory
Dept. of Electrical Engineering and Computer Science
The University of Michigan
Ann Arbor, MI 48109-2122

Higher order boundary conditions are presented for the simulation of non-metallic surfaces and thick dielectric layers. They are derived for a few configurations of practical interest and their accuracy is examined based on the predicted reflection coefficient. In particular, second, third and fourth order boundary conditions are presented for simulating homogeneous thick dielectric layers with or without metal backing, stacks of thin dielectric layers and a dielectric layer in the presence of a resistive sheet. It is found that a third order boundary condition is capable of providing an acceptable simulation for layers as thick as 1/4 of a wavelength, if lossless, or more in the case of lossy dielectrics. Finally, we discuss possible implications of these higher order boundary conditions when employed in analytical or numercial solutions.

B7-6
1520

TWO-DIMENSIONAL EM LENS DESIGN USING DIFFERENTIAL GEOMETRIC SCALING

A.P. Stone
University of New Mexico
Department of Mathematics and Statistics
Albuquerque, NM 87131
C.E. Baum
Air Force Weapons Laboratory
Kirtland AFB
Albuquerque, NM 87117

The study of inhomogeneous TEM plane waves which propagate on ideal cylindrical transmission lines with two or more independent perfectly conducting boundaries leads to the study of lens transition regions. These types of inhomogeneous media can be used to define lenses for transitioning TEM waves, without reflections or distortions, between different types of transmission lines. In the simplified situation considered here, we have a two-dimensional problem. In our generalized coordinate system, (u_1, u_2, u_3) we choose $u_3 = z$ and suppose that either the formal electric field or formal magnetic field has only a u_3 component. The remaining field has only a u_2 component and both field components are a function of u_1 only, with the result that we have a uniform TEM wave which propagates in the u_1 direction. Examples of two-dimensional lenses with parallel plate transmission lines are given. In these examples, either the electric field or magnetic field is parallel to the z-axis. The differential geometric scaling is given by complex analytic transformations. In one example, the transformation describes the potential distribution around a uniformly charged wire grid (in a homogeneous medium) terminating a uniform electric field. In another example, equal but opposite electric fields terminate the grid. In both cases the conductors and medium are cut off before the singularity on the z-axis is reached. The two-dimensional cases studied are part of the more general problem of using a differential geometric approach to transient lens synthesis.

B7-7
1540

RADIATION CHARACTERISTICS OF *CHIROSTRIP* ANTENNAS

Nader Engheta
The Moore School of Electrical Engineering
University of Pennsylvania
Philadelphia, Pennsylvania 19104-6390

It is has been shown that an isotropic chiral material can be described electromagnetically by the constitutive relations $\mathbf{D} = \varepsilon \mathbf{E} + i\xi_c \mathbf{B}$ and $\mathbf{H} = i\xi_c \mathbf{E} + (1/\mu)\mathbf{B}$ where scalar quantities ε, μ, ξ_c represent the permittivity, permeability and chirality admittance of the chiral medium, respectively. Such materials exhibit optical activity which refers to the rotation of the plane of polarization of electromagnetic waves traversing these media. This is due to the presence of two unequal characteristic wavenumbers $k_{\pm} = \pm\omega\mu\xi_c + \sqrt{k^2 + (\omega\mu\xi_c)^2}$ where ω is the radian frequency, $k = \omega\sqrt{\mu\varepsilon}$ and + and – refer to right- and left-circularly polarized eigenmodes, respectively. Optical activity differs from the phenomenon of Faraday rotation by the fact that the former is reciprocal and independent of the sense and direction of propagation whereas the latter is not.

We have introduced and investigated theoretically a new class of antennas which we name *chirostrip* antennas. These radiators consist of microstrip antennas printed on top of chiral substrates. Since chiral materials are, so-called "polarization sensitive", use of these materials as antenna substrates inevitably affects the radiation characteristics of such antennas. In this talk, we will present novel and interesting results obtained in our theoretical study of chirostrip antennas. It is observed that due to the fact that the eigenmodes of propagation in chiral media are left- and right-circularly polarized waves, the propagation of surface wave in chiral substrates is significantly reduced. This leads to higher radiation efficiencies and wider bandwidths. It is also observed that the state of polarization of radiation fields of chirostrip antennas is different from that of conventional microstrip antennas.

Since chiral materials are isotropic and reciprocal while they exhibit handedness, design of chirostrip antennas and other microwave elements with such materials will be considerably simplified. Use of chiral materials in microwave and millimeter-wave integrated-circuit antennas and components will introduce a new approach in the design of broadband and efficient devices.

B7-8
1600

REAL-VALUED RESISTIVE TAPERS THAT PLACE NULLS IN THE SCATTERING PATTERNS OF STRIPS

Randy L. Haupt
DFEE
USAF Academy
Colorado Springs, CO 80840

The scattering patterns of resistive strips may be modified by lowering the scattering sidelobe levels (R.L. Haupt and V.V. Liepa, IEEE AP-S, 35, 1217-1225, 1987) and placing nulls in the sidelobes (R.L. Haupt and V.V. Liepa, IEEE AP-S Symposium, , 1988). Complex resistive tapers for either low sidelobes or nulls in the sidelobes of a strip work well theoretically, but are difficult to physically realize. This presentation describes a method of placing nulls in the scattering patterns of a strip with a real-valued resistive taper. The figure below shows the real-valued resistive taper that places a null in the bistatic scattering pattern at 50° and the resultant bistatic scattering pattern (incident field is normal to the strip).

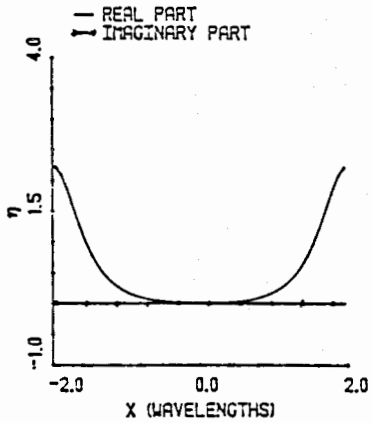

Normalized resistive taper for nulling

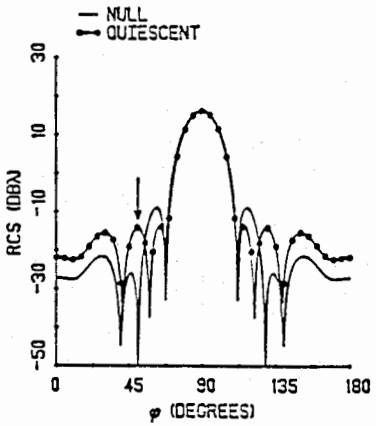

Bistatic scattering pattern, φ_i=90°

B7-9
1620

RIGOROUS ANALYSIS OF OPEN MICROSTRIP LINES WITH FINITE THICKNESS—THE MIXED-POTENTIAL INTEGRAL EQUATION APPROACH

K. A. Michalski and D. Zheng
Electromagnetics and Microwave Laboratory
Department of Electrical Engineering
Texas A&M University
College Station, Texas 77843

A rigorous analysis of an open microstrip line is presented, based on the mixed-potential electric field integral equation (MPIE) [K. A. Michalski, *Arch. Elek. Übertragung.*, **39**, 317-322, 1985]. The MPIE is preferable to several other possible variants of the electric field integral equation (EFIE), because it only requires *potential forms* of the Green's functions, which are less singular and converge faster than the *field forms* needed in other EFIEs. Another important advantage of the MPIE is its conformity with an existing, well-established moment method procedure, originally developed for surfaces of arbitrary shape in free space [A. W. Glisson and D. R. Wilton, *IEEE Trans. Antennas Propagat.*, **AP-28**, 593-603, 1980]. Hence, our technique can easily accomodate multiple strips, as well as strips of finite thickness.

Sample numerical results are presented for microstrip lines with both infinitesimal and finite thickness. These include dispersion characteristics and modal current distributions for the dominant mode and for first few higher modes. For the latter, results are given both for the bound regime (where the mode propagates unattenuated) and for the leaky regime (where the mode radiates as it propagates). Where possible, comparisons are made with published data. In particular, our result for the EH_1 mode in leaky regime is shown to agree with Oliver and Lee's work [*Digest of the AP-S Int'l Symp.*, Philadelphia, 443-446, 1986], which employed a transverse resonance method in conjunction with the Wiener-Hopf approach of Chang and Kuester [*Radio Sci.*, **16**, 1-13, 1981].

B7-10
1640

VALIDATION OF THE HYBRID QUASI-STATIC/FULL-WAVE METHOD FOR CAPACITIVELY LOADED ANTENNAS

R.G. Olsen and P.D. Mannikko
Electrical and Computer Engineering Department
Washington State University
Pullman, WA 99164-2752

Recently, a hybrid method in which quasi-static and full-wave integral equations are combined was developed (R.G. Olsen, G.L. Hower, and P.D. Mannikko, "A Hybrid Method for Combining Quasi-Static and Full-Wave Techniques for Electromagnetic Scattering Problems," IEEE Transactions on Antennas and Propagation, August 1988). The method is useful for scattering problems in which the geometry contains one or more electrically small but geometrically complex sub-regions composed of perfect conductors and/or dielectrics and which are "capacitive" in nature. The method is particularly advantageous for problems in which a detailed knowledge of the field within the subregion is necessary. Using quasi-static methods in the electrically small regions, full-wave methods in the remaining regions and coupling the regions as described in the recent publication results in improved numerical efficiency compared to using full-wave methods throughout the geometry. Since the writing of the recent communication, the hybrid method has been implemented, using the method of moments, for axially symmetric structures consisting of thin wires and electrically small "capacitive" regions.

As one means of validating the hybrid technique, a capacitor-loaded linear antenna was constructed. Its measured input admittance was compared with those predicted by the hybrid code. The antenna was modeled over a band of frequencies and over a range of dielectric constants available in the laboratory. Comparisons of predicted input admittances using the hybrid method with measured results for capacitor-loaded antennas show excellent agreement.

The hybrid results are also compared with numerical results obtained from MiniNEC for thin-wire antennas with a lumped-load. The value of the load was determined by the capacitance of the electrically small region. Results indicate that the hybrid method is a significant improvement over the lumped-load technique, especially in problems where the details of the fields within the subregion are important.

Session C-4 1355-Fri. CR1-40

NONLINEAR AND NONSTATIONARY SIGNAL PROCESSING

Chairman: Dennis Friday, National Institute of Standards and Technology, Boulder, CO 80303

C4-1 1400 A NONLINEAR OPTIMUM-DETECTION PROBLEM
T.T. Kadota, AT& T Bell Labs, Murray Hill, NJ 07974

An approximate log-likelihood ratio is derived for detecting a deterministic signal in linear stationary and nonlinear Gaussian noise. The new aspect of this detection problem is the inclusion of the nonlinear Gaussian noise which takes a quadratic form in the linear Gaussian noise and a certain interaction between the signal and the linear noise, such as modulation of the signal by the noise. Such a detection problem may arise in radar where the transmitted signal is reflected by clutter or random particles as well as by a target. The primary reflection by the clutter produces the linear Gaussian noise and the secondary reflection produces the nonlinear noise. It is assumed that the second is an order of magnitude smaller than the first, and the approximation used in the derivation is based on this assumption. The secondary reflection (by the clutter) of the target-reflected signal produces the signal-noise interaction. Monte Carlo simulation using simple examples is run to illustrate the effects of the newly derived nonlinear filters on detection performance.

C4-2 1440 POLYSPECTRA IN SIGNAL PROCESSING: C.L. Nikias, Northeastern Univ., Boston, MA 02115

C4-3 1540 A NON-GAUSSIAN TIME SERIES ANALYSIS, WITH APPLICATIONS
K.-S. Lii, Univ. of California, Riverside, CA 92521

C4-4
1620

DATA STRUCTURES AND ANALYSIS METHODS USEFUL IN IMAGE ANALYSIS

James J. Simpson, Scripps Institution of Oceanography, La Jolla, CA 92093

Remotely sensed images of the natural environment, when combined with quantitative analysis techniques, provide unique information on geophysical processes. The sampling protocols used by the satellites also can provide global observations of these processes on relatively short time scales. However, the satellite observations frequently are represented by completx multi-dimensional data structures which can impose severe computational and I/O limitations on any analysis procedure. A brief presentation of image data structures, followed by a discussion of three generic image analysis techniques, is given. The techniques include: statistical physical modeling of image data structures, convolution and spectral methods, and empirical orthogonal functions. These techniques are then applied to cloud screening, velocity and stream function generation, and pattern identification, respectively.

Session D-2 1335-Fri. CR2-28
GUIDED OPTICAL DEVICES
Chairman: J.W. Mink, Army Research Office

D2-1 COMPUTER ANALYSIS OF SURFACE MODE INTERACTION IN $LiNbO_3$
1340 INTEGRATED OPTICAL DEVICES

W. Charczenko, S.T. Vohra, and A.R. Mickelson
Department of Electrical and Computer Engineering
University of Colorado
Campus Box 425
Boulder, CO 80309

In this paper we analyze an archetypical optical CAD problem, a directional coupler which includes parallel and nonparallel waveguide regions. Numerical results are compared to experimental data on "in house" fabricated Ti indiffused $LiNbO_3$ directional couplers.

Coupled mode theory is used to analyze the parallel and nonparallel waveguide regions in integrated optical directional couplers (A. J. Weierholt, A. R. Mickelson, and S. Neegard, IEEE JQE, 23,1689-1700,1987). The propagation constants and the eigenmodes representing the transverse field distributions are obtained using a two dimensional effective index method (R. M. Knox and P. P. Toulios, Proc. of Symp. on Submillimeter Waves, 497-516, 1970). Given the input power distribution, the output power in each waveguide is calculated and compared to experimental data taken for various sets of devices fabricated under different conditions. The nonparallel waveguide regions influence on overall coupling length is examined.

This technique for calculating the optical properties of integrated optical structures shows much promise for use in optical CAD. The use of coupled modes allows one to store coupling coefficients and propagation constants in a fast look-up data base for use in the main program. This will allow for "real-time" interactive design and possibly even use in optomization routines. Data presented at the conference will show the technique to be sufficiently accurate for these purposes.

D2-2
1400

A NUMERICAL METHOD FOR DETERMINING INDEX PROFILES FROM NEAR-FIELD INTENSITIES OF OPTICAL GUIDED WAVE DEVICES

R. Fox, W. Charczenko, and A.R. Mickelson
Department of Electrical and Computer Engineering
University of Colorado
Campus Box 425
Boulder, Colorado 80309

In this paper we present a method for calculating the index of refraction profile given the near field intensity and propagation constant of integrated optical channel guides. Knowledge of the index of refraction profile is needed for any optical CAD system used in analyzing optical properties of guided wave devices.

We present a numerical method of fitting index of refraction profiles to experimental near-field intensity data. The technique is based on solving the wave equation using a Greens function for single moded optical waveguides with small index variations. The parameterized index distribution along with the near-field data and propagation constant are used in an integral expression for the fields. The fields in this integral expresion are calculated and compared to the near field data using a least squares fit for the index distribution paramaters to minimize the error.

This technique was used to determine the diffusion coefficients, and thereby index profiles for various indiffused $LiNbO_3$ waveguides. This method shows promise as a technique for analyzing near-field data to yield profiles, thereby offering a nondestructive means of determining the index profiles of integrated optical structures.

D2-3
1420

A FINITE DIFFERENCE/FINITE ELEMENT PROPAGATION ALGORITHM FOR INTEGRATED OPTICAL DEVICE

J.B. Davies*, T.B.Koch, D.Wickramasinge
University College
Department of Electronic and Electrical Engineering
London WC1E 7JE, England
*Currently Visiting Professor at:
Department of Electrical Engineering
University of Colorado
Boulder, CO 80309-0425

The simulation of wave propagation in integrated optical devices of arbitrary cross section and longitudinal geometry has become an important task as the performance of these components depend mainly on manufacture tolerances and also costs are high. Different versions of the Beam Propagation Method (BPM) currently in use have a number of disadvantages. The BPM with its spectral propagation characteristics is based on the assumption of scalar propagation, low refractive index change and the neglecting of reflected fields. Therefore the method is not able to model integrated optical devices involving large changes in refractive index in the longitudinal and transverse direction. As the BPM is derived from the scalar TE-wave equation, effects that involve a polarisation dependent propagation are totally neglected. Moreover most versions of the BPM can only be used efficiently in a one dimensional analysis due to the computational effort to transform the fields into the spectral domain and back after each step of propagation. To overcome these drawbacks, a different approach is suggested here, not based on a plane wave expansion. The new algorithm uses a Finite Element/Finite Difference discretisation of the TE-wave equation. It has also been successfully applied to the TM wave equation. The Finite Element method which solves for the modal and radiation fields in the cross section gives direct solutions to two dimensional or, for the sake of simplicity and comparison with the BPM, also for one dimensional cross sections. The main advantage of the new method however lies in the possibility of handling large changes in refractive index in the transverse direction. Combined with a method for longitudinal reflections, the new approach provides a powerful tool to model integrated optical components involving abrupt changes of refractive index, for example in a waveguide structure with totally reflecting corner mirrors.

Straight, curved and Y-shaped waveguides and other structures involving transverse discontinuities (TE and TM) have been successfully analysed. The Finite Difference algorithm which models the forward propagation (with the Finite Elements solving for fields in the cross section after each step of propagation) is unconditionally stable. We will present a comparison of this new algorithm with a two dimensional Finite Difference scheme and the BPM and show that our method requires less CPU-time. Also large propagation steps that would cause a breakdown of the BPM are now admissible.

D2-4
1440

OPTICAL DIRECTIONAL COUPLERS IN PROTON EXCHANGED $LiNbO_3$

S.T. Vohra and A.R. Mickelson
Center for OptoElectronic Computing Systems
Department of Electrical and Computer Engineering
University of Colorado
Campus Box 425
Boulder, Colorado 80309

Titanium indiffusion has been the predominant method of fabricating optical directional couplers in $LiNbO_3$. These couplers allow both TE and TM polarizations to be guided thus making it difficult to make single polarization guiding devices.

We report on the fabrication and characterization of optical directional couplers in proton exchanged $LiNbO_3$. This technique allows only single polarization to be guided (TE in X-cut and TM IN Z-cut $LiNbO_3$). We have characterized such devices for their coupling efficiencies and near-field patterns. Electrooptic switching characteristics are measured after depositing indium tin oxide (ITO) electrodes on the couplers.

D2-5
1500

GUIDED PROPAGATION IN GRADED-INDEX ANISOTROPIC FIBERS

S.F. Kawalko and P.L.E. Uslenghi
Department of Electrical Engineering and Computer Science
University of Illinois at Chicago
Box 4348, Chicago, Illinois 60680

A cylindrically symmetric optical fiber with a graded-index core which is anisotropic is considered. With respect to cylindrical coordinates, the three elements of the biaxial permittivity tensor are functions of the distance from the core axis.

The axial components of the electric and magnetic fields satisfy two coupled differential equations, that become uncoupled for azimuthally independent modes, corresponding to meridional rays. A WKB analysis of these TE and TM modes is performed.

For modes which are azimuthally dependent (corresponding to skew rays), a perturbation technique is developed. Some exact results, corresponding to specified permittivity profiles, are obtained and compared with the asymptotic results.

Session G-5 1335-Fri. CR2-6
IONOSPHERIC MODIFICATION
Chairman: M.C. Lee, Plasma Fusion Center, MIT, Cambridge, MA 02139

G5-1
1340 OBSERVATIONS HF-ENHANCED PLASMALINES IN ARECIBO AND EISCAT HEATING EXPERIMENTS

T. Hagfors and B. Isham
National Astronomy and Ionosphere Center
Space Sciences Building
Ithaca, New York 14853

Data taken at Arecibo during HF ionospheric modification experiments with and without chirping the 430 MHz diagnostic incoherent scatter radar include observations of natural plasma line spreading and reformation on the time scale of 30 sec, when a 30 sec on 30 sec off HF time sequence was used. The spreading of the chirped plasma line is thought to be due to small scale field-aligned striations with relative density fluctuations of 1 to 2 %. The frequency shift of some 100 kHz between the natural and the heater-enhanced chirped plasma lines previously reported and interpreted as small scale density depletions near the critical level is seen quite regularly. Some times, however, about 10 sec after the HF turn-on, a second scattering layer develops about 2 km below the initial level, often corresponding to the height of the natural plasma line. As a rule the return from the higher level disappears when this happens. There is some, but not yet conclusive, evidence that preconditioning is required for striations to develop.

Attempts to repeat these experiments with the Max-Planck HF facility and the EISCAT 933 MHz diagnostic incoherent scatter radar have so far been unsuccessful. During Tromsø heating experiments transient plasma line enhancements were observed at frequency offsets greater than the HF frequency by several hundred kHz, and at heights removed from the critical layer by several km. The normal symmetry of the plasma lines about the 933 MHz center frequency is not always in evidence. Observations of the ion line show that, in addition to the ion line enhancement in the vicinity of the critical level (i.e. where $X = 1$), there is also ion line enhancement at the top of the ionosphere near where the plasma frequency is equal to the HF frequency.

The possible cause of these observations is discussed, in particular in terms of plasma line excitation by suprathermal electrons originating in the critical layer and exciting plasma line enhancements in a turbulent plasma in its vicinity.

G5-2
1400 MAPPING OF THE POLAR ELECTROJET DOWN TO D-REGION ALTITUDES AND ITS CHARACTERIZATION BY THE ELF GENERATION TECHNIQUE

A. J. Ferraro, D. H. Werner and A. F. M. Zain

Communications and Space Sciences Laboratory
Department of Electrical Engineering
The Pennsylvania State University
University Park, PA 16802

The High Power Auroral Stimulation (HIPAS) facility near Fairbanks, Alaska has been used to modulate D-region ionospheric currents producing extremely low frequency (ELF) radio waves. The behavior of these ionospheric currents can be deduced from a comprehensive study of the polarization of these ELF signals received at a local field site. This paper examines the theory of mapping of the polar electrojet current down through the D-region where it can be modulated by the heater beam. Presented are theoretical profiles of the current density in the D-region for different spatial wavelengths and the direction of this D-region current for different electrojet heights. The measurement of the polarization of these ELF signals provides additional insight into the direction of flow of electrojet currents. This technique provides a means to study ionospheric currents in addition to the magnetometer, radar and satellite observations.

G5-3
1420 LARGE-SCALE MODIFICATION IN THE POLAR IONOSPHERE BY ELECTROMAGNETIC WAVES: A.H. Wong et al.

G5-4
1440

LARGE DENSITY MODIFICATIONS PRODUCED BY HF HEATING A NIGHTTIME IONOSPHERE*

G.J. Morales, L.M. Duncan#, J.D. Hansen, J.E. Maggs, and G. Dimonte§
Physics Department
University of California at Los Angeles
Los Angeles, CA 90024-1547

A theoretical and experimental study is made of the formation of large scale length (several km) density depletions having a magnitude on the order of 30% of the ambient density. The theoretical studies are based on a transport code that models the nighttime ionosphere using a protonosphere source. Dependences of equilibrium profiles on elevated electron temperatures (as may result from HF heating) are assessed. Studies of ray tracing in prescribed density cavities illustrate how field-aligned intense heating develops and results in narrow effective cavities when sampled by the diagnostic Thomson radar. A survey is made of an experimental campaign at Arecibo during May 3-6, 1988. Some of the highlights are: 1) generation of cavities at several HF frequencies, 2) transition from broad heating to narrow tubes, 3) cavity generation in a previously perturbed ionosphere, and 4) appearance of upper-hybrid wave phenomena.

* Work sponsored by ONR
# Clemson University
§ Lawrence Livermore Laboratory

G5-5
1500

IONOSPHERIC MODIFICATION WITH OBLIQUELY INCIDENT WAVES

E. C. Field, C. R. Warber, and R. M. Bloom
Pacific-Sierra Research Corporation
Los Angeles, California 90025

Nearly all ionospheric heaters operate at vertical incidence. Oblique waves cannot satisfy frequency-matching conditions necessary to excite the parametric decay instability, and they are weakened by geometric spreading below the ionosphere. Those spreading losses are mitigated, however, by focussing near caustics. This paper calculates fields near the caustics of oblique waves and calculates the corresponding increases in electron temperature and electron density. Heat conduction, diffusion, and the temperature dependence of the recombination coefficient are accounted for. First-order estimates of the propagation anomalies caused by the oblique heater are calculated and compared with experimental data published by Russian scientists.

G5-6
1520

DESIGN FOR A NEW IONOSPHERIC MODIFICATION EXPERIMENT*

Gary S. Sales, Bodo W. Reinisch, D.Mark Haines, Ian G. Platt
University Of Lowell Center for Atmospheric Research
Lowell, MA. 01854

We are now planning a set of ionospheric modification experiments using high power oblique HF transmissions. This transmitting system uses a new high gain antenna and a 1MW transmitter. The output of this system will range from 85 to 90 dBW, the actual achieved power depends on the selected frequency. The effects of ionospheric heating will occur near the midpoint of the propagation path where the caustic focusing increases the local field strength. An important part of this program will be to determine the existence of nonlinear effects in this region and the associated theshholds by varying the disturbing transmitter power output.

We are developing a new HF diagnostic system, a low power oblique sounder, to be used along the same propagation path as the high power disturbing transmitter. This concept was first utilized by Bochkarev, USSR to insure that the diagnostic signal always passes through the modified region of the ionosphere. This HF probe transmissions will be low power (150 W) and CW shifted in frequency by approximately 40 kHz from the frequency used by the high power system. The probe transmitter will be colocated at the high power facility while the probe receiver will be located down range from the transmitter at a distance such that the vertical sounder, used for frequency management, lies at the midpoint of the propagation path. There will be multiple receiving antennas as an interferometer to measure both the vertical and azimuthal angle of arrival as well as the Doppler frequency shift of the arriving probe signal. On-line signal processing and display will make it possible to see the heating effects in real-time. A frequency management system with real-time high speed ray tracing will be used at the midpoint site to provide real time frequency and elevation beam control. Simulation of the effects of a ionospheric depletion region on the HF probe signal passing through the "hole" is used to determine the optimum number and location for the down range receiving sites. These simulations indicate that regions of enhanced as well as reduced signal strength should occur during the heating experiment.

A description of the system and the analysis used in the design of the experiment is presented.

* This research was supported by the Air Force Office of Scientific Research and the AF Geophysics Laboratory.

G5-7
1540

RADIO WINDOW PROPAGATION NEAR THE SECOND ELECTRON GYRO-HARMONIC

E. Villalon; W. J. Burke

G5-8
1600

Study of Artificial Atmospheric Plasma

S.P. Kuo
Weber Research Institute
Polytechnic University
Farmingdale, New York 11735

We have used two crossed high power microwave pulses to produce a set of parallel plasma layers in the intersection region of the pulses in a plexiglass chamber. This experiment is intended to simulate the possible generation of artificial plasma layers as a reflector of EM waves in the upper atmosphere. Three probes including a microwave probe, an optical probe and a three dimensional movable Langmuir probe are used to measure the plasma parameters and microwave field intensity in the plasma. The breakdown paschen curve, plasma growth and decay rates, and electron density and temperature have been determined. We have also examined the effectiveness of such a plasma as the reflector of EM waves. Bragg scattering of test waves by the produced plasma layers has been considered. The reflection coefficient has been determined. We will show that our experimental results agree very well with the theory.

We have also studied the pulse propagation through the air. Two fundamental issues are addressed. One concerns the optimum pulse size for maximum energy transfer through the atmosphere by each pulse. The other concerns is with maximizing the ionizations in the destined altitude. In general, these two concerns are interrelated and must be considered together. We will first use the experimental results to demonstrate the significance of the concerns. Since chamber experiment alone can not resolve these concerns adequately, a theoretical model describing the pulse propagation in a nonuniform background pressure has been developed. A parametric study can thus performed to determine the optimum pulse parameters (Instability vs. Pulse width) for effective Ionization. These parameters are then used to evaluate the density profile of the plasma generated by a single microwave pulse or by two crossed beams. The results of this study will also be reported.

G5-9
1620

MICROWAVE BREAKDOWN LABORATORY EXPERIMENTS

D.E. Hunton, AFGL/LID, Air Force Geophysics Lab, Hanscom AFB, MA 01731; W.T. Armstrong, R. Karl, and R. Roussel-Dupre' Los Alamos National Lab; R. Alvarez, P. Bolton, and G. Sieger, Lawrence Livermore National Lab; L. Testermann and T. Tunnell, EG&G Energy Measurements; and D. Eckstrom and K. Stalder SRI Inc.

Chamber experiments to study ionization layers formed by crossed microwave beams (A.V. Gurevich, Sov. Phys. Usp., 23, 862, 1980) in conditions of low pressure air have been conducted. The experiments consisted of a high power (710 MW) 2.856 GHz microwave pulse focused in a pressure chamber onto a reflecting plate oriented at 45° to the incident beam such that the E-field of the beam is in the plane of the reflector. This geometry simulates two phase-locked microwave beams intersecting at 90° with respect to each other. The resulting air breakdown pattern consists of ionization layers at surfaces of constructive interference.

The experiment goals were to 1) measure ionization thresholds for single and multiple layer formation, 2) characterize the geometry of layer formation, and 3) determine density and effective collision rates in the ionization layer. We describe ionization threshold measurements (through measurements of transmitted microwave signal attenuation) over the parameter range of 75 to 1780 ns pulse lengths and 0.01 to 3.0 Torr air pressure. The measured thresholds are compared to previous threshold measurements and discussed in the context of optimization for lowest energy and lowest power requirements for ionization. Description of the breakdown geometry (through CCD camera imaging) is presented. Pressure dependent structure observed within the ionization layer is discussed.

Plans for future experiments will be presented.

G5-10
1640

IONOSPHERIC PLASMA MODIFICATIONS CAUSED BY THE LIGHTNING INDUCED ELECTROMAGNETIC EFFECTS

C. P. Liao, J. P. Freidberg, M. C. Lee
Plasma Fusion Center
Massachusetts Institute of Technology
Cambridge, Massachusetts 02139

The lightning-produced electromagnetic effects may produce significant modifications in the ionospheric plasmas. An outstanding phenomenon investigated in this paper is the so-called "explosive spread F", whose close link with lightnings was recently indentified. The parametric instability excited by the lightning-induced whistler waves is proposed as the source mechanism causing the explosive spread F. All the observed striking features of this phenomenon can be well explained by the proposed mechanism.

Session G-6 1335-Fri. CR1-46
IONOSPHERIC VARIATIONS AND PROPAGATION EFFECTS
Chairman: Haim Soicher, U.S. Army Communications-Electronics Command, Center for C3 Systems, Ft. Monmouth, NJ 07703-5000

G6-1
1340

SELECTED RESULTS FROM THE WAGS I CAMPAIGN: A STATUS REPORT

Robert Hunsucker
Geophysical Institute
University of Alaska Fairbanks
Fairbanks, AK 99775-0800
– and –
Paul Argo
Los Alamos National Laboratory
Los Alamos, NM 87545

The first "Worldwide Atmospheric Gravity-wave Study (WAGS I)" was carried out during the period 15-18 October 1985 by some 20 groups in various countries. Results of most of these studies have been presented at conferences and published in various journals, or are currently in Press. Selected results include some rather convincing "cause-effect" relationships between ionospheric source functions and AGW/TID phenomena, as well as rather detailed descriptions of certain ionospheric AGW sources and peculiarities of AGW/TID propagation. Descriptions of some continuing investigations and scheduling of future WAGS campaigns will also be presented.

G6-2
1400

ATMOSPHERIC GRAVITY WAVE AND DRIFT STUDIES WITH DIGITAL IONOSONDES

Z.-M. Zhang, T.W. Bullett and B.W. Reinisch
University of Lowell
Center for Atmospheric Research
450 Aiken Street
Lowell, Massachusetts 01854

High resolution Doppler and incidence angle measurements of ionospherically reflected HF radio waves are used to determine the ionospheric drift and the parameters of atmospheric gravity waves (AGWs). In the absence of gravity waves, the Doppler measurements at several spaced reflection points directly determine the ionospheric drift. When gravity waves are present, the phase velocity of the wave adds vectorially to the drift velocity affecting the observed Doppler shifts. Combining the information obtained from a fast sequence of ionograms and the Digisonde's high resolution Drift-AGW mode, the time sequence of electron density profiles allows one to clearly identify the gravity wave and to determine the wave amplitude. The wavelength of the AGW and the frequency are found in the high resolution mode. Once the phase velocity of the AGW is determined, the drift vector can be calculated. This paper explains the basic theory and shows first results.

G6-3
1420

COHERENT-ARRAY HF DOPPLER SOUNDING OF TRAVELING IONOSPHERIC DISTURBANCES

Abram R. Jacobson and Robert C. Carlos
Atmospheric Sciences Group
Earth and Space Sciences Division
Mail Stop D-466
Los Alamos National Laboratory
Los Alamos, New Mexico 87544

Medium- and small-scale acoustic-gravity waves (AGW's) are not amenable to propagation measurements using widely separated Doppler sounding stations. This is because the waves' Doppler signatures tend not to be coherent over the tens- or hundreds- of kilometers separations which are useful in another context (namely for tracking large-scale AGW's thought to be of auroral origin.)

We have recently adapted the approach of Pfister (1971) to multibaseline compact Doppler sounding arrays. By "compact" we mean that the dimensions are small compared to the radian wavelength (1/k) of the TID. This compactness precludes following the conventional approach to TID tracking, namely comparing arrival time at various stations of a common Doppler feature, because the lags are too small compared to the radian periods of the AGW. However, the correlations between complex modulation envelopes recorded at the various receivers serve as an efficient means of determining the wave velocity, in many cases. Use is made of the one-to-one relationship of zenith angle and instantaneous Doppler frequency when the HF reflection from the ionosphere is purely specular and when the ionospheric disturbance consists of a single, purely-propagating undulation.

The interest of multibaseline arrays for this application inheres in the cancelation of noise- and fading-based velocimetry errors by means of statistical averaging. The multiple baselines provide an ensemble of redundant measurements with which the sample mean velocity's variance can be reduced according to 1/N scaling. In addition, the multiplicity of baselines allows consistency checks to be performed regarding the hypotheses which must be satisfied to use Pfister's approach in the first place.

We will present a brief sketch of the coherent-array technique and will then illustrate its performance in the presence of noise and fading using data from our 16-channel (120-baseline) facility at Los Alamos. We will emphasise the use of baseline redundancy to mitigate errors and to recognize circumstances in which the model assumptions are not satisfied.

Reference:
Pfister, W., J. Atmos. Terr. Phys. 33, p.999 (1971).

G6-4
1440

POSITION ESTIMATION OF SHORT RANGE HF TRANSMITTERS

Zeb R. Jeffrey and Leo F. McNamara, Andrew Antennas, Technology Park 5095, Australia

Conventional HF direction finding techniques using crossed bearings fail for short-range transmitters, since the measured bearings fluctuate wildly because of the effects of travelling ionospheric disturbances (TIDs). The single station location (SSL) technique, which measures the zenithal angles of the arriving signals, can prove useful in these cases, provided that account can be taken of the effects of the TIDs. This paper will describe procedures based on simultaneous observations of a check target and the unknown target which have been found to take reasonable account of TIDs.

G6-5
1500

IONOSPHERIC CORRELATION STUDIES USING OBLIQUE-INCIDENCE SOUNDER DATA

John M. Goodman/Mark Daehler
Ionospheric Effect
Space Science Division
Naval Research Laboratory
Washington, DC 20375-5000

A number of procedures have been investigated by which ionospheric parameters such as foF2 and TEC are cross-correlated in order to establish the "area of applicability" for a prediction service based upon measurements at a single point. The largest correlation coefficients over space (and perhaps time) are typically associated with major disturbances which occur over global scales. Thus, if we can detect the onset of macroscopic disturbances of this kind, then there is a potential for achieving a prediction performance gain. On the other hand, if the disturbance is rapid as well as widespread (as in nuclear disturbance), a practical prediction improvement upper limit may be reached because of the system overhead required to monitor the changes and apply them to the remote region of interest.

This paper addresses the correlation of Maximum Observable Frequency (MOF) which for a specified range of coverage will depend upon both ionospheric height and critical frequency. Since travelling ionospheric disturbances (TID's) impact these parameters somewhat differently, we anticipate that MOF correlation "ellipses" will be different from either TEC or foF2 ellipses.

The paper will address the correlation of MOF for a set of mid-latitude sites for two epochs of solar activity.

G6-6
1520

ON THE VARIABILITY OF SPORADIC-E

Adolf K. Paul
Naval Ocean Systems Center,Code 542
Ocean and Atmospheric Sciences Division
San Diego,California 92152-5000

The analysis of digital ionograms taken in short time intervals show rapid changes of sporadic-E parameters. The lifetime (observation time) of an individual layer can be shorter than 1 minute. Frequently two or more Es-layers are observed in a given ionogram. Angle of arrival measurements show that the echoes are returned from two or more distinctly different areas in the sky implying a relatively small scale structure in horizontal directions. This conclusion is supported by the fact that almost 25% of the Es-layers found in our data set of more than 4,000 ionograms showed tilt angles of 20 degrees or more. The tilt angles were often highly variable. In many cases where continuity of the top frequency ftEs was observed over relatively long sequences of ionograms, the variation of the tilt angles still indicated some instability of the layer.

G6-7
1540

STATISTICAL ANALYSIS OF IONCAP PREDICTION ERRORS

A. A. Tomko
Johns Hopkins University Applied Physics Laboratory
Johns Hopkins Rd
Laurel, MD 20707

HF field strength predictions generated using the IONCAP model (Version 85.04) have been compared to the median observed skywave field strengths contained in the CCIR database (Data Bank D). IONCAP (Method 20) was run for 15,788 cases, comprising a wide range of geophysical conditions. The IONCAP output was merged with the CCIR database and the prediction error was computed for each case.

Using the entire data set, one finds that the distribution of prediction errors is approximately Gaussian, with a median error of -3 dB and a standard deviation of about 19 dB. Analysis of various subsets of the error population reveals the dependence of the error on key parameters, like the radio frequency, path length and time of day. The results of the error analysis suggest areas where the model could be improved, such as the over-the-MUF loss formulization.

G6-8
1620

NOCTURNAL TRANS-EQUATORIAL PROPAGATION OF RADIO WAVES AT 23.4 KHZ

J. A. Ferguson
Ionospheric Propagation Branch (Code 542)
Ocean and Atmospheric Sciences Division
NAVOCEANSYSCEN
San Diego, CA 92152-5000

In 1969, very low frequency transmissions at 23.4 kHz from a transmitter in Hawaii were measured aboard an in-flight aircraft between Hawaii and Samoa. Although the overall variation of the signal strength as a function of distance was explained at the time, there remained an unexplained rapid variation of the signal strength as a function of distance (Bickel et al., Radio Sci. 5, 19-25, 1970). This rapid variation was suggestive of scattering but a source of was lacking. Recent work by Pappert and Hitney (Radio Sci. 23, 599-611, 1988) suggests that differential penetration of the ionosphere at different latitudes may provide the explanation for the rapid variation.

The data and earth-ionosphere waveguide mode parameters for the path are presented. The variation of penetration into the ionosphere is shown for a representative set of points along the path.

G6-9
1640

VLF TRANSMITTING SATELLITE COVERAGE PREDICTIONS

Francis J. Kelly
Ionospheric Effects Branch
Space Sciences Division
Naval Research Division
Washington, DC 20375-5000

The potential coverage of a VLF transmitting satellite discussed. Results of ray-tracing calculations and full-wave signal and signal-to-noise ionospheric transmission calculations will be given. Coverage maps for the North Polar Area for a VLF transmitting satellite will be shown.

Index

Condensed Technical Program
(Continued from inside front cover)

Thursday, 5 January

0830-1200
PLENARY SESSION — Duane G0-30

1335-1700

B-4	ANTENNAS	CR2-28
E-1	HIGH POWER ELECTROMAGNETICS, COUPLING AND SHIELDING	CR0-36

1355-1700

A-2	ELECTROMAGNETIC MEASUREMENTS	CR1-42
B-3	EM THEORY I	CR0-30
C-2	INVERSE PROBLEMS	CR1-40
F-3	MILLIMETER-WAVE PROPAGATION	CR1-9
G-3	HIGH LATITUDE EFFECTS	CR2-6
GH-1	ELECTROMAGNETIC ANALYSIS FOR IONOSPHERIC PROPAGATION	CR1-46
J-4	SOLAR AND STELLAR RADIO BURSTS	CR2-26

1700-1800

Commission A Business Meeting	CR1-42
Commission D Business Meeting	CR0-30
Commission E Business Meeting	CR0-36
Commission F Business Meeting	CR1-9
Commission H Business Meeting	CR1-46

Friday, 6 January

0835-1200

B-5	EM THEORY II	CR0-30
C-3	FITTING THEORETICAL MODES TO EXPERIMENTAL DATA	CR1-40
G-4	COMPUTATIONALLY FAST IONOSPHERIC MODELS AND THEIR APPLICATIONS	CR2-6
H-3	WAVES IN IONOSPHERIC AND MAGNETOSPHERIC PLASMAS—RECENT THEORETICAL AND EXPERIMENTAL DEVELOPMENTS	CR1-46

0855-1200

DB-2	WAVE GUIDING STRUCTURES	CR0-36

1335-1700

B-7	THEORY AND DESIGN	CR0-30
D-2	GUIDED OPTICAL DEVICES	CR2-28
G-5	IONOSPHERIC MODIFICATION	CR2-6
G-6	IONOSPHERIC VARIATIONS AND PROPAGATION EFFECTS	CR1-46

1355-1700

C-4	NONLINEAR AND NONSTATIONARY SIGNAL PROCESSING	CR1-40

1515-1700

B-6	SCATTERING II	CR2-28